Lehigh University
Lehigh Preserve

Theses and Dissertations

1985

Observations of whisker growth from tin electroplate /

Barbara A. Shollock
Lehigh University

Follow this and additional works at: https://preserve.lehigh.edu/etd

 Part of the Metallurgy Commons

Recommended Citation
Shollock, Barbara A., "Observations of whisker growth from tin electroplate /" (1985). *Theses and Dissertations*. 4574.
https://preserve.lehigh.edu/etd/4574

This Thesis is brought to you for free and open access by Lehigh Preserve. It has been accepted for inclusion in Theses and Dissertations by an authorized administrator of Lehigh Preserve. For more information, please contact preserve@lehigh.edu.

OBSERVATIONS OF WHISKER GROWTH FROM TIN ELECTROPLATE

by

Barbara A. Shollock

A Thesis

Presented to the Graduate Committee

of Lehigh University

in Candidacy for the Degree of

Master of Science

in

Metallurgy and Materials Engineering

Lehigh University

1985

Certificate of Approval

This thesis is accepted and approved in partial fulfillment of the requirements for the degree of Master of Science in Metallurgy and Materials Engineering.

September 9, 1985

Date

Yoshinari Nakada

Supervisor, AT&T Bell Laboratories

Walter C. Hahn, Jr.

Professor in Charge

David A. Rowan

Department Chairman

ACKNOWLEDGEMENTS

It is a great pleasure to acknowledge my thesis advisors, Professor W.C. Hahn and Dr. Y. Nakada for their invaluable advice and encouragement.

Technical discussions with Drs. J.S. Crompton and M.C. Lin have been very helpful. I also wish to extend additional thanks to Dr. J.S. Crompton for his assistance in proof reading, for his many excellent suggestions and for all his help.

K.J. Leachman deserves special recognition for her expert computer and typing skills.

I would also like to acknowledge AT&T Bell Laboratories and the Graduate School of Lehigh University for financial assistance.

TABLE OF CONTENTS

LIST OF TABLES

LIST OF FIGURES

ABSTRACT

Tin whisker growth from electroplated pure tin poses a reliability question for the microelectronics industry. The present research program concentrates on the formation of tin whiskers from both commercial and laboratory samples. Scanning electron microscope examinations reveal that the tin plated leads of dual-in-line packages manufactured by Motorola, Fairchild and Texas Instruments contain tin growths in the as-received and all aged conditions.

Results from laboratory bright acid tin plated lead frames demonstrate that tin whiskers grew only from plated copper lead frames aged at 75 and 100°C for 9 months. In contrast, plated copper lead frames aged at room temperature and 50°C as well as plated alloy 42 (Fe-42 wt % Ni) lead frames in all aged conditions did not produce whiskers. Plating macrostresses evaluated by means of x-ray diffraction appear unrelated to tin whisker growth for the laboratory plated lead frames.

Observations of whisker morphology support a whisker formation mechanism that includes basal growth; however, an exact mechanism for whisker growth remains unresolved. The driving force for tin whisker growth appears to be partially provided by a combination of intermetallic compound formation and plating microstresses.

The maximum length of whiskers observed under the optimum whisker formation conditions was only 60μm. Since the minimum lead separation on a dual-in-line package (DIP) is 1270μm, the probability of whiskers causing inter-lead shorts is very small. Therefore, tin plating on integrated circuits does not pose a reliability problem.

1. INTRODUCTION

1.1 Statement of the Problem

The spontaneous formation of thin single crystal filaments, or whiskers, from electroplated pure tin has long concerned the electronics industry.[1] [2] [3] It has been shown that although the growth of tin whiskers does not adversely affect the protective quality of the tin coating, whiskers have the inherent potential to bridge closely spaced circuit elements by 1) growing to sufficient length, 2) breakage and relocation, and 3) swaying and touching due to localized air currents.[3] [4] When any of these events occur, whiskers may provide low resistance paths between conducting surfaces resulting in short circuiting of the equipment.

Various investigations [5] [6] have found that the current carrying capacity of tin whiskers ranges from 1550 to 4500 Amm^{-2}. In addition, it has been observed [7] that whiskers carrying short (<100ns) pulses with a repetition rate of approximately 100 Hz can support currents in excess of 1A. This current carrying capacity in combination with the closely spaced leads and the lower operating voltages of modern integrated circuits has increased the potential of tin whiskers as a reliability problem in electronic equipment.

Several reports [1] [2] [8] in the literature describing whisker growth on components in telecommunications equipment prompted AT&T Bell Laboratories to investigate the cause of tin whisker growth and methods of its suppression and elimination.[6] [7] [9] As a result of these investigations, electroplated pure tin has been replaced with electroplated gold as a lead finish for devices manufactured by AT&T Technologies. In addition, commercial suppliers are required to use reflowed tin on the leads of devices produced for AT&T to reduce the possibility of whisker growth.[7] [10] The process of reflow involves heating the tin plated leads to 240° — 250°C to relieve residual stresses and volatilize organics that are trapped in the plating. The use of gold electroplating and tin reflowing increase the cost of the device;

further, the thermal treatments involved in reflow may induce severe stresses causing microcracking and delamination between the leads and the plastic packages.

In 1984, Lin [11] from AT&T Bell Laboratories conducted an extensive survey which revealed that no failures of dual-in-line package (DIP) devices have conclusively been attributed to the growth of tin whiskers. In view of this, it is questionable whether the expense and problems associated with the alternatives to as-plated pure tin are justified. It is the purpose of this work to investigate the effects of various critical parameters on tin whisker growth on tin plated leads of commercial integrated circuit devices and on laboratory plated lead frames in order to evaluate the influence of these variables on the reliability of modern telecommunications equipment.

2. REVIEW OF THE LITERATURE

2.1 Whiskers and Whisker Growth

Scientific interest in the filamentary growth of crystals existed long before the advent of the electronics industry.[12] [13] [14] In his 18th century writings, mineralogist Johann Henckel discussed possible origins of hair silver on argenite (Ag_2S).[14] The hair silver Henckel described is a well known example of whisker growth. According to Nabarro and Jackson,[15] any fibrous growth of a solid may be regarded as a type of whisker. Whiskers are generally defined as crystals with one dimension much larger than the other two with no side branching, thus allowing a distinction to be made between whiskers and branched crystals such as dendrites.

Whiskers may grow from the solid, from the vapor, from the melt and from chemical solutions. Regardless of the whiskers' origin, whiskers typically exhibit properties similar to a perfect crystal lattice, exhibiting high strength and have also been observed to have a low dislocation density.[16] [17]

A large number of materials including metals, polymers, semiconductors, minerals and organic crystals have been grown in whisker form.[15] [18] [19] [20] [21] [22] Hair silver and other filamentary growths of metals on non-metals have been documented for two centuries. It was not until 1946, however, when H. L. Cobb [23] observed whiskers growing from the cadmium plated steel of a capacitor that the filamentary growth of metals on metals became of widespread interest. Metallic growths such as those reported by Cobb are defined as "proper" whiskers. Proper whiskers grow from the solid without the atoms which form the whisker passing through another phase.[15] The term whisker in the present work will exclusively refer to proper whiskers.

Numerous investigators have observed spontaneous room temperature growth of whiskers on tin, zinc and cadmium.[24] [25] Arnold [1] found that tin-lead solder (30 weight percent lead), tin-lead-silver solder (34 weight percent lead, 6 weight percent silver) and tin-aluminum alloys also develop whiskers at room temperature. Similarly, Koonce and Arnold [26] grew filaments on alpha brass, niobium, copper, gold, iron, magnesium, nickel, palladium, silver, tantalum, and tungsten by heating these metals in air at 400°C for 60 to 100 hours. In addition, they reported growths on lead after exposure for 30 hours at 200°C. Although the compositions of the filaments were not determined in their study, it was proposed that some of the growths may have been oxides. In comparison, the noble metals are resistant to oxidation at elevated temperatures, and the observed growths are postulated to be metallic whiskers.

In another study, Arnold [6] found that whiskers grow easily from thin metallic coatings ($\approx 0.25 \mu m$), less readily from thicker metallic coatings ($\approx 12 \mu m$), with difficulty on bulk polycrystalline metals, and never on bulk polycrystalline metals of high purity (99.9999 percent pure) or on single crystals of nominal purity. Since whiskers were observed to grow on bulk metal as well as on thin layers it was concluded that whiskers do not grow as a result of a galvanic reaction between the coating and the substrate.[6]

Further evidence for this conclusion can be found in an extensive investigation to characterize whisker formation on thin metallic coatings conducted by Compton, Mendizza, and Arnold.[2] In this study, whisker growth was also observed from bulk metal and from thin coatings on mica and paper. In addition, Compton, Mendizza and Arnold [2] used x-ray diffraction studies to show that whiskers were not corrosion products. These findings also support the conclusion that whisker growth is not a consequence of a galvanic reaction between the coating and the substrate. Compton, Mendizza and Arnold [2] also performed numerous tests in an attempt to establish possible links between whisker growth and

temperature, relative humidity or presence of organic compounds in the environment such as sulfurous rubber. Their results showed that an increase in temperature accelerates the growth of whiskers. This relationship was further defined by other investigations [6] [27] which found an optimum temperature of approximately 50° — 60°C for the growth of tin whiskers. In contrast, relative humidity was reported to be unimportant to whisker formation. The presence of organic compounds in the environment did not affect whisker growth; copper and silver, however, developed shiny black dendritic or tapered filaments in the presence of sulfurous rubber. Based upon the previously mentioned observations of growth from thin films of tin and cadmium evaporated onto mica and paper, Compton, Mendizza, and Arnold [2] also concluded that whisker formation from thin metallic coatings is independent of the substrate material. This conclusion was later refuted by studies concerning whisker growth from electroplated tin on various substrates.[28] [29] Details of these investigations are described in a subsequent section.

2.2 Physical Characteristics of Tin Whiskers

Numerous investigations [17] [30] [31] have concentrated on discovering the physical characteristics of tin whiskers such as length, diameter, surface morphology and growth direction. In an early study, Compton, Mendizza and Arnold [2] observed a large variation in whisker length; some whiskers were barely distinguishable from surface irregularities while others had developed to a length of approximately 1 cm. In contrast to this wide variation of length, whiskers were generally found to have a diameter of approximately 2 microns which remained relatively constant along the length. Compton, Mendizza and Arnold [2] also rotated individually illuminated fibers about their longitudinal axes. The reflections observed revealed the presence of distinct facets on the whisker surface. These observations of whisker length, diameter and surface morphology have been supported and further defined by various studies.[5] [30] [31] [32] [33] Typically, tin whiskers possess diameters ranging from

0.05 to 5.0 microns, vary in length from 0.03 to 10.0 mm and often exhibit striations parallel to their long axis.

Key [31] conducted a detailed scanning electron microscope (SEM) study of the surface morphology of tin, zinc and cadmium whiskers. Whiskers of all three metals shared the same general characteristics: approximately uniform diameter from base to tip, large variations in length and the presence of surface striations. In addition, Key determined that whisker diameter and length are apparently independent of each other. In this study, Key also discussed whisker morphology in terms of the tip of the whisker, the shaft of the whisker and the base of the whisker.

The tip of the whisker was usually smooth or rounded without any significant structural features although occasionally whiskers in which the tip appeared to be bent sharply were observed. Koonce and Arnold [34] noted that the general shape of the initial whisker tip persisted during the growth of the whisker; consequently, whiskers appear to grow from the base. This conclusion is significant when evaluating the proposed models for whisker growth as discussed later in this thesis.

According to Key,[31] the shaft of the whisker was either smooth or longitudinally striated with the striations extending over the entire length of the whisker. The pattern and depth of these striations changed only slightly on an individual whisker. However, since the pattern and number of striations varied between whiskers, Key considered that the striations were not crystallographically significant. Electron microscope examination of plastic replicas [35] and metallographic cross sectioning [36] [37] have also revealed the presence of these striations or "fluting" extending along the external surface of the whisker shaft. In addition, metallographic cross sectioning has demonstrated that some whiskers are hollow for at least part of their shaft length.[36] This observation is supported by a comparison of measured and calculated whisker weights which show that there must exist solid and nearly solid whiskers

as well as hollow whiskers.[38]

The last portion of the whisker described by Key [31] was the base which revealed two distinct structures. In one case, whiskers may emerge directly from the electroplating while in the other case whiskers may develop from a distinct nodular growth. These nodules may be smooth or contain some structure, and for samples on which nodular growths appear, all the whiskers emerge from these growths. The existence of nodules, however, may not be considered as indicative of whisker formation since they are also observed in the absence of whiskers.[31] In the case of both types of basal morphology, Key did not observe depressions or evidence of thinning of the electroplating adjacent to the whisker's base. Similarly, Dunn's [5] scanning electron microscope observations of whiskers also noted the absence of depressions at whisker bases. In addition, metallographic cross sectioning [5] indicated an absence of microscopic voids or pores in the plating surrounding the whiskers.

Numerous x-ray diffraction studies [17] [30] [39] have supplemented the information on whisker morphology. Tin whiskers exhibit the β-tin crystallographic structure, body centered tetragonal. Ellis [30] investigated the distinct striations on the external surfaces of whiskers in an attempt to determine potential crystallographic significance. Although Key [31] concluded that these features had no crystallographic relevance, Ellis found that the discrete optical reflections [2] of a tin whisker are associated with specific crystallographic directions.

X-ray diffraction studies [17] [30] [39] revealed that a variety of growth directions may exist. In addition, transmission electron microscopy [40] has also been used to determine the growth directions of tin whiskers. The results of the numerous x-ray diffraction and the transmission electron microscopy investigations are summarized in Table I.

Although tin whiskers are generalized as being both cylindrical and straight, whiskers may also consist of a small number of kinks joining straight sections,[5] [6] [37] [41] [42] and a few tin whiskers have been in the form of spirals. [2] [32] [37] [43] The distribution of

observed angles in these kinked tin whiskers is predominated by angles clustered around 30°, 45°, 60° and 90°.[5] [41] [43]

Table I : Whisker Growth Directions

Source of Whiskers	Method	Growth Directions Crystallographic Indices	Investigation
spontaneous growth from tin electroplate	x-ray diffraction	<100>, <101>, [001]	Treuting and Arnold [39]
spontaneous growth			
a) tin electroplate on zinc	x-ray diffraction	<111>, [111]	Ellis [25]
b) tin electroplate on brass	x-ray diffraction	<111>, [011]	Ellis [25]
c) tin electroplate on low carbon steel	x-ray diffraction	[100] or [010], [010]	Ellis [25]
spontaneous growth from tin-zirconium alloy (tin rich)	x-ray diffraction	[001], [100], [101], [111]	Smith and Rundle [17]
"squeeze" growth	transmission electron microscopy	<101>, <100>, <210>, <001>, <110>	Morris and Bonfield [40]

2.3 Mechanisms of Whisker Growth

A number of theories has been proposed to explain the spontaneous growth of metallic whiskers. Two basic models have emerged: dislocation based models [44] [45] [46] [47] [48] and models based on grain growth or recrystallization and grain growth.[30] [49] [50] [51] [52] Dislocation models have been proposed in which the required driving forces for dislocation motion are obtained from surface energy effects [45] [46] and internal or external stresses.[47]

Considering the proposed dislocation based models, Peach [53] presented the earliest whisker growth mechanism. Peach suggested that metal atoms are transported by diffusion along the core of a screw dislocation. As a result, metal atoms are deposited at the surface as single atomic layers. Continuation of the process produces a whisker with a screw dislocation coincident with its axis. This mechanism, however, must be discarded based on the accepted observation that whiskers grow from the base rather than from the tip.[33] [52]

The dislocation models of Eshelby [46] and Frank [45] both describe mechanisms in which the oxidation of the new surface as a filament grows provides the necessary driving force for whisker growth. In both theories, the oxidation is equivalent to a negative surface tension. According to Eshelby,[46] this surface tension causes a small pre-existing hump on the surface to pull out into a whisker. In addition, these surface tension forces provide a retaining pressure at the base of the growing whisker. Eshelby further assumed the presence of a dislocation generating mechanism such as a Frank-Read source of length l parallel to the surface at a distance l beneath the hump. Under the influence of the surface tension, the source emits dislocations which glide vertically toward the surface, each one adding one atomic layer to the base of the hump (Figure 0).

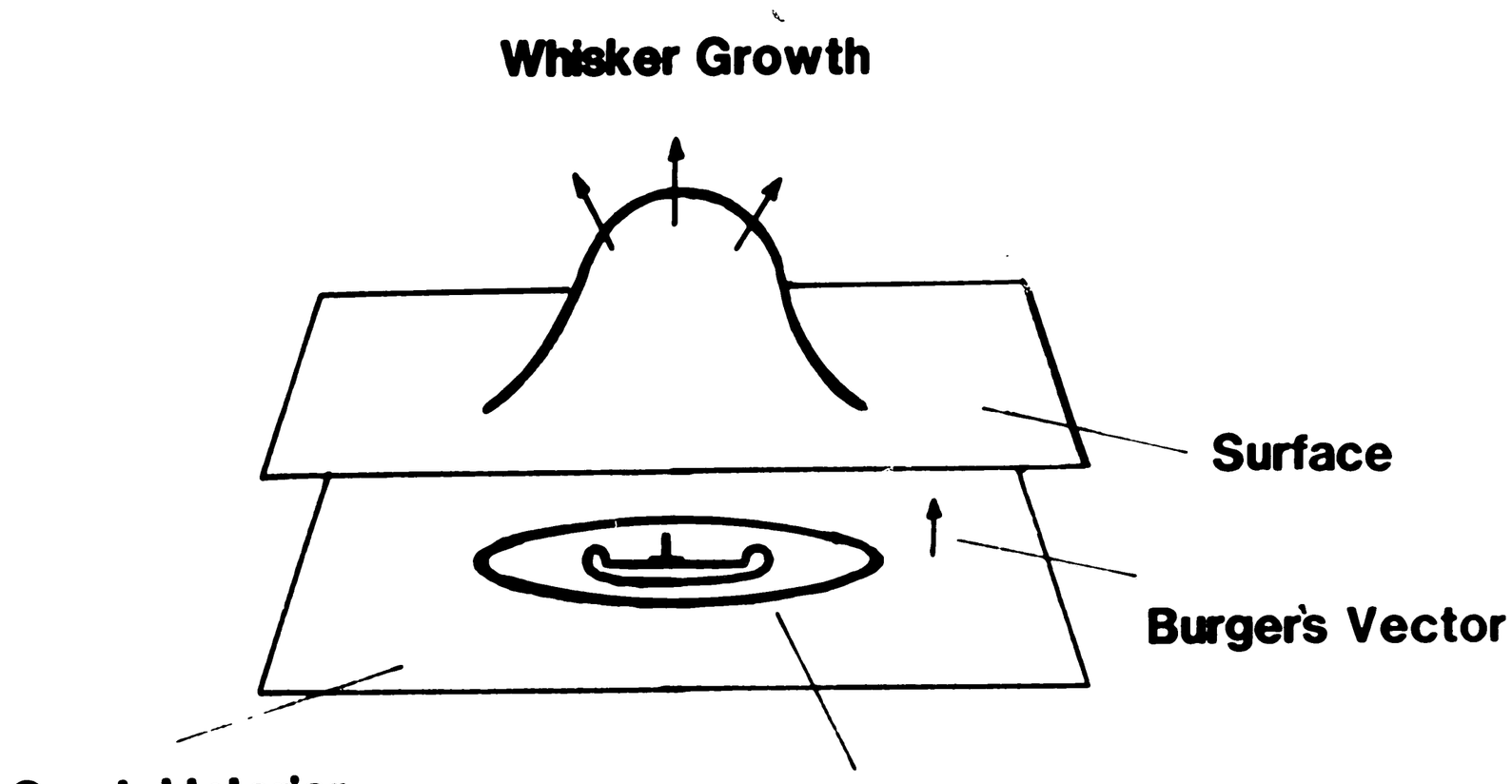

FIGURE 0: DISLOCATION MODEL FOR WHISKER GROWTH (AFTER ESHELBY[46])

The linear growth rate of the resulting whisker is given by: [46]

$$\frac{V}{\pi R^2} \approx K\beta nD \left(\frac{b}{l}\right)^2 \left(\frac{\gamma b^2}{kT}\right)$$

where V is the volume transferred in unit time, R is the radius of the hump, K is a stress distribution factor, b is the Burgers vector, D is the diffusion coefficient, n is the number of dislocation loops in transit between the source and the surface and γ is the surface tension.

The other general dislocation based model which used the negative surface tension generated as a result of oxidation for a driving force is that of Frank.[45] According to Frank's whisker growth mechanism, a dislocation terminating at the free surface will move over the metal surface until it reaches an equilibrium position. If the dislocation is anchored in the form of a closed loop, unless the anchor point provides an equilibrium position, the dislocation will continue to travel around this point indefinitely. Under the driving force of a negative surface free energy resulting from oxidation, each circuit travelled will displace a knob by a distance and direction corresponding to the Burgers vector of the dislocation. As a result, a whisker that grows from its base is formed. Frank [45] calculated the growth rate of a whisker as

$$\left(\frac{12D_s}{\pi r}\right)\left[\exp\left(\frac{4Qa}{rkT}\right) - 1\right]$$

where D_s is the self-diffusion coefficient, r is the radius of the whisker, Q is the free energy released by oxidation per surface lattice site of the metal and a is the interatomic distance.

Franks' [47] model adapted the proposed mechanisms of Eshelby and Frank and derives the required driving force from applied pressure or from internal stresses. This theory takes dislocation loops from an Eshelby type source but supposes that rather than gliding unobstructed to the surface, the loops intersect other dislocations with the same Burgers vector. The portion of the second dislocation which intersects the loop is carried to

the surface by the loop; however, this portion is connected to the remaining stationary sections outside the loop by screw dislocations. These screw dislocations may glide to the surface. If the screw dislocations reach the surface, they are anchored at the base of the whisker and migrate around the whisker base. If the screw dislocations do not reach the surface, they produce spiral edge dislocations as described by Frank.[45] Franks attributes the cessation of whisker growth to the formation of stacking faults.

In the three dislocation models for whisker growth the rate of whisker growth is dominated by the rate of self-diffusion in the whisker growing medium regardless of the proposed driving force. The grain growth or recrystallization and grain growth model [30] [49] [51] relies on the presence of stored strain energy or applied external stresses [52] [50] to provide the necessary driving force for whisker growth. Ellis, Gibbons, and Treuting [30] suggest a whisker growth mechanism based on recrystallization and grain growth in which the driving force arises from internal strain energy or external stress.[50] [52] In general, whisker growth occurs by the extension of the free surface of a critical size crystal that is already present or formed by recrystallization. The basic hypothesis is that the growth of whiskers is more energetically favorable for the release of stored strain energy although the final state achieved may have a higher energy than the state reached by bulk recrystallization and grain growth. According to Ellis and co-workers,[30] the grain boundary of the nucleating crystal must be immobile so the decrease in energy occurs by whisker growth rather than by grain boundary migration. The exact mechanisms for this grain boundary pinning are not clear, but oxide films,[30] [49] and specific dislocation configurations [30] are suggested as possible factors. Ellis and co-workers [30] describe the growth process in view of normal grain growth with atoms migrating from strained regions to unstrained regions. As a consequence of the fixed grain boundary, atoms diffuse into the nucleating crystal while vacancies diffuse away; the surface of this grain must grow outward. A whisker results by the continuous addition of

atoms, and the growth of the whisker ceases when the internal stress is reduced below a critical level. In addition, Ellis, Gibbons and Treuting [30] state that the whisker may be the extension of an entire grain or of a portion of a grain.

2.4 Factors Affecting Tin Whisker Growth

Numerous factors are known to affect the growth of tin whiskers. The previously described investigation of cadmium, tin and zinc whisker growth by Compton, Mendizza and Arnold [2] provided a foundation for later studies which attempted to characterize the parameters which influence tin whisker growth.[24] [27] [28] [37] [9] [54] [55] [56] Various investigators have found that the major variables affecting tin whisker growth are the type of tin coating,[4] [8] [57] [58] [59] coating thickness,[6] [8] mechanical stress,[6] [52] storage temperature [6] [27] and substrate metal.[8] [24] [55] [60]

2.4.1 Type of Tin Coating Arnold [6] reported that whiskers developed on hot-dipped, sprayed and evaporated tin coatings as well as tin electroplate; however, it has been shown [3] [8] that hot dipped and reflowed tin coatings are less prone to whisker growth than electroplated tin. Tin electroplate may roughly be classified into three categories: matte pure tin plating, bright pure tin plating and tin-alloy plating. Both matte and bright tin electroplates are susceptible to whisker growth.[8] [55] Bright tin coatings, however, exhibit more rapid whisker growth as compared to matte tin, possibly due to the higher content of organic impurities in the bright tin electroplate.[37] In terms of the previously described theories of whisker growth, the presence of these organic impurities may affect the internal stress state of the plating, thus providing a driving force for whisker growth.[37] Considering tin-alloy coatings, a tin-nickel (65 weight percent tin) electroplate has been found to be immune to whisker growth and tin-lead (40 weight percent lead [5] to as little as 1 weight percent lead [9]) electroplates were shown to suppress whisker formation. Although tin-lead electroplate appears to be the most commercially viable alloy coating, Arnold [9] discovered

that tin electroplate alloyed with antimony, cobalt, copper, germanium or gold also showed a reduction in whisker growth. It has been suggested [4] that the alloying constituents can change the state of the internal stress of the deposit and may therefore reduce the driving force for whisker growth.

2.4.2 Post-Plating Treatment Another factor that affects tin whisker growth is post-plating treatments. Arnold [1] has shown that pre-plating chemical treatments of the substrate have no effect on whisker growth; however, a post-plating immersion of tin electroplated brass in an alkaline solution containing a polycation was found to eliminate whisker growth.[59] In contrast to post-plating chemical treatment, post-plating heat treatments have been extensively investigated.[3] [8] [57] [58] [61] Reflowing the tin electroplate at 240 - 250°C in a non-oxidizing atmosphere has been found to reduce the possibility of whisker formation.[8] [57] [61] Post-plating annealing of the tin electroplate in a non-oxidizing atmosphere has also been shown to retard the growth of whiskers.[3] [8] [54] [58] Annealing temperatures typically range from 180 - 218°C and annealing times vary between 1 to 3 hours.[3] [8] [54] In the specific case of tin electroplate on copper, it has been suggested [58] that a post-plating heat treatment in a non-oxidizing atmosphere at a temperature just below the copper-tin eutectic temperature decreases the formation of whiskers.

2.4.3 Coating Thickness In addition to the effects of tin coating type and post-plating treatments, tin whisker growth is sensitive to coating thickness. As mentioned previously (Section 2.1), Arnold [6] found that whiskers develop more readily on thin ($\approx .25\mu m$) coatings. This correlation between thin electroplates and enhanced whisker growth has been supported by subsequent studies.[8] [27] It has been postulated that thinner coatings contain higher internal stresses which may provide the required driving force for whisker growth. [30] Arnold [9] also observed that for a constant final thickness of tin electroplate, varying the plating current and time did not greatly affect whisker formation. This observation,

however, does not agree with later studies which suggest that higher cathodic current densities increase the defects and stresses in the metal film, thus promoting whisker formation.[3] [37]

2.5 External Stress

External stresses also influence whisker growth from tin electroplate.[3] [8] [52] Fisher, Darken and Carroll [52] reported that the growth rate of tin whiskers can be accelerated by several orders of magnitude by the application of a compressive force. The growth rate increased linearly with pressure; under an applied compressive stress of 7500 psi, rates as high as 10,000 A/second were observed.[52] In addition, electroplated coatings previously suspected to be immune to whisker growth, such as tin-lead electroplates, developed whiskers under the influence of a sufficiently high local pressure.[6] [8]

2.5.1 Temperature Temperature has been observed to have a marked effect on tin whisker growth.[6] [27] [56] It has been suggested that the optimum temperature for whisker growth from tin electroplate is 50 — 60°C;[6] [37] [56] however, in one investigation [27] whiskers were observed to occur most frequently in the 20 — 50°C temperature range with the occurrence of whiskers very low at -30°C and 120°C.

2.5.2 Substrate Metal The substrate metal onto which the tin is electrodeposited plays a critical role in whisker formation. Numerous investigations [8] [55] [60] have demonstrated that tin electroplated directly onto brass exhibits the maximum whisker growth rate as well as the highest density of growths. Whiskers [27] [60] also grow profusely from electroplated tin on copper substrate. In contrast to brass and copper substrates, steel, iron, nickel and silver substrates appear to eliminate or substantially reduce the growth of tin whiskers.[8] [37] [62]

In addition to the effect of the substrate metal, it has also been found that cold working of a copper substrate before tin plating may accelerate whisker formation.[37] A

subsequent investigation,[56] however, revealed no relationship between degree of cold working and whisker growth for tin plated copper substrates.

2.5.3 Parameters to be Investigated in the Present Study The present investigation of tin whisker growth will concentrate on two variables which have been proven to influence tin whisker formation: temperature and substrate. All other factors will be held constant. In addition, the influence of macrostress in the tin electroplate on whisker growth will be characterized.

3. EXPERIMENTAL PROCEDURE

3.1 Materials

3.1.1 Commercial Devices Commercial devices with tin plated leads that had not been reflowed or solder dipped were obtained. The devices were 16 lead dual-in-line packages, DIPS (Figure 1). Three manufacturers were represented, Texas Instruments (device day code 8220), Fairchild (device day code 8224), and Motorola (device day code I8413). Table II provides an explanation of these day codes.

3.1.2 Laboratory Plated Lead Frames Unplated alloy 42 (Fe-42 weight percent Ni) and copper lead frames were purchased from Paul Hamer Associates. The material was in strips 21 cm long by 2.5 cm wide in which there were ten frames (Figure 2). Strips of both materials were tin plated using the MacDermid B.A.T. 432 process, a bright acid sulfate tin plating process. The plating solution composition and operating conditions are given in Table III and Table IV, respectively. Prior to immersion in the plating solution the strip was cleaned by dipping in a NaOH solution (concentration 75g/l) at approximately 72°C followed by deionized water rinsing and then dipping in a 5 percent by volume aqueous H_2SO_4 solution followed by a deionized water rinse. It was determined experimentally that a plating time of four minutes produced a tin coating of approximately 5.0 μm (See 3.3.1 for thickness measurement). The electroplated strips were then cut into individual lead frames for subsequent heat treatments.

3.2 Heat Treatment

After initial scanning electron microscope examination (Section 3.3.2), the commercial devices were divided into groups for heat treatment, that is, four groups of fifty Texas Instruments DIPs, four groups of fifty Fairchild DIPs, and four groups of fifty Motorola DIPs. In addition, the laboratory plated lead frames were divided into groups,

Table II : Day Codes of Commercial Devices

Manufacturer	Device Day Code	Year of Manufacture	Week in Year of Manufacture
Texas Instruments	8220	1982	20
Fairchild	8224	1982	24
Motorola	I8413*	1984	13

* I designates a chip processing parameter

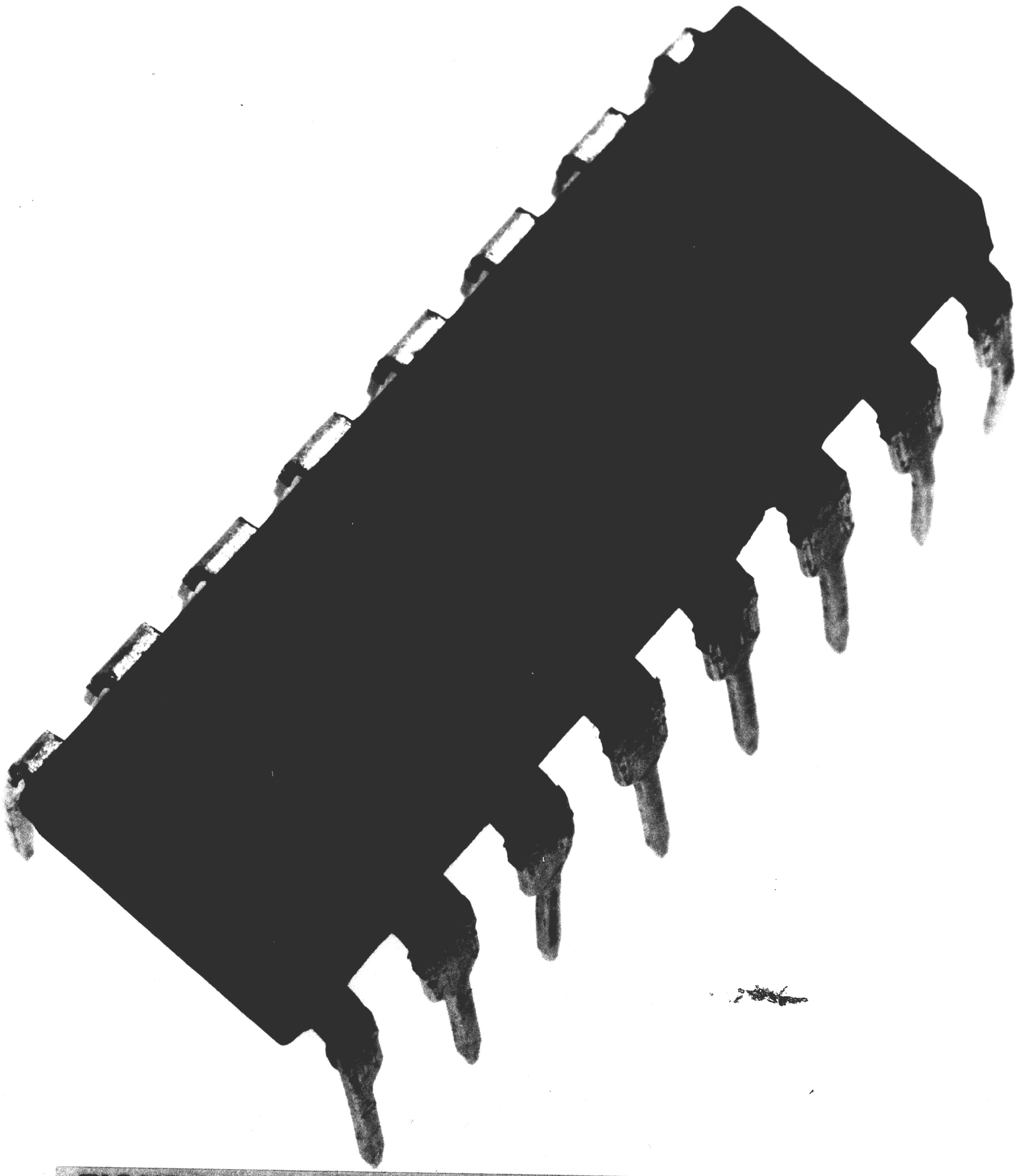

FIGURE 1: DUAL-IN-LINE PACKAGE (DIP)

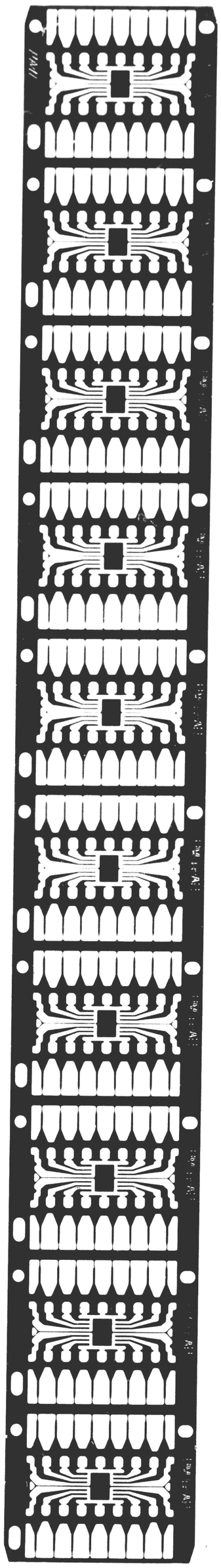

FIGURE 2: STRIP OF LEAD FRAMES

Table III : Tin Plating Bath Solution

stannous sulfate	567.0 gram
sulfuric acid, C.P.	2.0 liter
MacDermid B.A.T. 432 solution	0.95 liter
deionized water	19.0 liter

Table IV : Tin Plating Operating Conditions

anode	:	99.99 percent pure tin
cathode	:	alloy 42 or copper
voltage	:	0.8V
current	:	1.2A

four groups of fifty tin plated alloy 42 lead frames and four groups of fifty tin plated copper lead frames. A group of devices from each manufacturer, a group of plated copper lead frames, and a group of plated alloy 42 lead frames were aged in air for various times at each selected temperature. The temperatures chosen for this study were 25°C, 50°C, 75°C, and 100°C. based on the optimum temperature for tin whisker growth suggested by Arnold.[6]

3.3 Metallography

3.3.1 Optical Microscopy Optical microscopy was used to determine the tin plating thickness on both the leads of the commercial devices and the laboratory plated lead frames. Cross sections of the leads of a DIP from each manufacturer and cross sections of a plated alloy 42 lead frame and a plated copper lead frame were prepared by conventional metallographic techniques. Prior to metallographic preparation, the five specimens were overplated with approximately 2.5 μm of copper. This overplating was done to retain edge definition of the tin plating during subsequent polishing operations. The laboratory plated copper lead frame was etched with 2% nitric acid to improve contrast between the plated layers and substrate. The polished cross sections were then photographed at 500x using a Zeiss Axiomat optical microscope. The tin plating thickness was determined from these photographs.

Optical metallography was also performed on the as-received alloy 42 and copper lead frames. A cross section parallel to the length and width of the lead frame and a cross section parallel to the thickness of the lead frame (Figure 2B) of these two materials were prepared using standard metallographic techniques. The etchants used are presented in Table V. The polished and etched cross sections were then examined in a Zeiss Axiomat optical microscope to determine the grain structures.

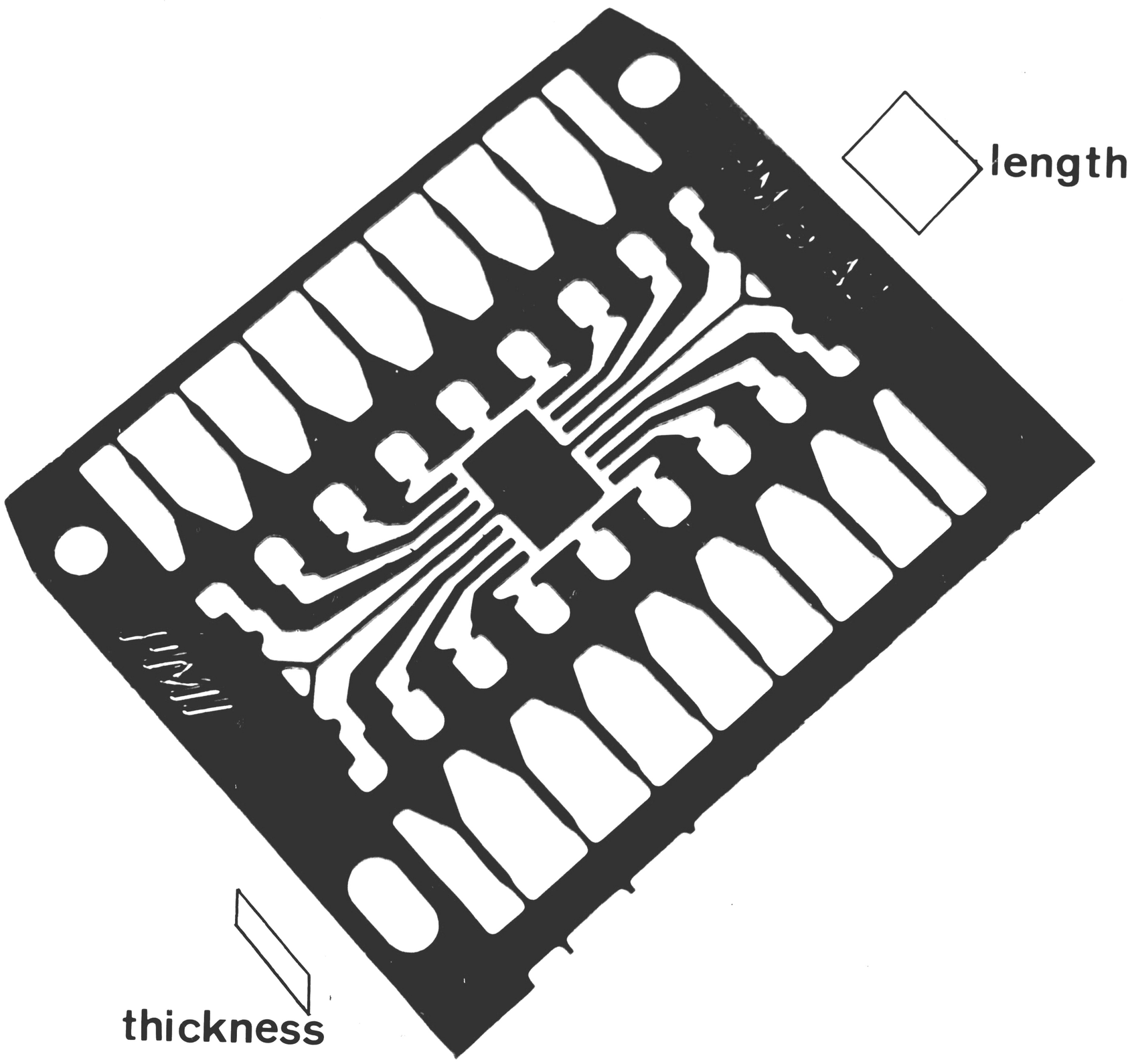

FIGURE 2B: LEAD FRAME SHOWING CROSS SECTIONS

Table V : Etchants used for As-Received Lead Frames

Material	Etching Reagent	Composition
Alloy 42	ferric chloride and	5g $FeCl_3$
	hydrochloric acid	50 ml HCl
		100 ml distilled H_20
Copper	ammonium hydroxide and	5 parts NH_4OH
	hydrogen peroxide	5 parts H_20
		3 parts H_2O_2 (3 percent)

3.3.2 Scanning Electron Microscopy (SEM) Both the as-received commercial devices and the laboratory plated lead frames were examined in an Amray 1000A SEM to determine if whiskers were initially present and to characterize the plated surface topology.

After subsequent heat treatments, the tin plating of the commercial devices and the laboratory plated lead frames were re-examined in the SEM for whisker growth and topological changes.

3.3.3 Energy Dispersive Spectroscopy (EDS) Energy dispersive spectroscopy conducted on an Amray 1000A SEM equipped with Kevex x-ray analysis apparatus was used to examine the composition of the leads and plating of the commercial devices.

3.4 X-ray Analysis

3.4.1 Background One of the theories proposed to explain whisker growth is based on the development and relief of internal stresses; it has been suggested that whisker formation may be a stress relief mechanism.[26] In an attempt to correlate the presence or absence of whiskers to stresses in the tin electroplating, x-ray diffractometer studies were performed on the laboratory tin plated lead frames.

Bragg's Law states

$$n\lambda = 2d_o \sin \theta_o$$

where n is the order of reflection, λ is the wavelength of the incident x-rays, d_o is the interplanar spacing in an unstressed lattice, and θ_o is the Bragg angle for the unstressed condition.

From this relationship, it can be seen that the Bragg angle ,θ_o, for the diffraction of x-rays from a set of crystal planes is sensitive to all factors that affect the interplanar spacing of these reflecting planes. Since stresses can alter the spacing of reflecting planes, d_o, enough to change the Bragg angle θ_o by a measurable amount, the magnitude of the stresses that are altering the normal spacing of the planes can be estimated from the observed $2\theta_o$ angles. This effect is illustrated in Figure 3 for a set of crystal planes lying normal to the applied stress. Figure 3a represents an x-ray intensity distribution for an unstressed set of crystal planes. The x-ray peak position occurs at $2\theta_o$ corresponding to an unstressed crystal with an interplanar spacing d_o. Under a compressive stress, Figure 3b, the lattice spacing becomes d where d is less than d_o, and the associated x-ray peak has moved with respect to $2\theta_o$ (from the equation above, it can be seen that as d decreases, θ must increase). Thus, any experimentally determined shifts in x-ray peak position may be related to changes in interplanar spacing caused by local stresses.

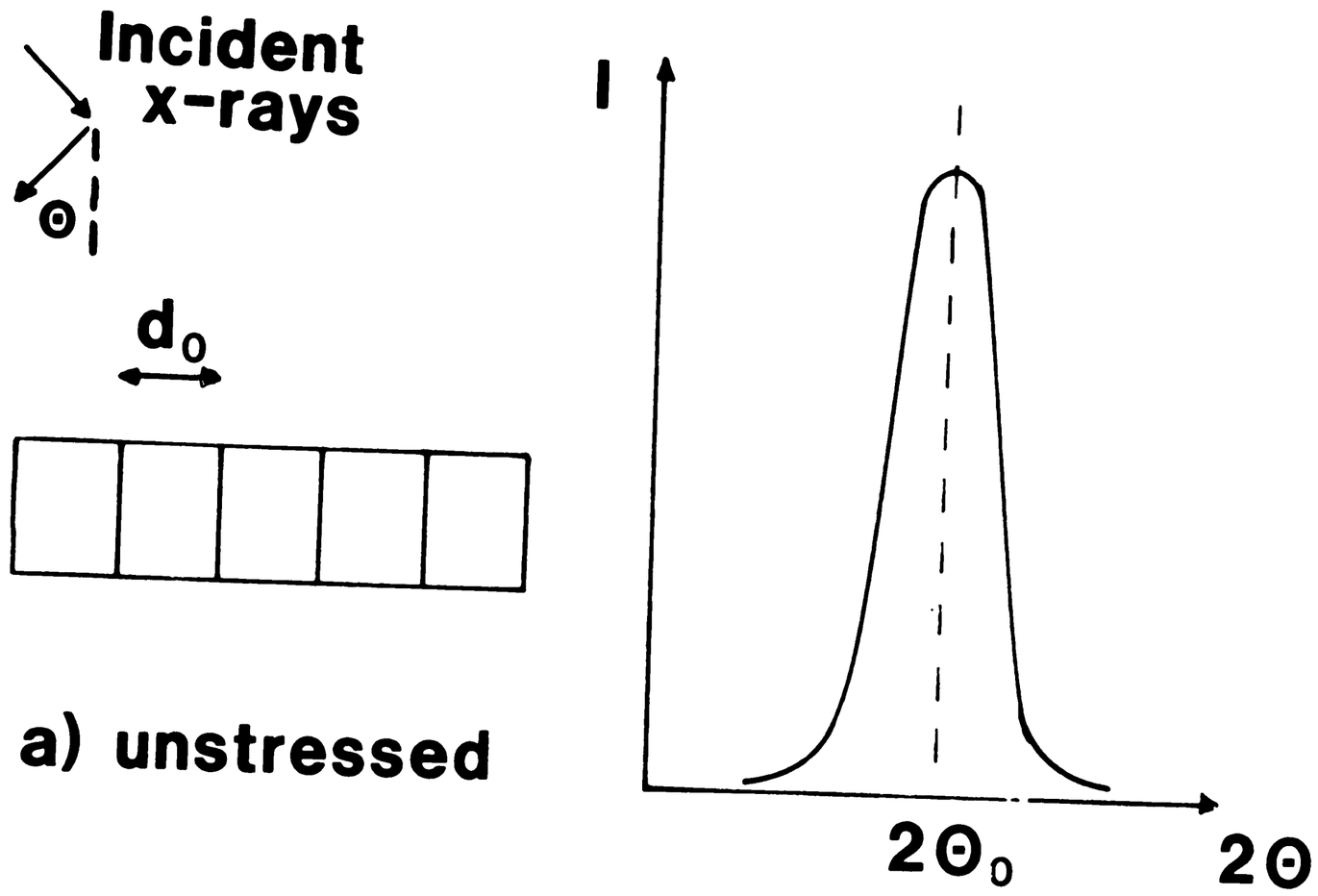

Figure 3: Effect of stress on x-ray diffraction peak position.

3.4.2 Experimental X-ray Technique To ensure that stress analysis was conducted only on material in the tin plating layer, initial x-ray diffractometer scans were used to determine a tin peak that was isolated from peaks of both lead frame materials. These preliminary diffractometer data consisted of full scans of a block of annealed tin (200°C, 113 hr.) taken from an unused portion of the plating anode, an alloy 42 lead frame, and a copper lead frame, both as-received. These data were obtained using a Philips XRG-5000 unit with a copper tube ($CuK_{\alpha 1}$, λ = 1.405A) operating at 40kV, 30mA and a 2θ scan speed of 2°/minute.

Since the evaluation of the internal stresses is based on the measurement of shifts in x-ray peak position, it is essential to monitor variations in the diffractometer data between scans resulting from specimen to specimen geometry changes. Silicon powder (200 mesh, 99.99+ percent pure) was chosen as the internal standard since it has a peak close to the x-ray peak of tin used for stress evaluation.

Samples of as-plated and aged laboratory electroplated alloy 42 and copper lead frames used for the internal stress studies were coated with a thin layer of the finely ground silicon powder prior to diffractometer scans. The x-ray data of the plated lead frames were obtained using a Philips APD 3600 automated x-ray powder diffractometer. All collected data ranged from an initial 2θ value of 28.00° to a final 2θ value of 34.00° using a 2θ angle increment of 0.01° and a count time of 1.2 seconds.

The results from the x-ray diffractometer scans were initially corrected for specimen to specimen geometry changes using the internal standard. The corrected tin x-ray peak position of the laboratory plated lead frames was compared to the x-ray peak obtained from the annealed block of tin.

4. RESULTS

The results of microstructural examination, x-ray stress measurement and surface examination after aging at various temperatures will be presented. These results will be described for the commercial devices and the laboratory plated alloy 42 and copper lead frames.

4.1 Material Characterization

4.1.1 Plating Thickness The tin plating thicknesses of the commercial devices and the laboratory plated lead frames were measured using optical metallography. A typical micrograph is presented in Figure 4. The left portion of the micrograph is the substrate, the layer immediately adjacent to the substrate is the tin plating, the final layer is the copper plating used for edge retention during metallographic preparation and the large dark region is the metallographic mounting material. Table VI contains the measured tin plating thicknesses for the three commercial devices and the two laboratory plated materials.

4.2 Composition Determinations

In order to further characterize the commercial devices, the plating and lead material were evaluated using qualitative energy dispersive spectroscopy (EDS). The plating material of the devices from all three manufacturers was determined to be tin.

However, EDS analysis showed that the underlying lead frame material of the three commercial manufacturers was different. The lead material of the Fairchild and Motorola devices was copper whereas that of the Texas Instruments devices was an iron-nickel alloy.

Similarly, the composition of the laboratory plated coating was confirmed to be tin by the EDS analysis. The lead frames used for the laboratory electroplating were analyzed and found to be copper and an iron-nickel alloy.

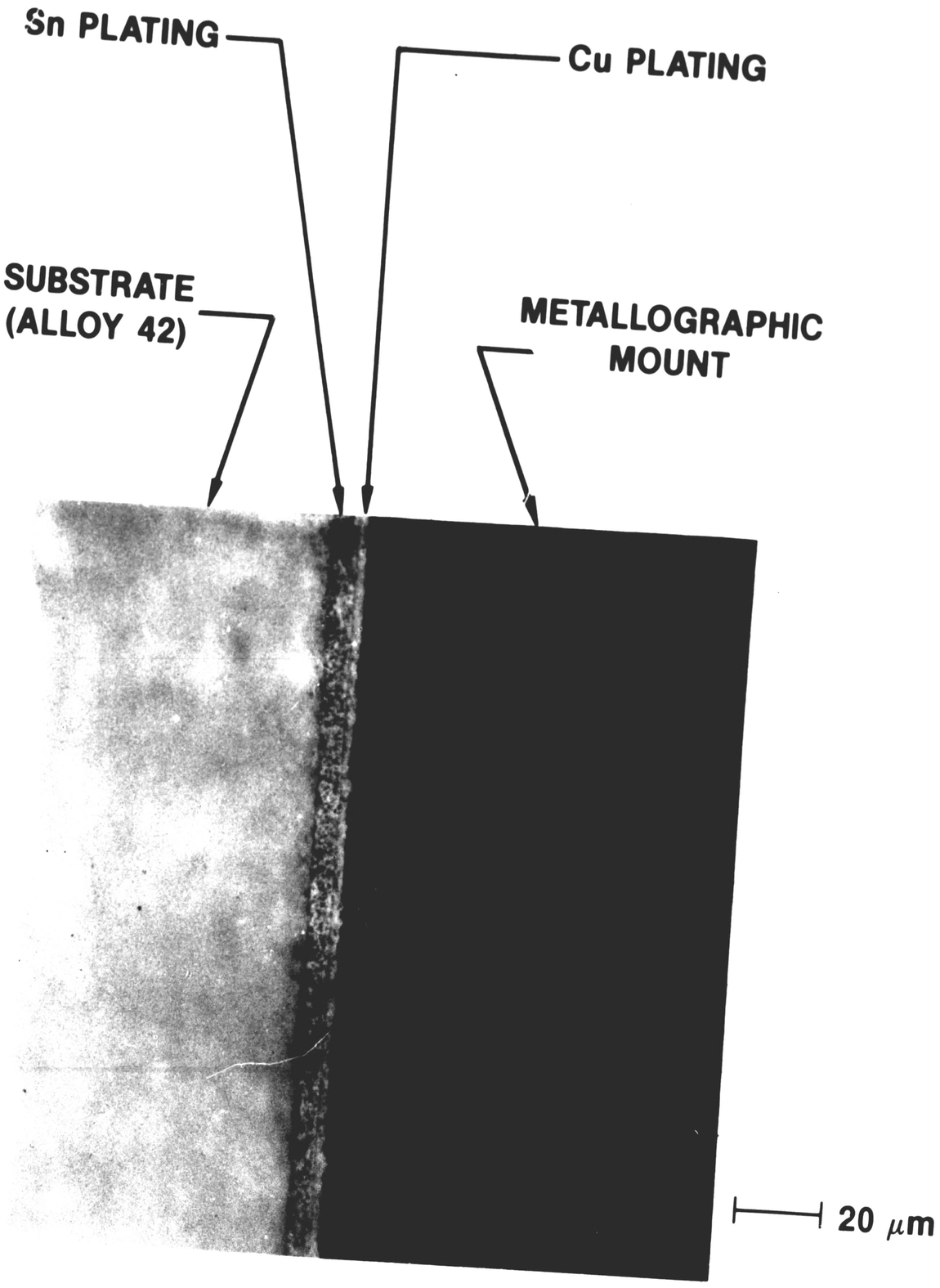

FIGURE 4: METALLOGRAPHIC CROSS SECTION OF TIN PLATED ALLOY 42 LEAD FRAME.

Table VI : Measured Tin Plating Thicknesses

Laboratory Lead Frame Material or Commercial Manufacturer	Measured Tin Plating Thickness at 500x, mm	Actual Tin Plating Thickness, μm
Alloy 42	2.7	5.4
Copper	2.0	4.0
Texas Instruments	2.8	5.6
Fairchild	4.8	9.6
Motorola	2.3	4.6

4.2.1 Microstructural Characterization Metallographically prepared and etched samples of as-received lead frames of copper and of alloy 42 were examined to characterize the microstructures. Micrographs of sections parallel to the length and width of the frame and sections parallel to the thickness (Figure 2B) for each material are presented in Figures 5 to 8.

Examination of the alloy 42 micrographs (Figures 5 and 6) reveals a relatively equiaxed grain structure for each section with comparable grain sizes. Inclusions are also visible generally forming aligned arrays thus suggesting that the alloy 42 was rolled into strips and recrystallized after forming.

The micrographs of the copper lead frames (Figures 7 and 8) display little resolvable grain structure. The through thickness section (Figure 7) shows a layered structure with aligned inclusions. These characteristics suggest that this material was rolled into strips with no associated recrystallization. This is expected since annealed copper will be too soft to function as a lead frame.

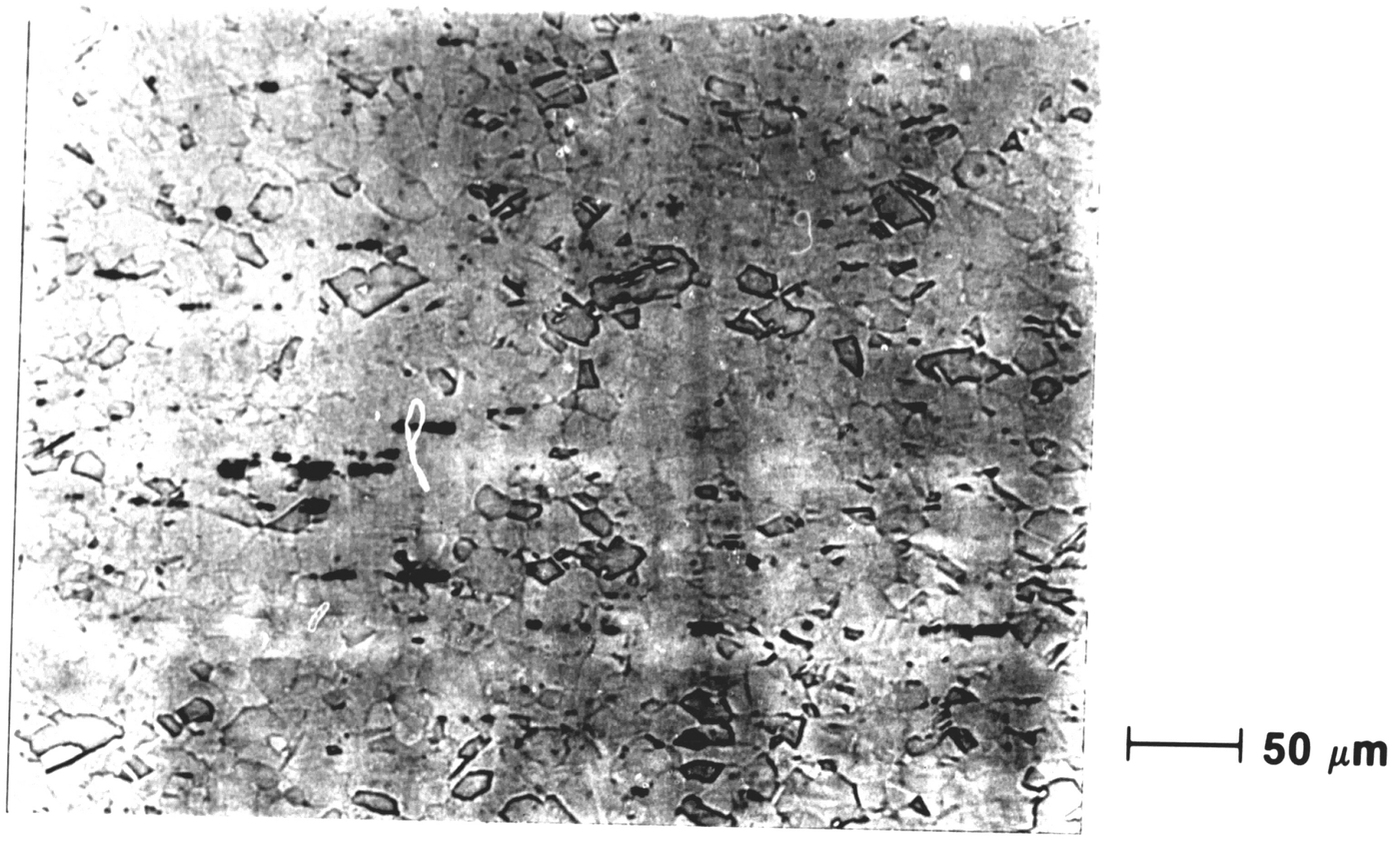

FIGURE 5: MICROSTRUCTURE OF WIDTH SECTION OF ALLOY 42 LEAD FRAME (SEE TABLE V FOR ETCHANT).

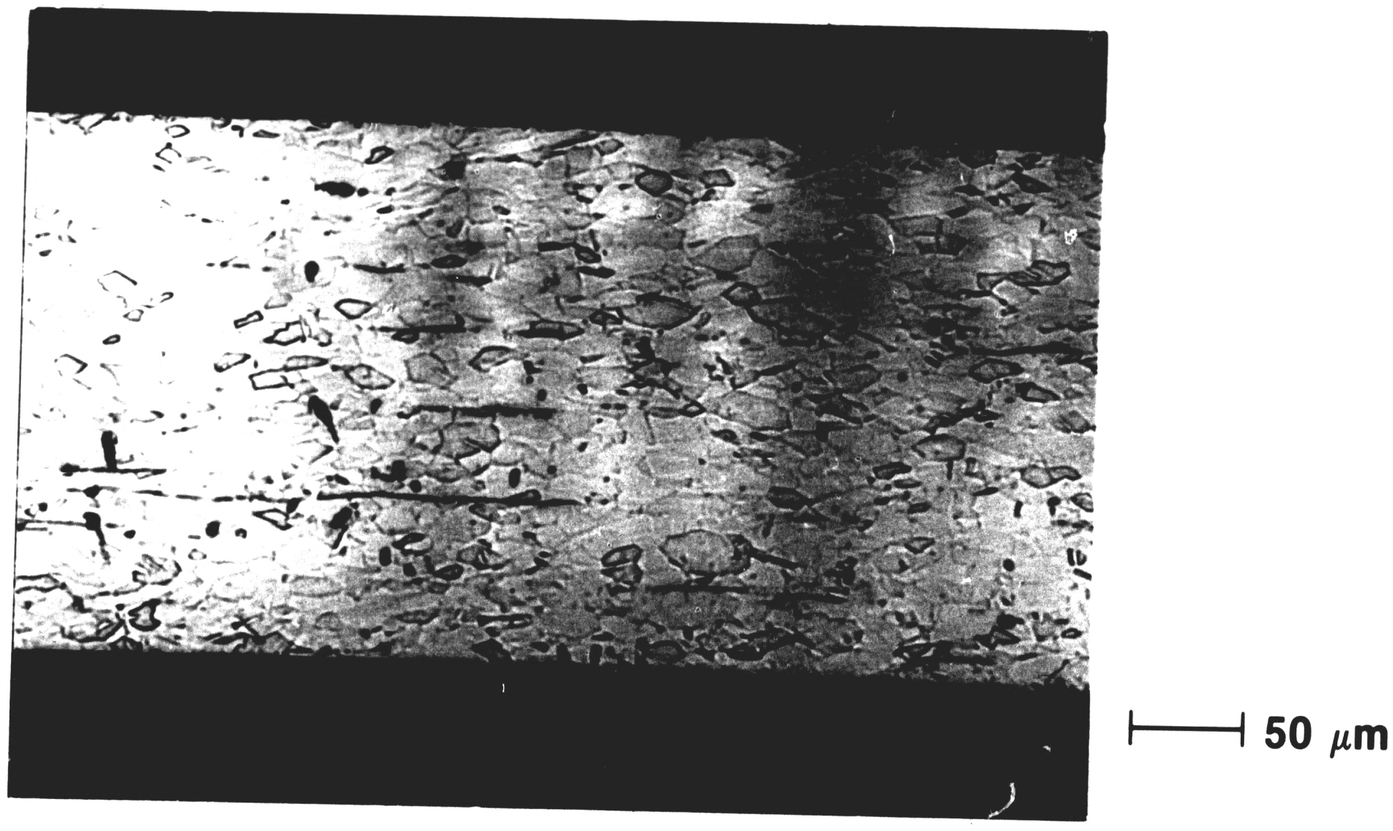

FIGURE 6: MICROSTRUCTURE OF THICKNESS SECTION OF ALLOY 42 LEAD FRAME (SEE TABLE V FOR ETCHANT).

FIGURE 7: MICROSTRUCTURE OF WIDTH SECTION OF COPPER LEAD FRAME (SEE TABLE V FOR ETCHANT).

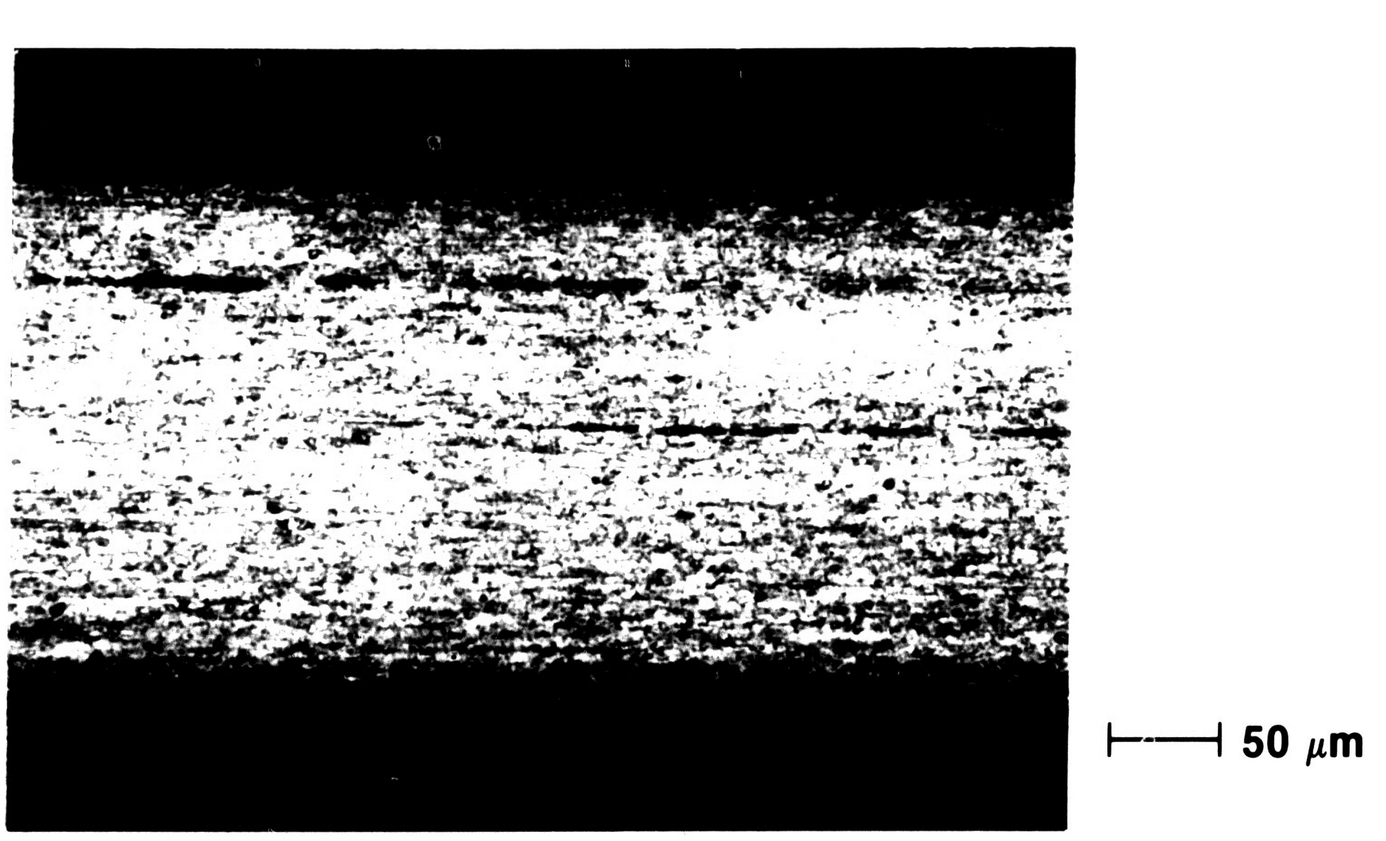

FIGURE 8: MICROSTRUCTURE OF THICKNESS SECTION OF COPPER LEAD FRAME (SEE TABLE V FOR ETCHANT).

4.3 X-Ray Macrostress Measurements

4.3.1 Data Treatment Each x-ray diffractometer scan yielded a printout of x-ray counts for 2θ values in 0.01° increments using copper radiation ($CuK_{\alpha 1}$, λ = 1.5405A). The data were subsequently plotted on an intensity versus 2θ axis with the maximum on the intensity scale corresponding to the maximum intensity for the silicon internal standard peak. The angular positions of the silicon standard peak and the (101) tin peak were determined from measurements of the half width of the peak at half the maximum intensity. The position of the experimental silicon diffraction peak was compared to the known position of the peak, 2θ = 28.46°. The difference between the experimentally determined and expected position of the silicon peak was used to correct the tin diffraction data. This correction is necessary to account for geometrical changes in the experimental set up between scans. After correction, diffraction peak shifts resulting from the presence of macrostresses in the tin plating were measured by comparison of the position of the plated tin (101) diffraction peak to that of the annealed tin. For the annealed tin, the standard position was taken to be that corresponding to 2θ = 32.30° with d = 2.769 A.

The results of this analysis for the tin plated alloy 42 and copper lead frames are presented in Tables VII and VIII, respectively. The data are given in terms of the measured positions of the silicon standard and the tin peaks together with the corrected values for each of the conditions investigated. Finally, the inferred shifts ($\Delta 2\theta_{sn}$) in the tin diffraction peaks for each condition are listed; these shifts are all negative (to the left) compared to the annealed tin standard.

Table VII : X-Ray Diffraction Data for As-Plated and Aged Tin Electroplating on Alloy 42

Condition	Measured 2θ value of Si internal standard diffraction peak, degrees	$\Delta 2\theta_{Si}$, degrees	Measured 2θ value of Sn diffraction peak, degrees	Corrected 2θ value of Sn diffraction peak, degrees	$\Delta 2\theta_{Sn}$, degrees
as-plated	28.63	-0.17	32.16	31.99	-0.31
aged at room temperature for 6244 h.	28.69	-0.23	32.28	32.05	-0.25
aged at 50°C for 6227 h.	28.78	-0.32	32.38	32.06	-0.24
aged at 75°C for 6225 h.	28.69	-0.23	32.30	32.07	-0.23
aged at 100°C for 6221 h.	28.78	-0.32	32.40	32.08	-0.22

Table VIII : X-Ray Diffraction Data for As-Plated and Aged Tin Electroplating on Copper

Condition	Measured 2θ value of Si internal standard diffraction peak, degrees	$\Delta 2\theta_{Si}$, degrees	Measured 2θ value of Sn diffraction peak, degrees	Corrected 2θ value of Sn diffraction peak, degrees	$\Delta 2\theta_{Sn}$, degrees
as-plated	28.81	-0.35	32.38	32.03	-0.27
aged at room temperature for 6203 h.	28.94	-0.48	32.53	32.05	-0.25
aged at 50°C for 6198 h.	28.91	-0.45	32.50	32.05	-0.25
aged at 75°C for 6195 h.	28.85	-0.39	32.44	32.05	-0.25
aged at 100°C for 6179 h.	28.88	-0.43	32.50	32.07	-0.23

4.3.2 Macrostress Calculations The development of macrostress in the plated layer will cause a change in the spacing of the crystal planes such that a strain, ϵ, will be obtained. It can be shown[63] [64] that the strain in the crystal planes lying parallel to the plating surface can be given by:

$$\epsilon = \frac{d_n - d_o}{d_o}$$

where d_n is spacing of the planes parallel to the surface in a stressed condition and d_o is the spacing of the same planes in the absence of stress (see for example Figure 3, in which the plane of the plated surface is vertical). The resulting stress in the material parallel to the surface is given by:[63] [64]

$$\sigma = -\frac{E}{\mu}\left(\frac{d_n - d_o}{d_o}\right)$$

where E is Young's modulus and μ is Poisson's ratio. For fine grained tin, $\mu = 0.33$ and E $= 41.6 \times 10^9$ MPa.[65] The calculated stresses in the electroplated tin parallel to the substrate material for both as-plated and aged conditions are presented in Table IX for the plated alloy 42 and in Table X for the plated copper.

The calculated macrostresses in the tin electroplate parallel to the alloy 42 substrate are all negative, meaning compressive. (Table IX). The macrostresses in the plating perpendicular to the substrate, therefore, are positive, or tensile. The change in the interplanar (101) spacing parallel to the substrate is significant in the as-plated condition as compared to the annealed tin standard. The changes in the interplanar spacing in the aged samples are not significant since they fall within the errors associated with the diffraction peak position measurements.

The results of the macrostress analysis for tin plating parallel to the copper lead frames are all negative, meaning compressive (Table X). As with the alloy 42, the macrostresses perpendicular to the substrate are therefore tensile. In the as-plated condition,

the change in the interplanar (101) spacing parallel to the copper substrate is significant when compared to the annealed tin standard. In contrast the change in the interplanar spacing values in the aged condition are not significant. As with the plated alloy 42, the macrostresses in the aged plated copper lead frames fall within the errors of the technique and therefore cannot be considered significant.

Table IX : Calculated Macrostresses for As-Plated and Aged Electroplated Tin on Alloy 42.

Condition	d_n, A	ϵ	σ, MPa
as-plated	2.795	0.009	-11.3×10^2
aged at room temperature for 6244 h.	2.790	0.007	-8.82×10^1
aged at 50°C for 6227 h.	2.789	0.006	-7.56×10^1
aged at 75°C for 6225 h.	2.788	0.006	-7.56×10^1
aged at 100°C for 6221 h.	2.788	0.006	-7.56×10^1

Table X : Calculated Macrostresses for As-Plated and Aged Electroplated Tin on Copper

Condition	d_n, A	ϵ	σ, MPa
as-plated	2.792	0.008	-10.1×10^2
aged at room temperature for 6203 h.	2.790	0.007	-8.82×10^2
aged at 50°C for 6198 h.	2.790	0.007	-8.82×10^1
aged at 75°C for 6195 h.	2.790	0.007	-8.82×10^1
aged at 100°C for 6179 h.	2.788	0.006	-7.56×10^1

4.4 Surface Morphology Characterization

Morphological changes in the tin plating were examined using scanning electron microscopy (SEM) techniques. In general, two types of growths were encountered which in the present work are referred to as hillocks and whiskers. Hillock type growths displayed a rounded morphological nature while whisker type growths displayed a general cylindrical configuration with distinct striations along the length of the whisker.

4.4.1 Commercial Devices A preliminary SEM examination of the tin plated leads of commercial devices from all three manufacturers was conducted prior to aging. The general appearance of the leads was similar for Motorola and Fairchild devices. The leads of these devices exhibited large areas of scratches in the base region which did not continue onto the slender tip, as shown in Figures 9 and 10. Although the general low magnification appearance of the Motorola and Fairchild tin plated leads was similar, at higher magnifications differences in the surface morphologies were evident. The plating surface of the Motorola device leads consisted of a fine ($\approx$ 1 micron) raised grain-like structure (Figure 11). In contrast, the surface morphology of the Fairchild device leads consisted of a larger ($\approx$ 2 to 8 microns) faceted grain structure (Figure 12). Examinations of Motorola and Fairchild device leads in both the as-received and aged conditions revealed the presence of whiskers. The composition of the observed whisker growths was confirmed to be tin using energy dispersive (EDS) analysis. Figure 13 shows a tin whisker on a tin plated lead of an as-received Motorola device. Figures 14 to 17 present whiskers observed on the tin plated leads of aged Fairchild devices. In general, more whisker growths were observed on Fairchild device leads as opposed to Motorola device leads.

In contrast to the general appearance of Motorola and Fairchild device leads, the tin plated leads of Texas Instruments devices appeared relatively smooth (Figure 18) with small pores in the as-received condition without the grain-like features observed for the

Motorola and Fairchild device leads (Figure 19). Growths on the tin plating surface were evident in both the as-received and aged condition. EDS analyses revealed them to be composed of tin. Figures 20 and 21 show hillock type growths on the leads of as-received Texas Instruments devices. A whisker type growth on the lead of an aged Texas Instruments device is presented in Figure 22. As compared to both the Motorola and Fairchild devices, fewer growths were observed on the leads of Texas Instruments devices.

Table XI presents a summary of the results for the commercial devices with the approximate whisker density defined as the average number whiskers on the lead surface. In addition, it is important to note that the Texas Instruments and Motorola devices were stored at room temperature for approximately two years prior to use for this study.

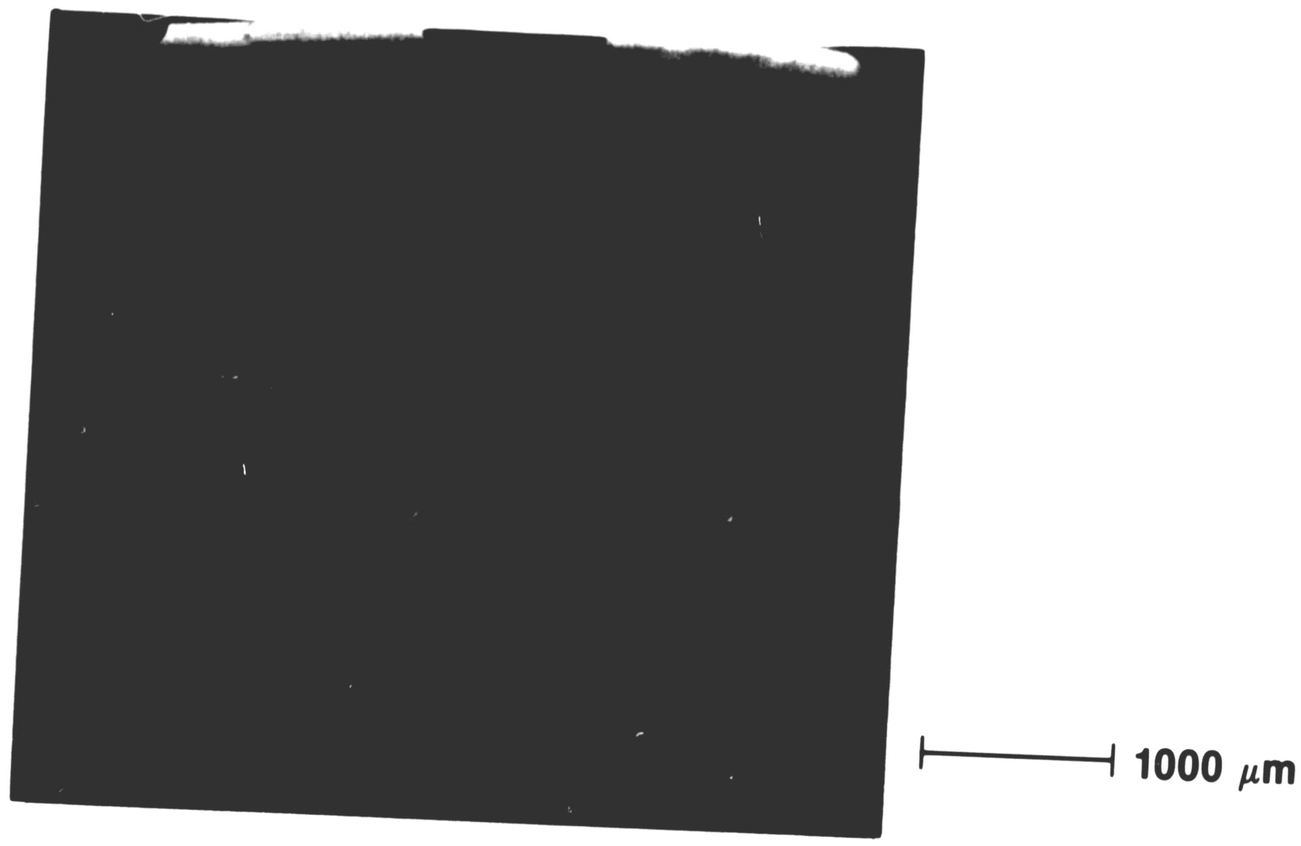

FIGURE 9: SEM MICROGRAPH OF TIN PLATED LEADS OF AS-RECEIVED MOTOROLA DEVICE.

FIGURE 10: SEM MICROGRAPH OF TIN PLATED LEADS OF AS-RECEIVED FAIRCHILD DEVICE.

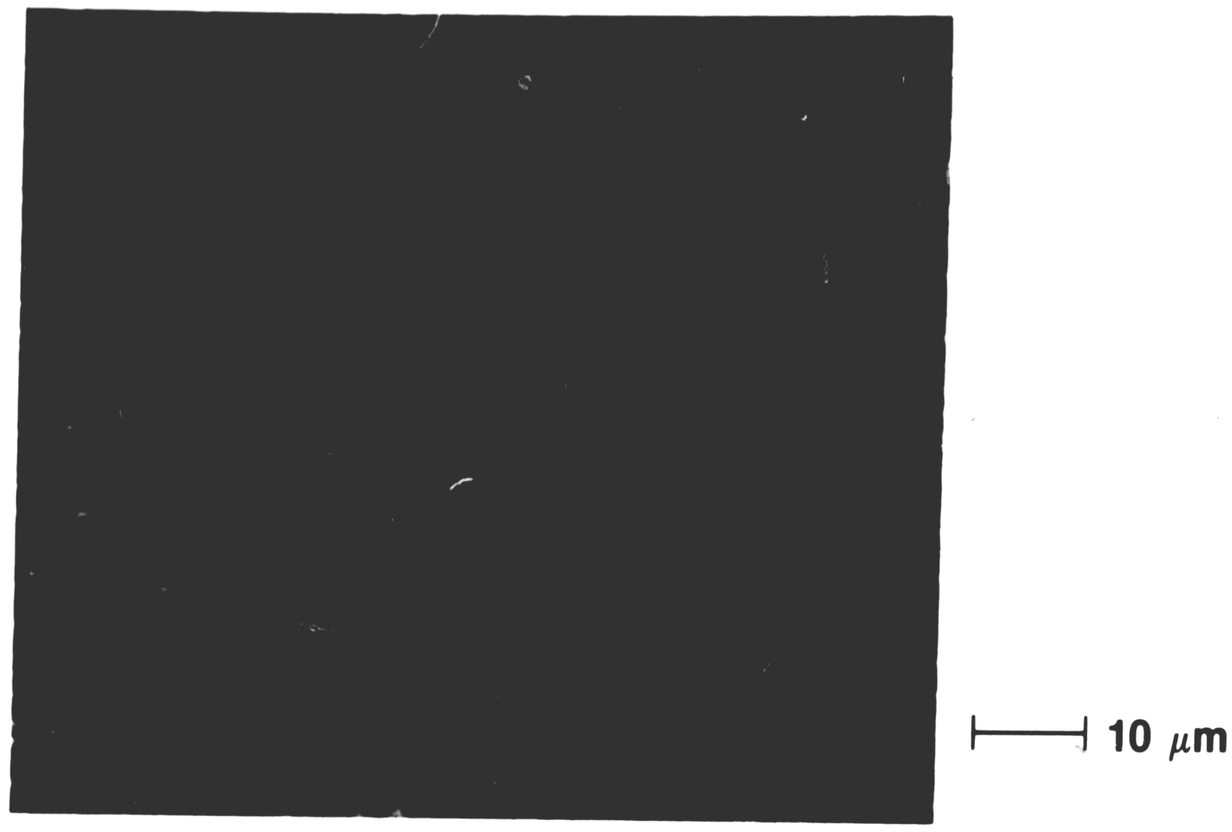

FIGURE 11: SEM MICROGRAPH OF PLATED SURFACE OF AS-RECEIVED MOTOROLA DEVICE.

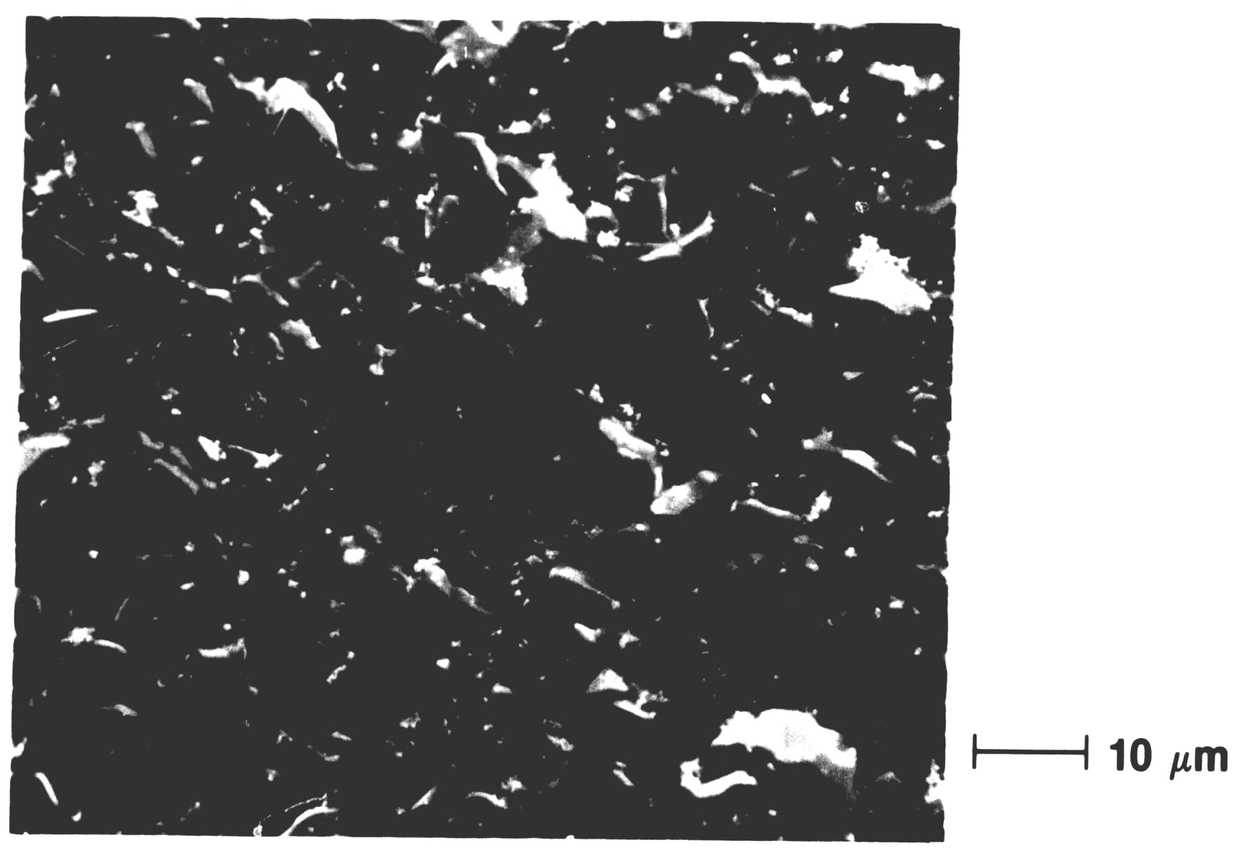

FIGURE 12: SEM MICROGRAPH OF PLATED SURFACE OF AS-RECEIVED FAIRCHILD DEVICE.

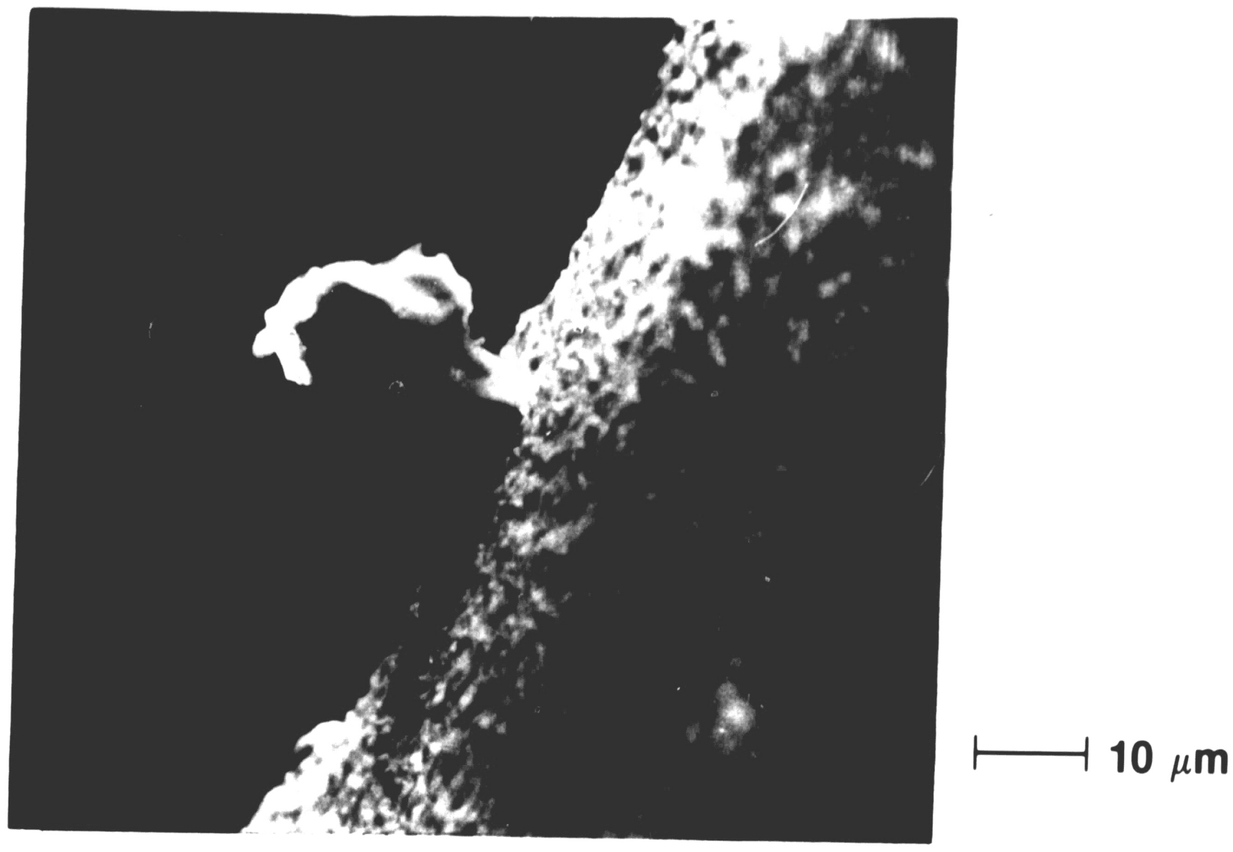

FIGURE 13: SEM MICROGRAPH OF TIN WHISKER ON LEAD OF AS-RECEIVED MOTOROLA DEVICE.

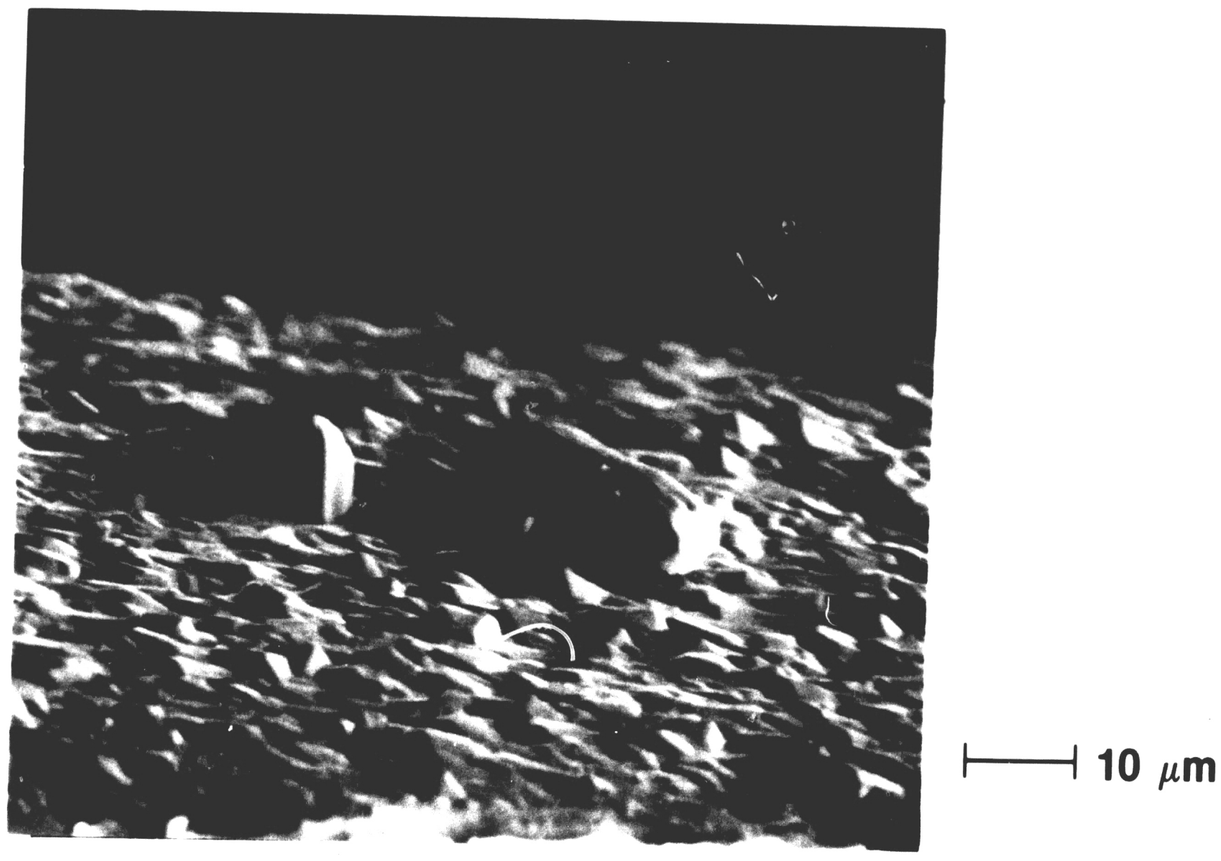

FIGURE 14: SEM MICROGRAPH OF TIN WHISKERS ON LEAD OF AGED (25°C, 7000 h.) FAIRCHILD DEVICE.

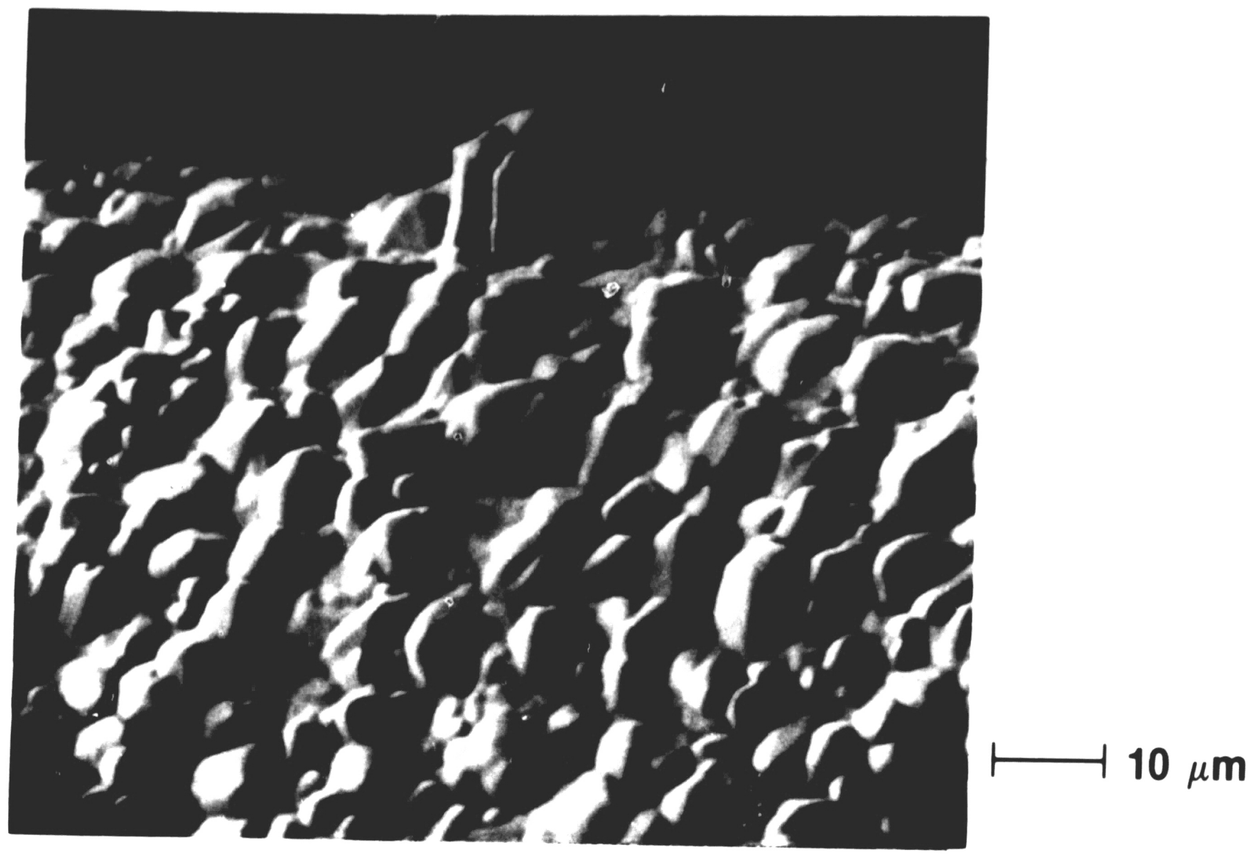

FIGURE 15: SEM MICROGRAPH OF TIN WHISKER ON LEAD OF AGED (50°C, 7000 h.) FAIRCHILD DEVICE.

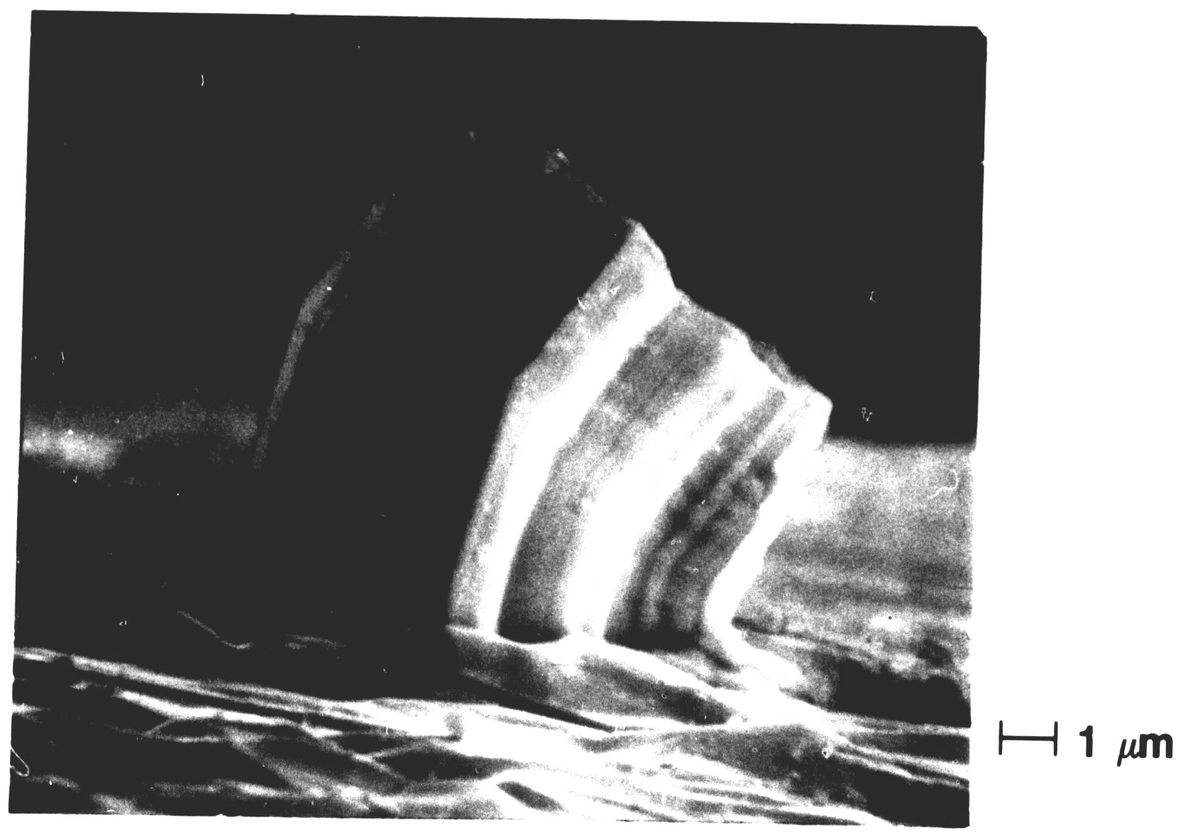

FIGURE 16: SEM MICROGRAPH OF TIN WHISKER ON LEAD OF AGED (75°C, 7000 h.) FAIRCHILD DEVICE.

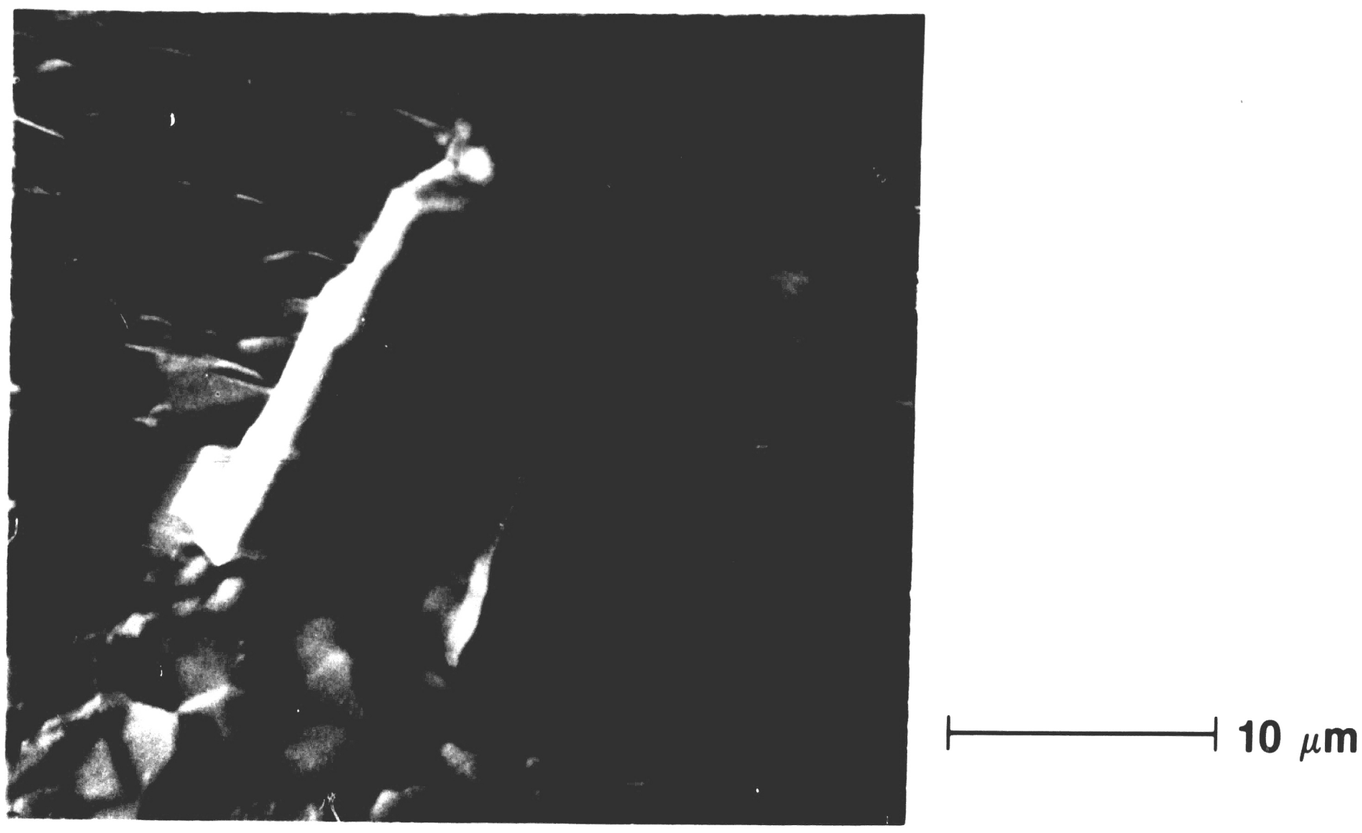

FIGURE 17: SEM MICROGRAPH OF TIN WHISKER ON LEAD OF AGED (100°C, 7000 h.) FAIRCHILD DEVICE.

FIGURE 18: SEM MICROGRAPH OF TIN PLATED LEADS OF AS-RECEIVED TEXAS INSTRUMENTS DEVICE.

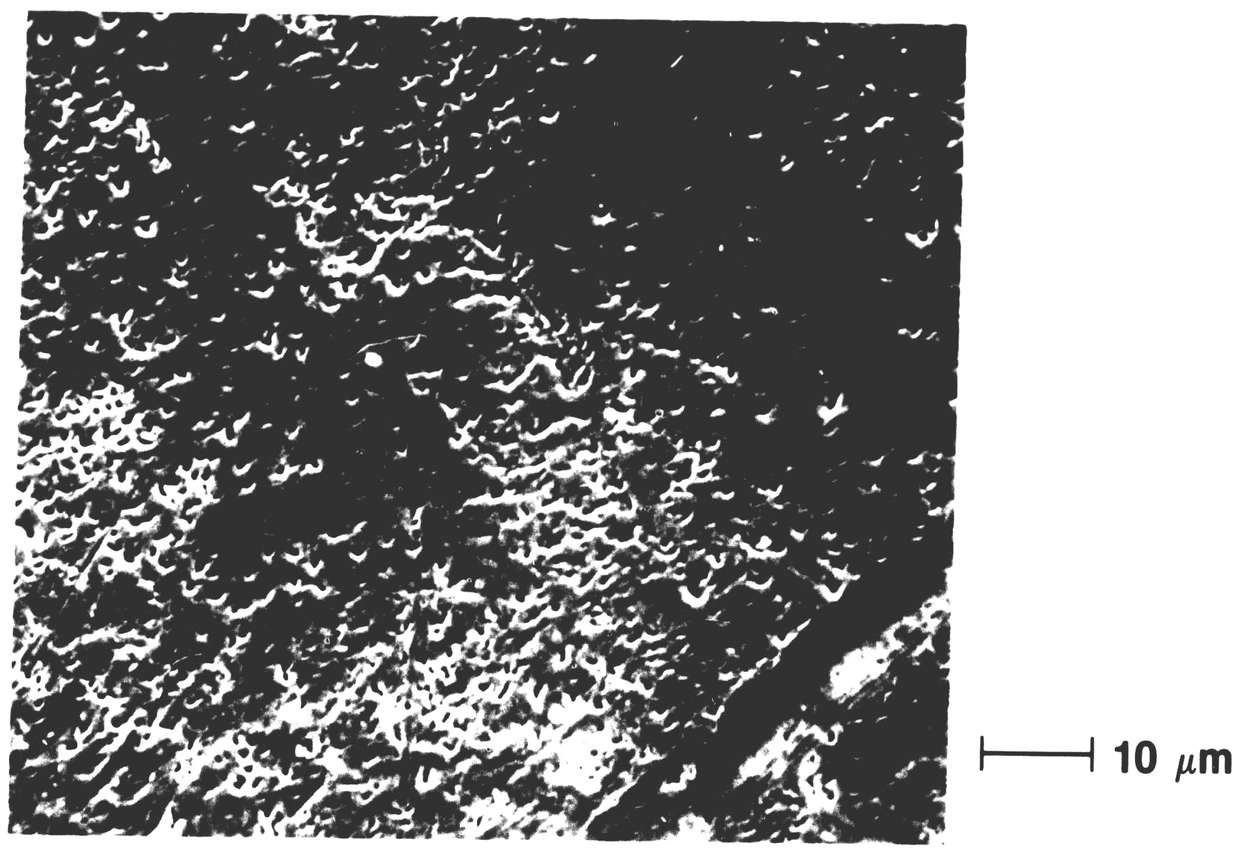

FIGURE 19: SEM MICROGRAPH OF PLATED SURFACE OF AS-RECEIVED TEXAS INSTRUMENTS DEVICE.

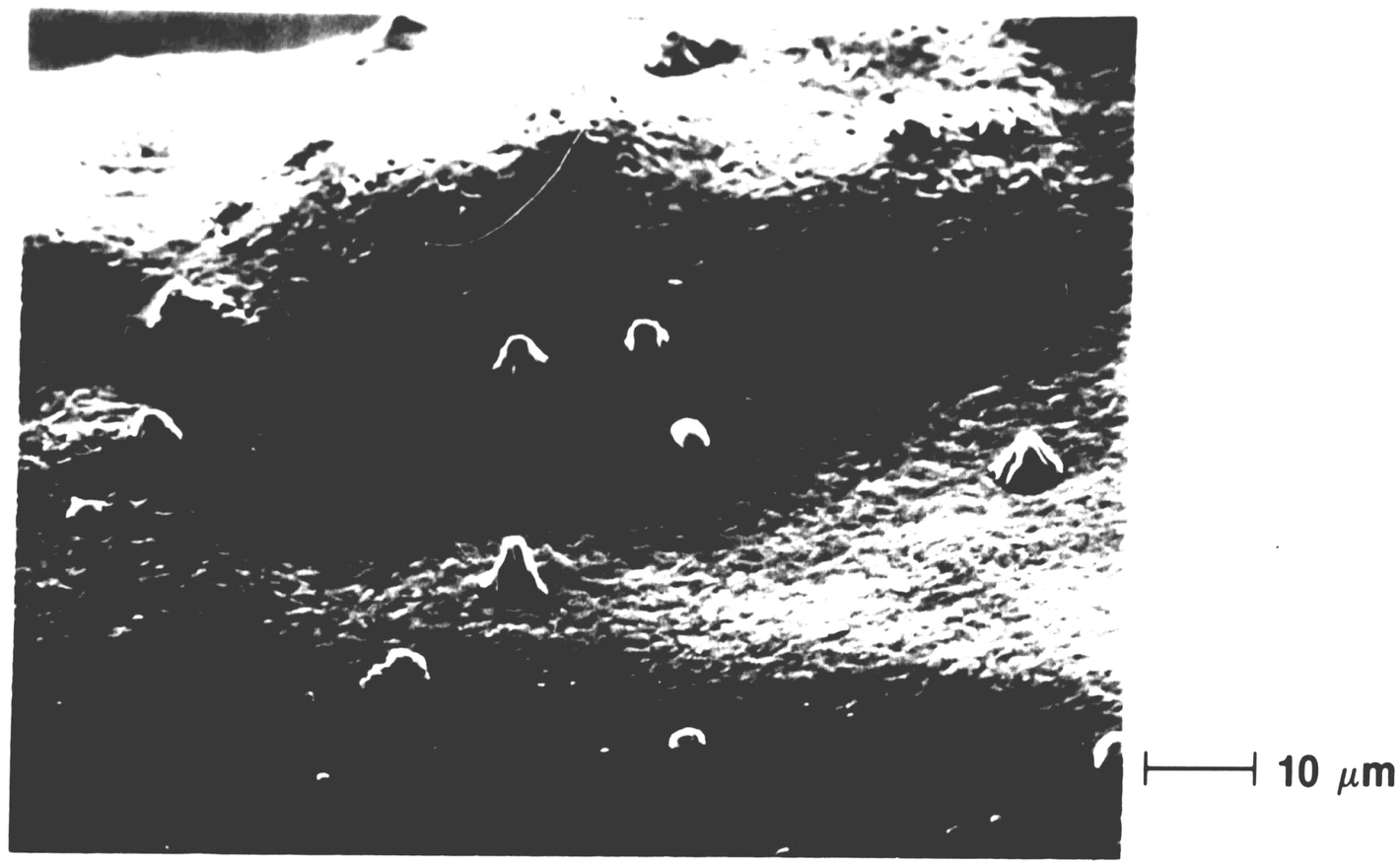

FIGURE 20: SEM MICROGRAPH OF TIN HILLOCKS ON LEAD OF AS-RECEIVED TEXAS INSTRUMENTS DEVICE.

FIGURE 21: SEM MICROGRAPH OF TIN HILLOCKS ON LEAD OF AS-RECEIVED TEXAS INSTRUMENTS DEVICE.

FIGURE 22: SEM MICROGRAPH OF WHISKER TYPE GROWTH ON LEAD OF AGED (100°C, 7000 h.) TEXAS INSTRUMENTS DEVICE.

Table XI : Whisker Data for Commercial Devices

Manufacturer	Approximate whisker density, whiskers/mm^2	Average whisker diameter, μm	Average whisker length, μm
Motorola			
as-received	1/10	10	20
25°C, 7000 h.	1/10	10	20
50°C, 7000 h.	1/10	10	20
75°C, 7000 h.	1/10	10	20
100°C, 7000 h.	1/4	10	20
Fairchild			
as-received	4/10	6	10
25°C, 7000 h.	4/10	6	14
50°C, 7000 h.	4/10	6	14
75°C, 7000 h.	4/10	8	9
100°C, 7000 h.	4/10	9	16
Texas Instruments			
as-received	1/1*	3*	4*
25°C, 7000 h.	1/40	5	6
50°C, 7000 h.	1/40	5	6
75°C, 7000 h.	1/40	5	6
100°C, 7000 h.	1/20	5	6

*hillocks

4.4.2 Laboratory Plated Lead Frames The as-plated lead frames were examined in the SEM to characterize the plating surface prior to aging. Figure 23 shows the as-plated surface of an alloy 42 lead frame; the surface is smooth and featureless with the exception of a few small pores. Aging at room temperature (25°C), 50°C and 75°C for approximately 7000 hours resulted in a change from the as-plated surface morphology. Small (≈ 0.5 micron) bumps are visible on the tin plating (Figure 24) for all three aging temperatures. After aging at 100°C for approximately 7000 hours, hillock type growths were observed on the plated surface (Figure 25); EDS analysis confirmed these growths to be tin. No whiskers were observed on laboratory tin plated alloy 42 lead frames in the period of this study (7000 hr.).

The as-plated morphology of the tin plated copper lead frames did not differ significantly from the as-plated surface of the alloy 42 lead frames; the surface is smooth with small pores (Figure 26). After aging at 50°C for approximately 300 hours, no observable changes in the tin plated surface were noted (Figure 27). In contrast, the plated surface displays hillock type growths after aging at 100°C for approximately 300 hours (Figure 28). These growths were found to be tin by means of EDS analysis.

After aging for approximately 7000 hours at the various temperatures, changes in the tin plated surface morphology were evident. The surfaces of the tin plated copper lead frames appeared similar after aging at room temperature (25°C), 50°C and 75°C (Figure 29). Approximately 0.5 micron diameter bumps are visible on the plated surface, much like the plated alloy 42 lead frames aged under the same conditions (Figure 24). In addition, a few small whisker-like growths, which were found to be tin using EDS analysis, were observed on the plating surface after aging at 50°C for approximately 7000 hours (Figure 30). In contrast, numerous whiskers were present after aging the tin plated copper lead frames at 75°C for 7000 hours. An example of a whisker is presented in Figure 31 and as before, was confirmed to be tin by EDS analysis. After aging at 100°C for approximately 7000 hours a

marked change in the plating surface morphology was noted. Numerous hillocks and whiskers as well as small regions of buckling were evident (Figure 32). Whiskers were also observed on the surface such as the one shown in Figure 33. EDS analysis confirmed these growths to be tin.

In summary, tin whisker growths were observed on the plated copper lead frames after aging at 50°C, 75°C and 100°C. The growths on the lead frames aged at 50°C for approximately 7000 hours were small and very few in number. After aging at 75°C for the same time, the whiskers were more numerous as well as larger. After aging at 100°C for approximately 300 hours, small hillocks were observed, and after 7000 hours at 100°C many whisker growths were present. The whiskers observed after aging at 100°C for approximately 7000 hours, however, were shorter than those observed after aging at 75°C for the same time. Table XII presents a summary of the results for the laboratory plated lead frames with the approximate whisker density calculated from the entire lead frame surface. The maximum observed whisker length was 60 microns.

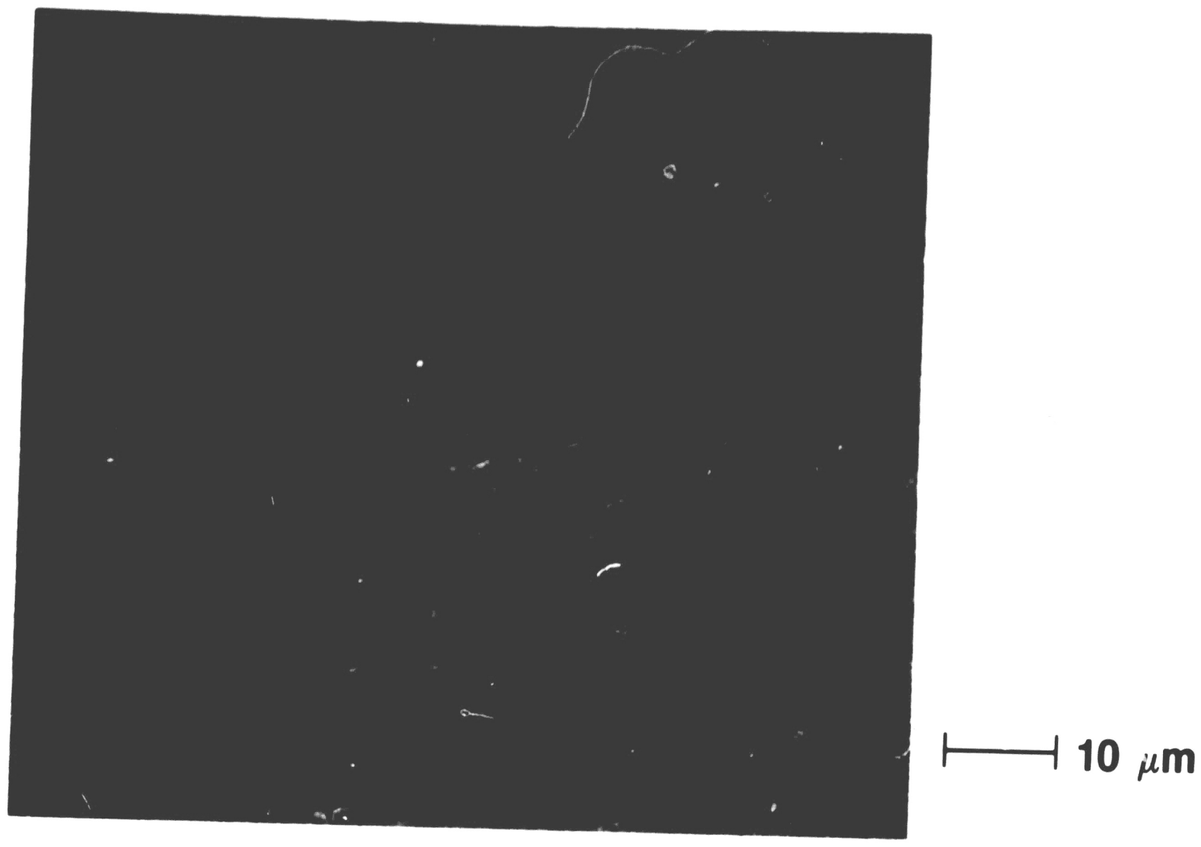

FIGURE 23: SEM MICROGRAPH OF AS-PLATED SURFACE OF ALLOY 42 LEAD FRAME.

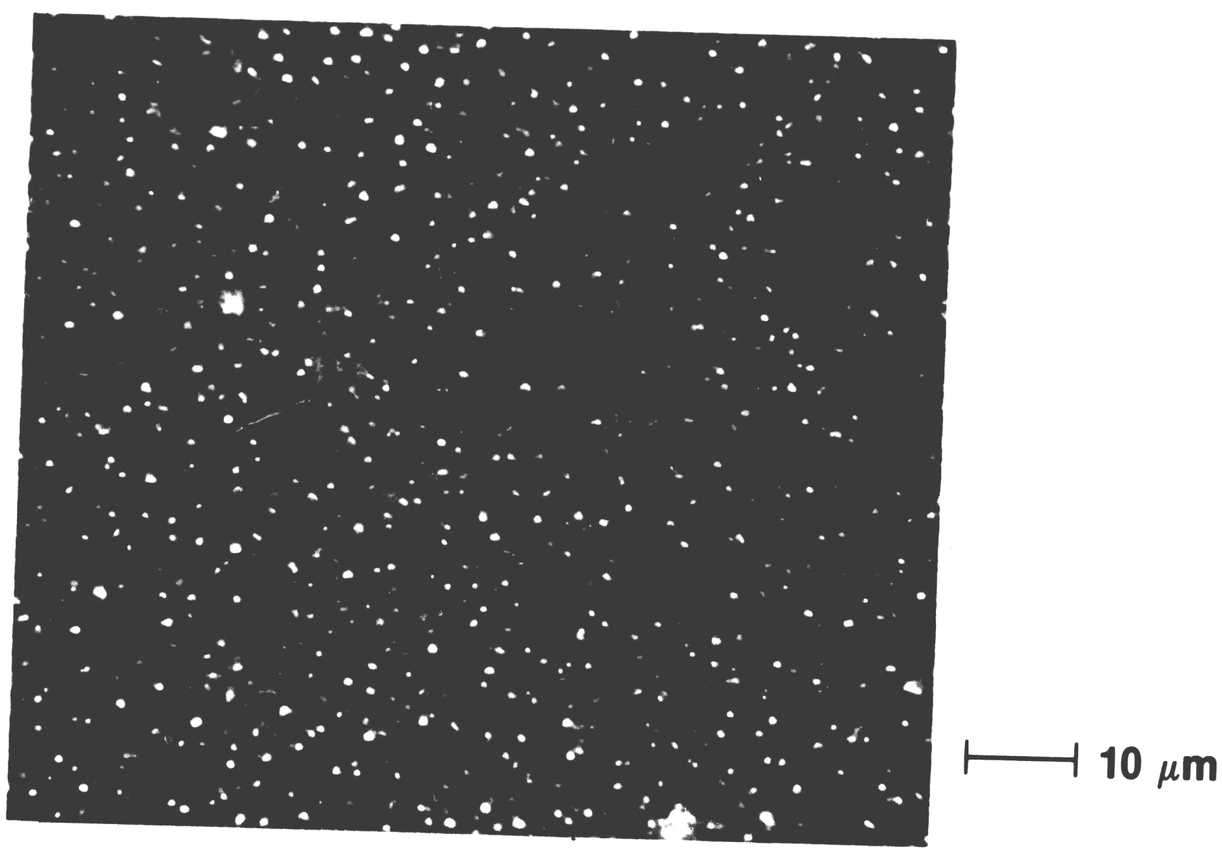

FIGURE 24: SEM MICROGRAPH OF AGED (25°C, 7000 h.) PLATED SURFACE ON ALLOY 42 LEAD FRAME.

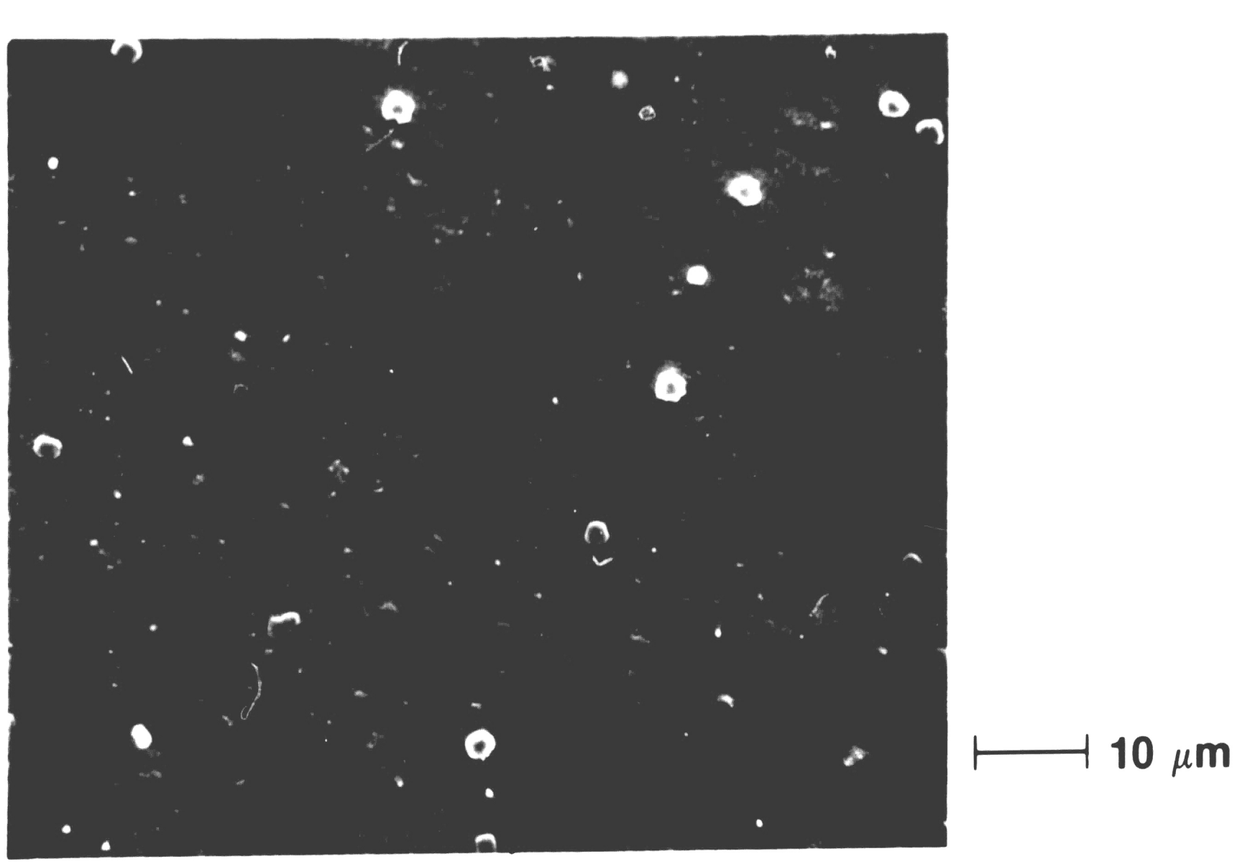

FIGURE 25: SEM MICROGRAPH OF TIN HILLOCK TYPE GROWTHS ON AGED (100°C, 7000 h.) PLATED SURFACE ON ALLOY 42.

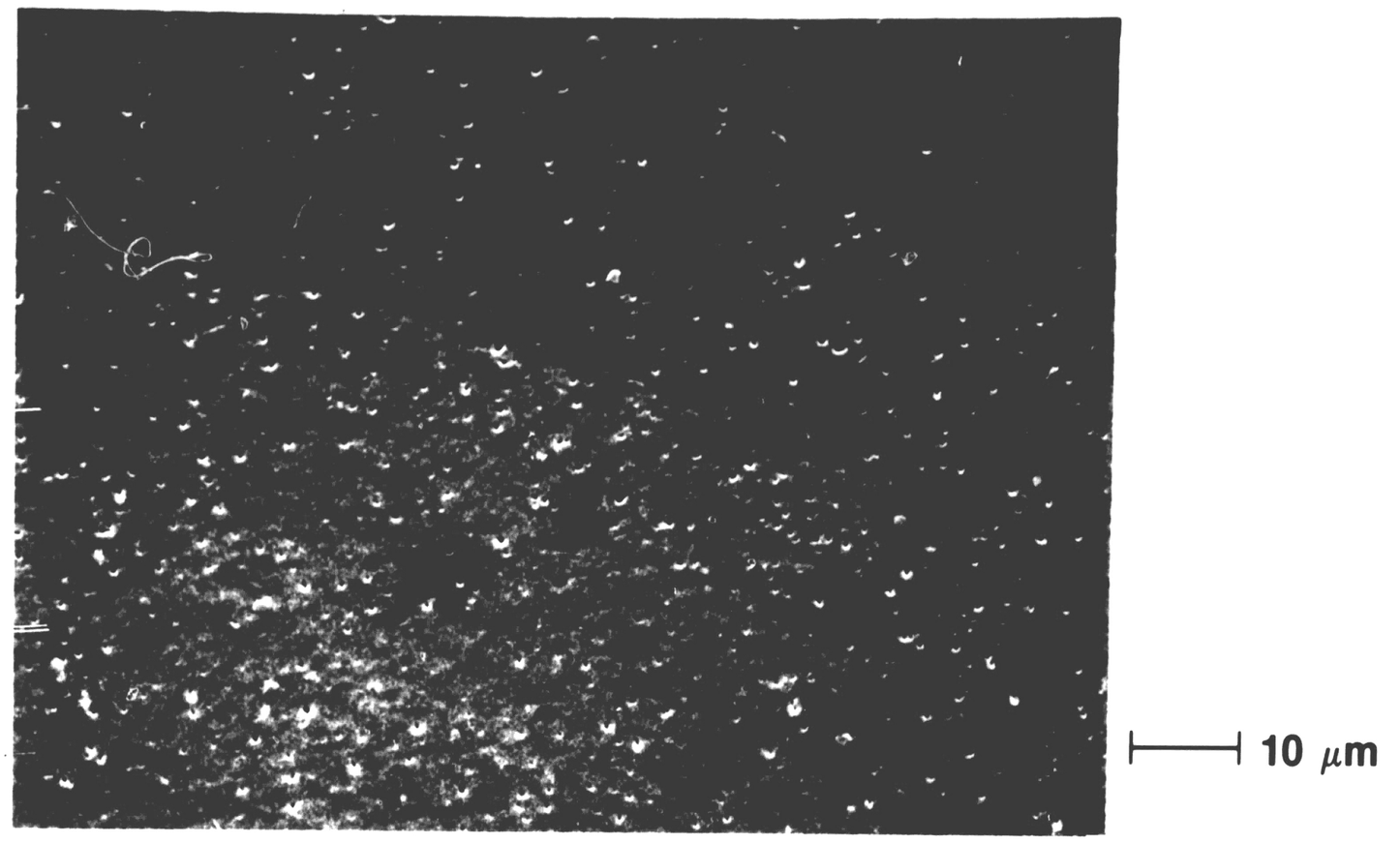

FIGURE 26: SEM MICROGRAPH OF AS-PLATED SURFACE OF COPPER LEAD FRAME.

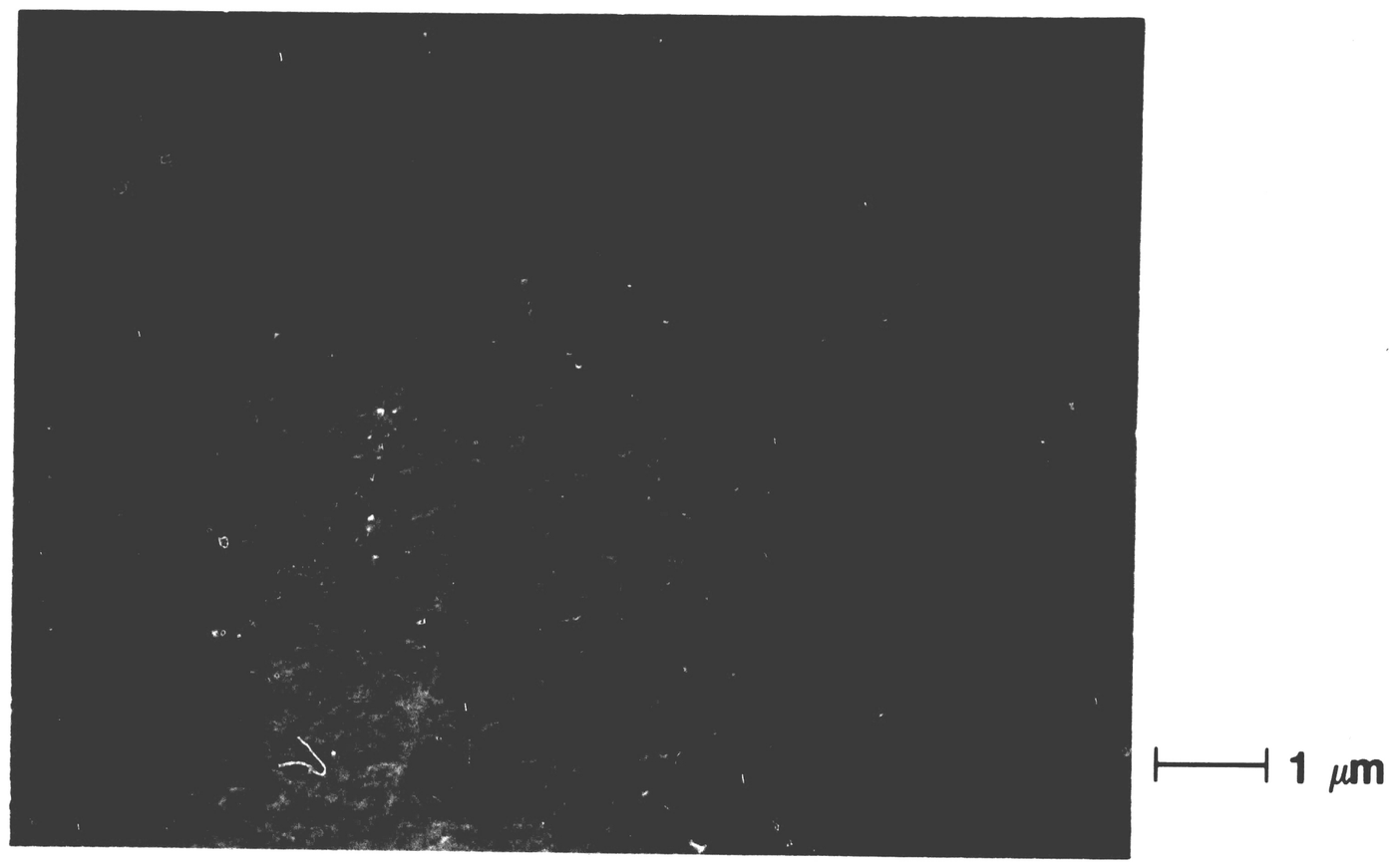

FIGURE 27: SEM MICROGRAPH OF AGED (50°C, 300 h.) PLATED SURFACE ON COPPER.

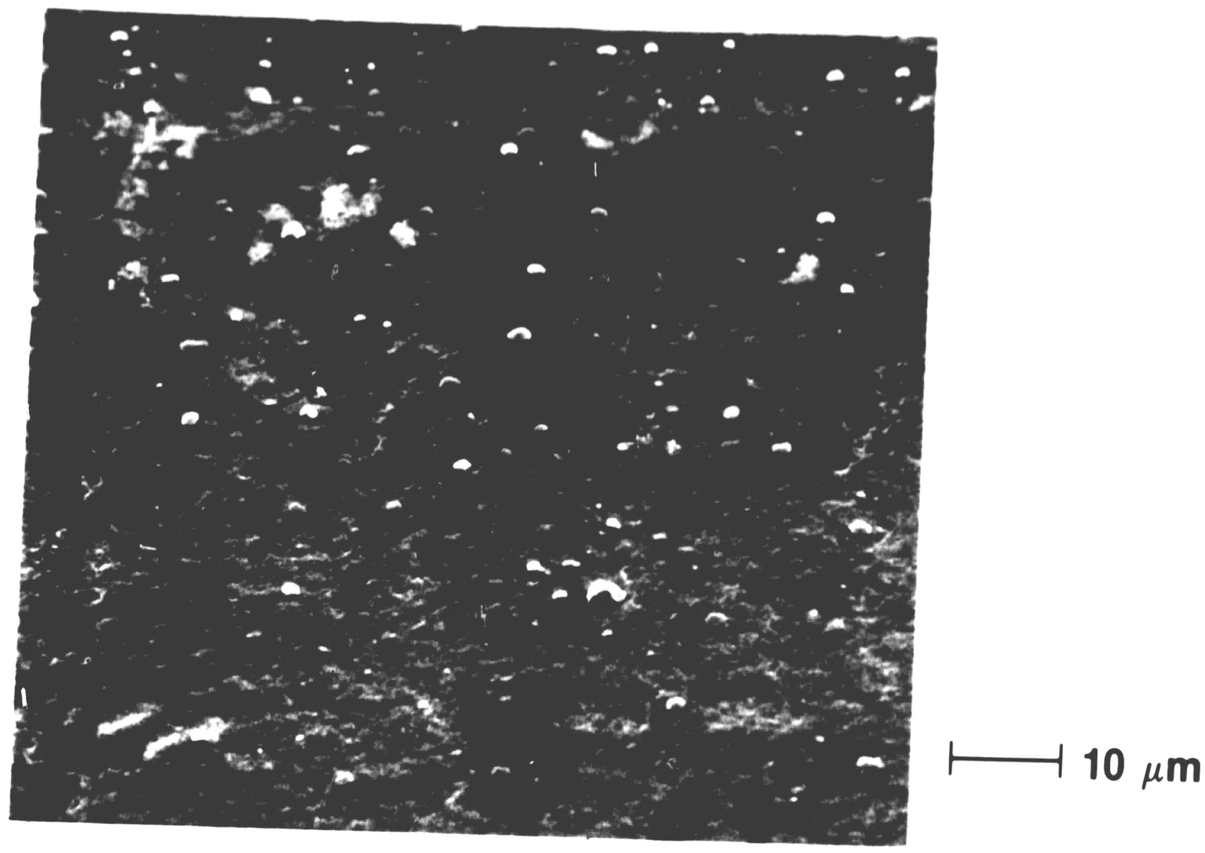

FIGURE 28: SEM MICROGRAPH OF TIN HILLOCK TYPE GROWTHS ON AGED (100°C, 300 h.) PLATED SURFACE ON COPPER.

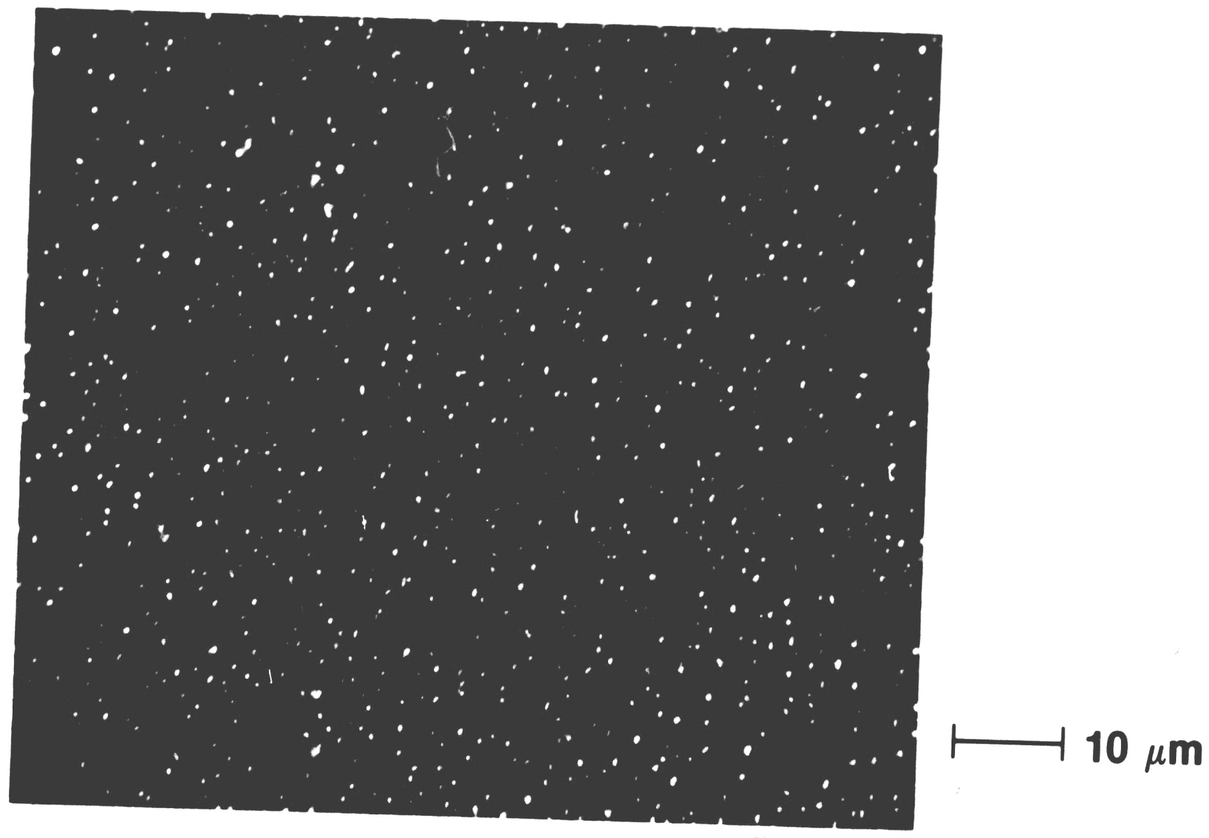

FIGURE 29: SEM MICROGRAPH OF AGED (25°C, 7000 h.) PLATED SURFACE ON COPPER.

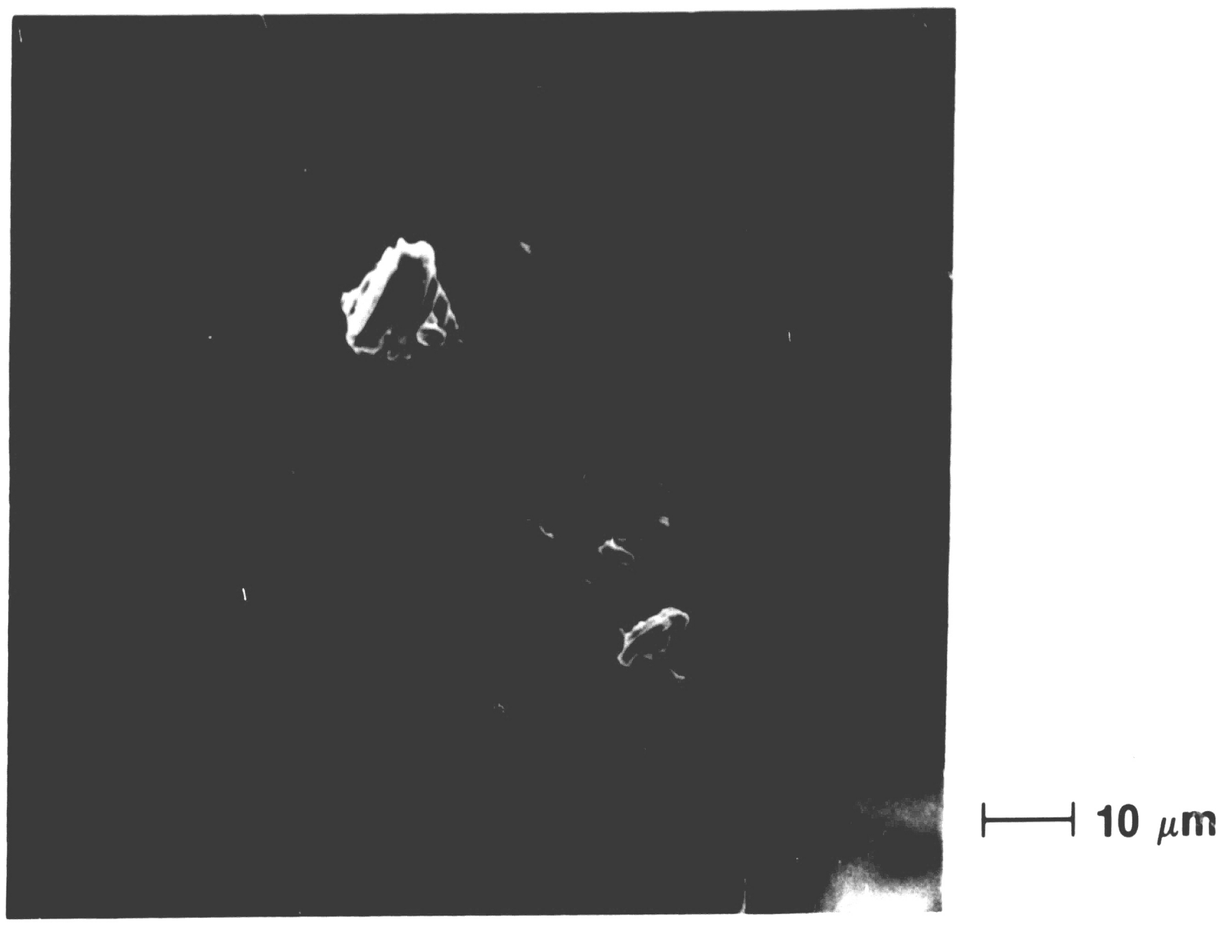

FIGURE 30: SEM MICROGRAPH OF TIN WHISKER TYPE GROWTHS ON AGED (50°C, 7000 h.) PLATED SURFACE ON COPPER.

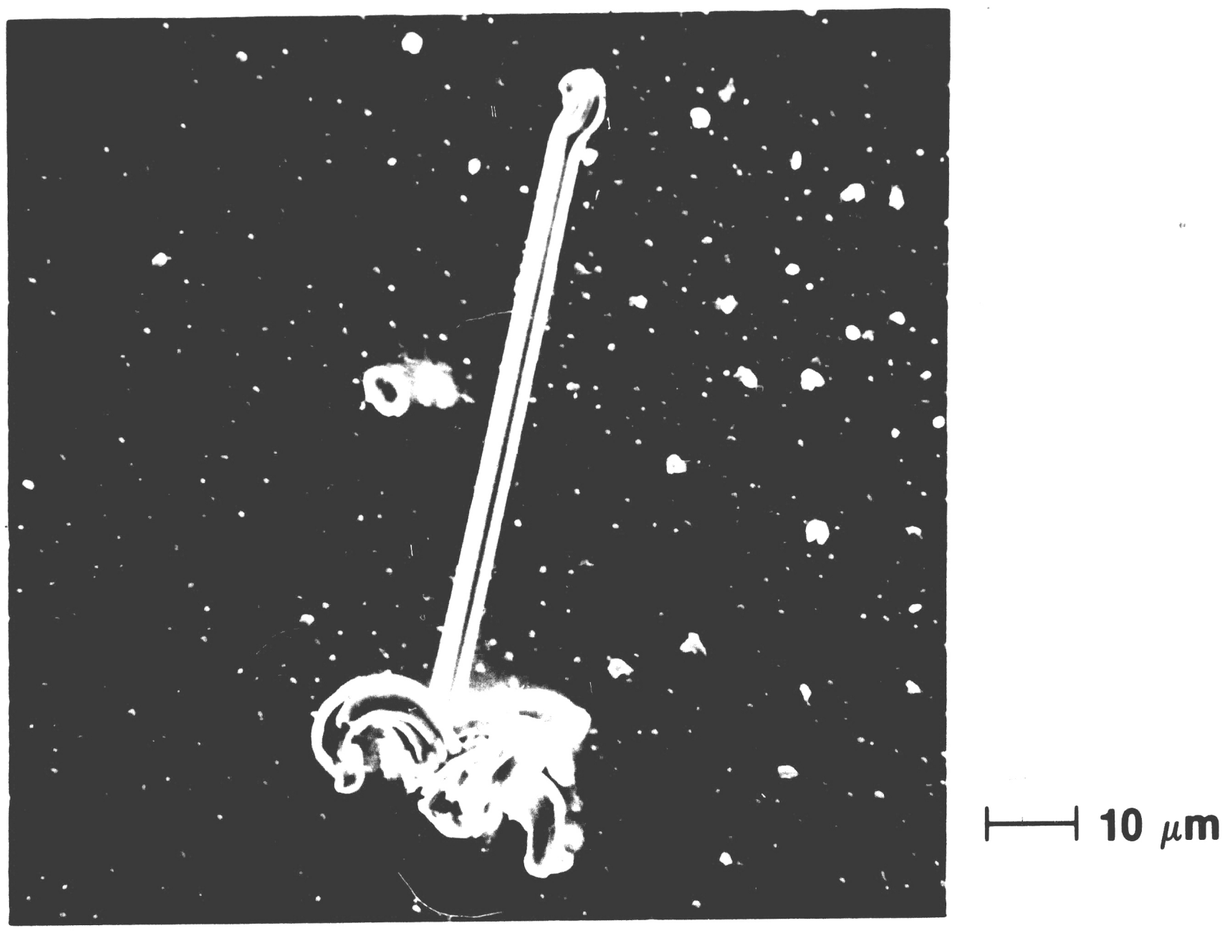

FIGURE 31: SEM MICROGRAPH OF TIN WHISKER ON AGED (75°C, 7000 h.) PLATED SURFACE ON COPPER.

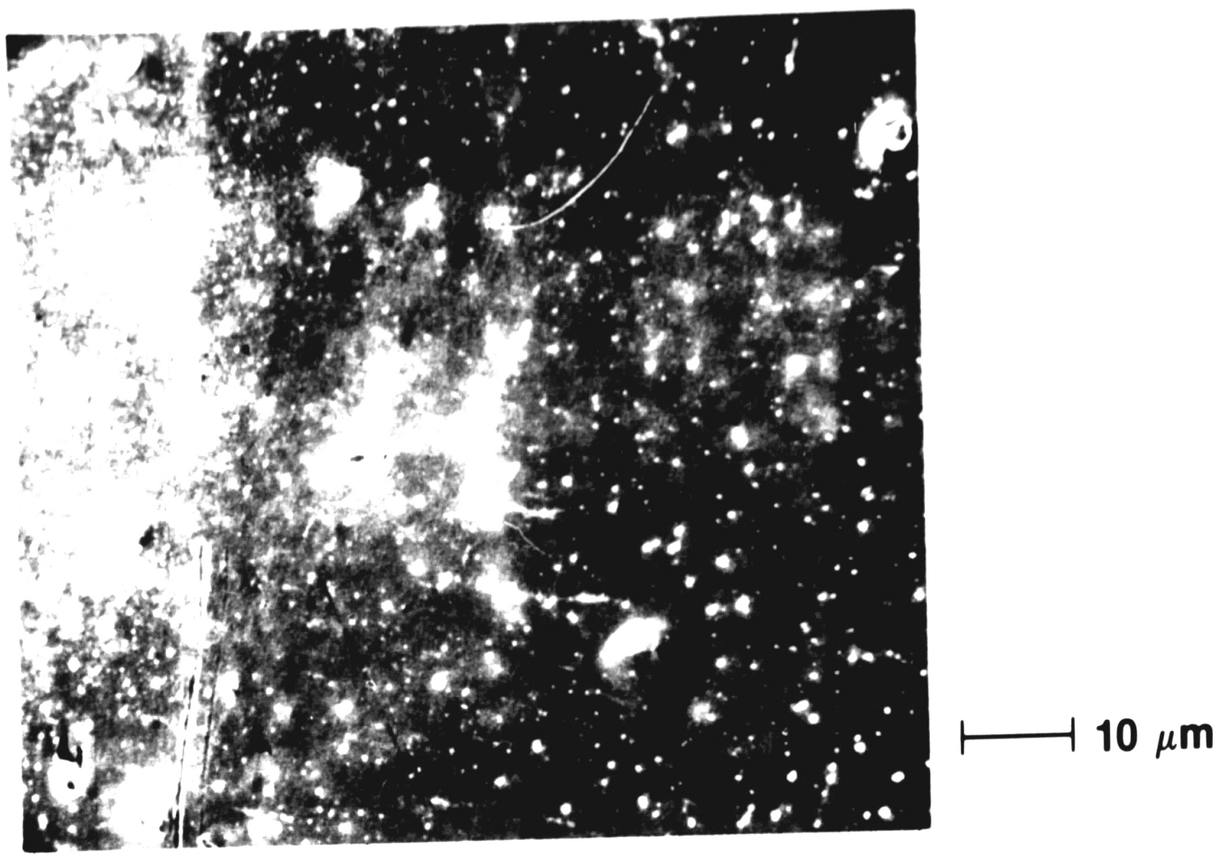

FIGURE 32: SEM MICROGRAPH OF AGED (100°C, 7000 h.) PLATED SURFACE ON COPPER.

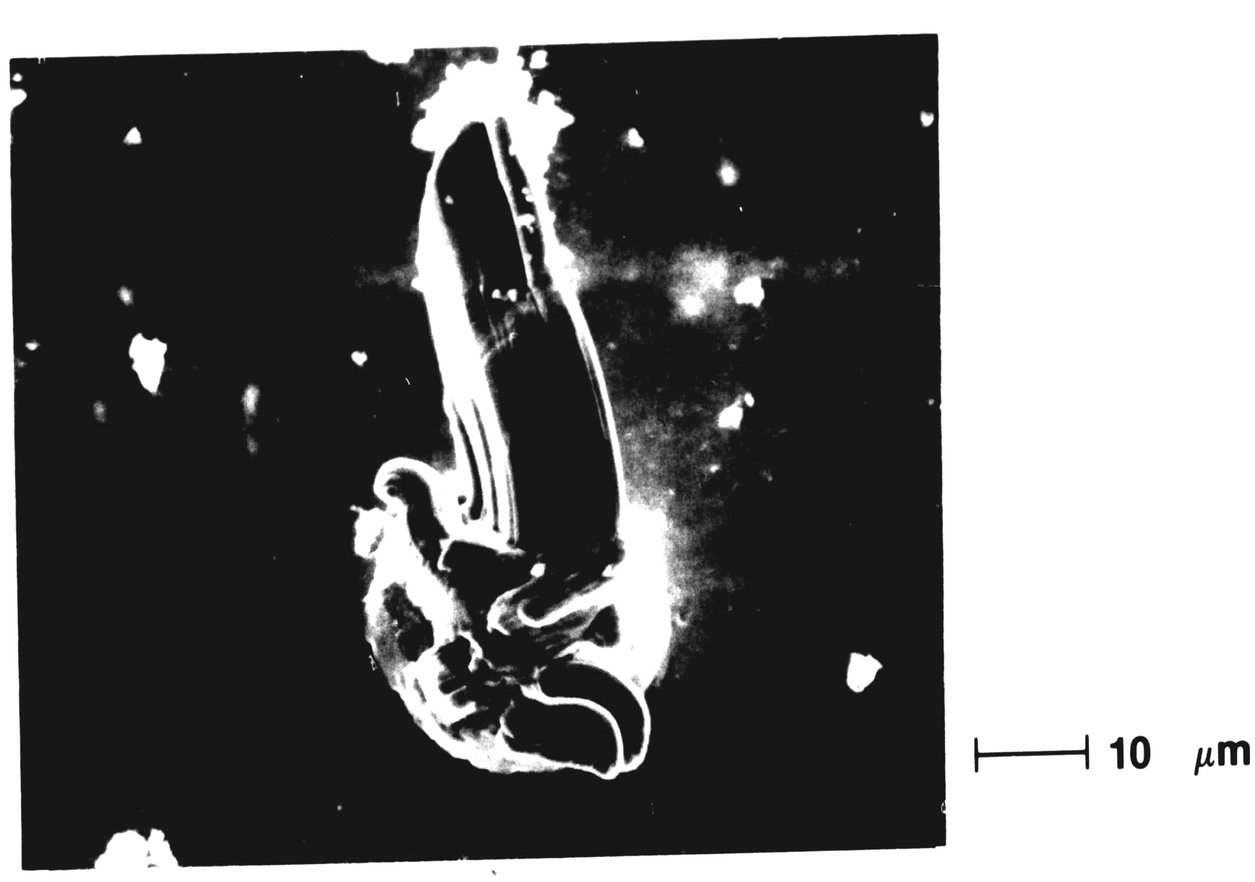

FIGURE 33: SEM MICROGRAPH OF TIN WHISKER ON AGED (100°C, 7000 h.) PLATED SURFACE ON COPPER.

Table XII : Whisker Data for Laboratory Plated Lead Frames

Lead Frame Material	Approximate whisker density, whiskers/μm^2	Average whisker diameter, μm	Average whisker length, μm
alloy 42			
as-plated	0	-	-
25°C, 7000 h.	0	-	-
50°C, 7000 h.	0	-	-
75°C, 7000 h.	0	-	-
100°C, 7000 h.	1/250*	3*	1*
copper			
as-plated	0	-	-
50°C, 300h.	0	-	-
100°C, 300 h.	1/91*	2.5*	2*
25°C, 7000 h.	0	-	-
50°C, 7000 h.	1/9000	2	4
75°C, 7000 h.	1/180**	6***	51***
100°C, 7000 h.	1/90**	8***	23***

* hillocks
** hillocks & whiskers
*** whiskers

5. DISCUSSION

The discussion of the results for this investigation of tin whisker growth on both commercial devices and laboratory tin plated lead frames will be considered in two sections. First, a short evaluation of the observations for the commercial devices will be presented. Next, a discussion of tin whisker growth from the laboratory plated lead frames will be presented in terms of observed whisker morphologies and substrate, temperature and macrostress effects.

5.1 Commercial Devices

The tin coated leads of devices from all three manufacturers exhibited nodular, whisker or both nodular and whisker growths in the as-received and aged conditions. Recalling that the Motorola and Texas Instruments devices were two years old at the time of acquisition for this study, and due to problems encountered during scanning electron microscopy examination of intact devices resulting from specimen geometry, it is difficult to unequivocally define trends concerning tin whisker growth and aging for commercially manufactured devices.

Closer examination reveals that Fairchild device leads displayed the highest whisker density followed by Motorola device leads. The leads of Texas Instruments devices exhibited the lowest density of whisker growths. A partial explanation for the differences in whisker densities may lie in the substrate material for the device leads. Substrate metal is known to affect tin whisker formation;[8] [55] [60] copper substrates initiate whisker growth more readily than steel, iron and nickel. The lead material of the Fairchild and Motorola devices is copper, whereas that of the Texas Instruments devices is an iron nickel alloy. Based on the observed whisker densities for the commercial devices as related to base material, it appears that copper substrates promote whisker growth from electroplated tin.

Variations in whisker growth resulting from base material will be discussed with the laboratory lead frames.

In addition to the difference in whisker density between the Motorola and Fairchild devices and the Texas Instruments devices, a marked difference in the morphology of the observed growths between those of the Motorola and Fairchild devices and those of the Texas Instruments devices is evident (compare Figures 34 and 35).

As stated previously, the tin plated surface of the Motorola and Fairchild device leads consists of rough grain-like particles (Figures 11 and 12). For both manufacturers, characteristic surface striations [31] extend from the base to the tip of the whiskers (Figure 13 to 17). In addition, the plating appears continuous to the base of the whiskers with no depressions visible. This lack of depressions around the whisker base implies long range tin atom transport provided the source of material for the whisker. It is interesting to note that the diameter of the whiskers observed on the Fairchild device leads are approximately the same as the diameter of the faceted grains present on the surface (Figures 14 to 17 and Figure 35). In fact, the whiskers generally appear to be three dimensional extensions of grains as seen in Figure 35. This observation correlates well with the recrystallization and grain growth theory of Ellis, Gibbons and Treuting [30] in which whisker growth occurs by the extension of the free surface of a portion of a grain or of an entire grain. In the case of the Motorola device, the whisker diameter is typically larger than the grain-like particles observed on the plating surface (Figure 13). It has been determined that a whisker need not be discrete but may be a bundle of smaller whiskers.[31] In view of the theory of Ellis, Gibbons, and Treuting, a number of adjacent small grains may have extended out of the plating surface to form whiskers. The irregular tip of the whisker presented in Figure 13 may be evidence of varying lengths of the small whiskers which may comprise the growth. Equally, this irregularity may indicate that the growth pushed up through the plating layer

with the displaced plating surface remaining adhered to the surface, thus implying basal growth. In contrast, the leads of the Texas Instruments devices did not exhibit the high density of whiskers of the other commercial devices. In addition, the morphology of the growths on the Texas Instruments device leads is different.

Figure 34 presents nodular growths which are smooth and rounded on the relatively smooth surface of a lead of an aged Texas Instruments device. According to Key,[31], whiskers may originate from such nodules and this type of behavior may be seen in Figure 22 in which a whisker appears to be emerging from the center of the left portion of the nodule.

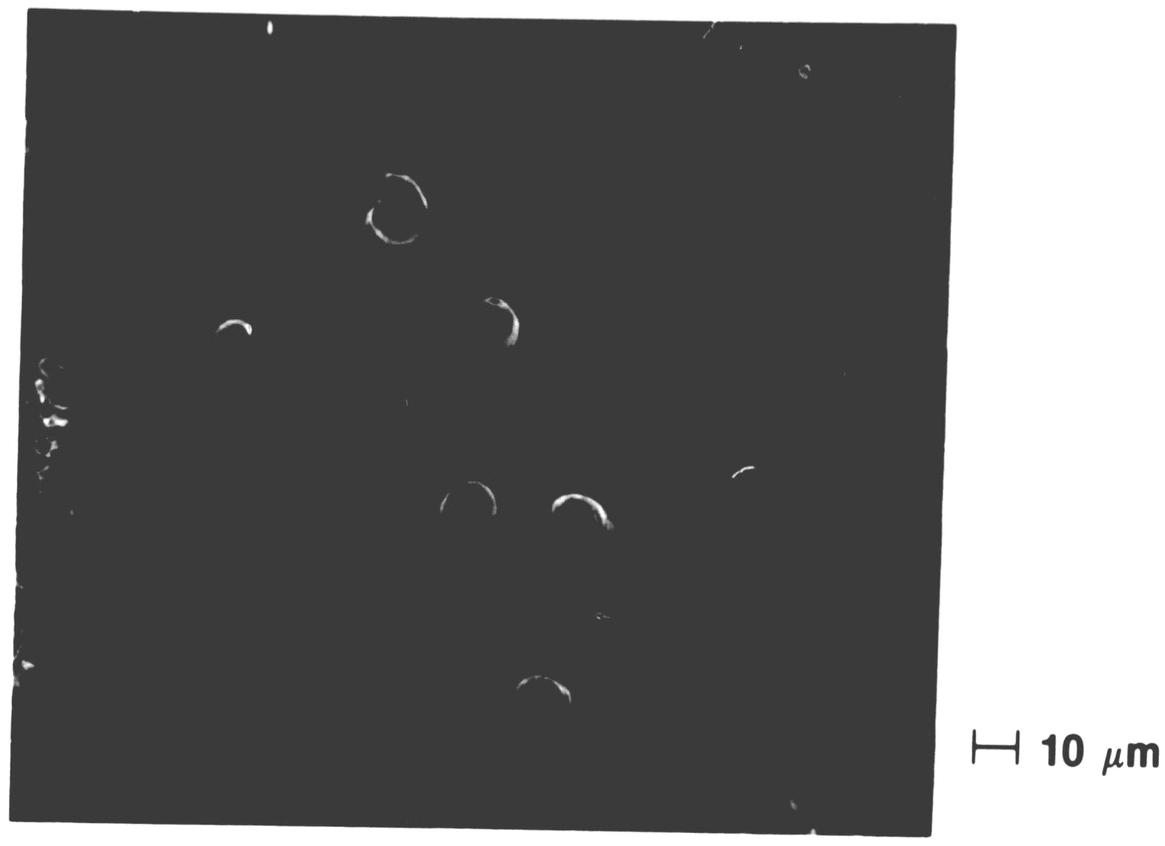

FIGURE 34: SEM MICROGRAPH OF NODULES ON LEAD OF AGED (100°C, 7000 h.) TEXAS INSTRUMENTS DEVICE.

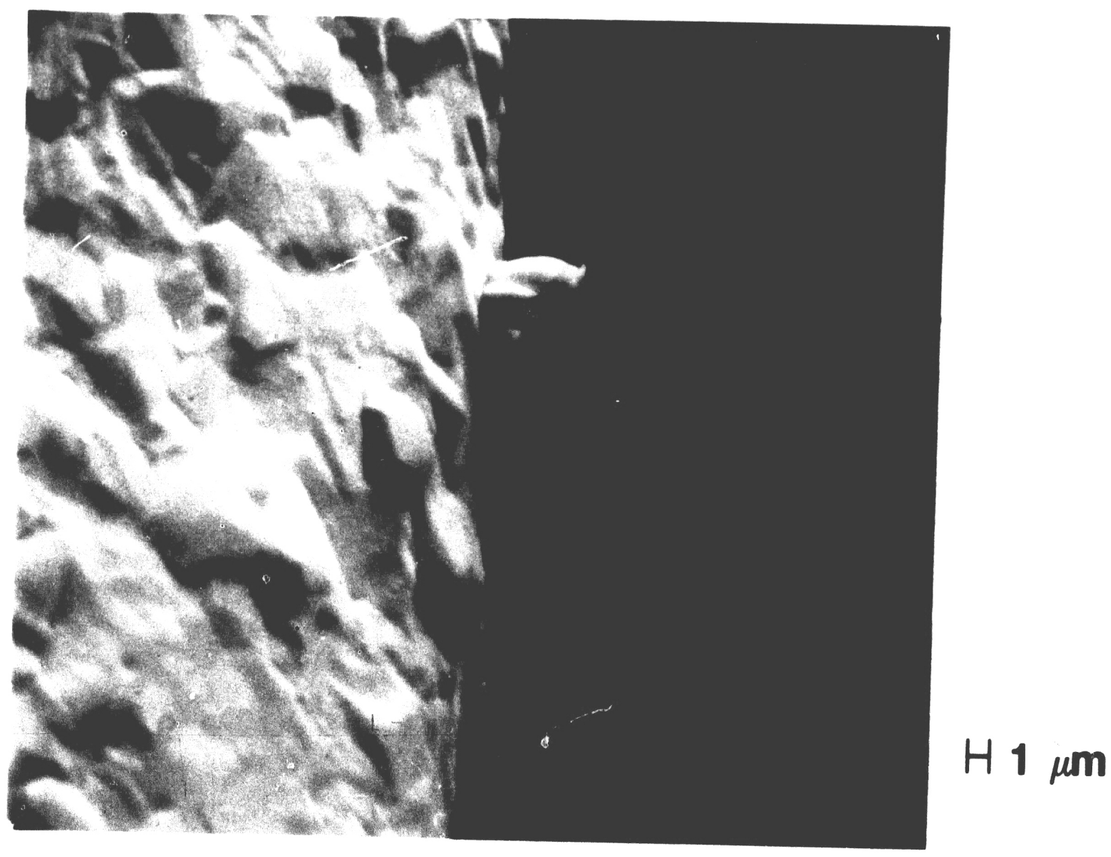

FIGURE 35: SEM MICROGRAPH OF TIN WHISKER ON LEAD OF AGED (25°C, 7000 h.) FAIRCHILD DEVICE.

5.2 Laboratory Plated Lead Frames

5.2.1 Observed Whisker Morphologies In this investigation, tin whiskers grew only from laboratory plated copper lead frames aged at 75° and 100°C for 7000 hours; therefore, the discussion of whisker morphologies derives from observations of these lead frames.

Three parts comprise the typical whisker structure: the shaft, the base and the tip. Previous investigations [30] [31] characterized the shaft of tin whiskers as straight or sharply kinked with a nearly uniform diameter from base to tip. In addition, striations typically extend along the length of the whisker shaft. This generally accepted description of the tin whisker shaft applied for only a few cases in the present investigation.

Figures 36 and 37 show two whiskers that exhibit the characteristic whisker shaft. Figure 36 presents a whisker with a straight shaft, uniform diameter and striations extending from base to tip. Previous investigations [30] [39] concluded that tin whiskers were single crystals with characteristic growth directions, suggesting that this straight whisker may be a single crystal with a low index crystallographic growth direction. Figure 37 presents whiskers with straight and kinked shafts. In both cases, the shaft diameter is uniform and striations extend along the length of the shaft. Figure 38 shows details of the striations of the straight whisker in Figure 37. The striations vary in depth and the spacing between striations differs; however, the depth and spacing stays constant along the whisker shaft. Furthermore, the striations remain parallel to the whisker length and unchanged in depth and spacing as the whisker kinks (Figure 39).

In the whiskers observed, the surface striations persisted along the whisker length and remained unchanged across kinks. Any pertubation of a smooth surface automatically leads to an overall increase in the surface area and the associated surface energy. As such, it is necessary to consider how the striations occur and how the striations influence the whisker

growth process.

Since the process of whisker growth must occur as a means of reducing the total energy of the system, the presence of the striations must contribute to this reduction. It is known that in crystalline solids the density of atomic packing is a function of the orientation of the crystallographic plane. In general, certain low index planes are more closely packed than others and represent orientations in which a minimization of energy is achieved. The specific planes on which this occurs are a function of the material's crystal structure.

During whisker growth, surface area is being continually created. In view of the fact that specific low index planes represent minima in surface energy, it is energetically favorable for a facetted surface to form over a smooth surface containing many randomly oriented crystal planes. Therefore, a facetted surface may form which evidences itself as striations on the whisker surface. As such, the surface striations are consistent with energy considerations; these striations represent low index crystallographic planes with a lower overall surface energy.

Figure 37 shows a sharply kinked whisker that also corresponds to the typical shaft morphology. The kinks occur from a change in the growth direction of the whisker with a return to the original growth direction. Measurements found the angles of the outer edges of the kinks to be between 105 to 110°. Numerous investigators [39] [41] suggest that twinning at the whisker base during growth reorients the whisker and produces kinks. Assuming that the observed kinks result from twinning and using the {101} plane [64] as the twinning mode, the growth directions of the whisker segments can be tentatively identified. Geometric calculations reveal the angle between the twin direction and the growth directions to be approximately 37°. Based on experimentally determined growth directions (Table I) and the angles between directions in β-tin, the growth directions of the whisker segments correspond to <100>. This exercise merely demonstrates that the principle of kinking may be related to

local twinning of the whisker during growth.

In contrast to the whiskers presented in Figures 36 and 37, the majority of whiskers observed exhibited a highly irregular shaft morphology. Most whiskers differed from the characteristic structure with the exception of the striations extending from base to tip. Figures 40 to 45 present the variety of whisker morphologies. The shafts of the whiskers in Figures 40 and 41 and of the individual whiskers in Figure 42 appear nearly uniform in diameter from base to tip and slightly curved rather than straight or sharply kinked. This curving may result from minute reorientations at the whisker base as growth proceeds.

The whiskers shown in Figures 43, 44 and 45 do not possess the characteristics of a typical whisker shaft with the exception of the striations. In these cases, the whiskers appear to be "extruded" from the plated surface with no evidence of a specific crystallographic orientation. In contrast to the striations shown in Figures 37 and 38, that are postulated to be low energy crystallographic planes, the striations on these irregular whiskers seem to reflect the shape of the extrusion channel. The irregularities may result from the process of reorientation for energy minimization during growth; if so, the whiskers may later assume straight growth and single crystal character.

Considering the next section of the whisker, the base, two morphologies prevailed. Figure 36 depicts a whisker emerging directly from the electroplate. In contrast to this basal morphology, the majority of whiskers observed appear to grow from a featureless nodular base (Figures 37, 41 and 42). No growth theory accounts for the presence of these nodules. In general, the featureless nodular base suggests that localized buckling of the plating surface may occur. Copper-tin intermetallics Cu_6Sn_5 have been observed to form readily at bimetallic copper-tin interfaces.[66] The formation of these compounds is associated with a local volume change that forces the tin electroplate up. Non-uniform formation of this

compound may result in isolated buckling and eruptions of the tin electroplate.

The last portion of the whisker morphology is the tip. In agreement with previous investigations, [31] observation of the whisker tips revealed either a smooth surface (Figures 3b) or a sharp bend (Figures 31 and 37). Based on the postulation that whisker growth proceeds according to energy reduction, the bent tip may result at the onset of growth when the newly forming whisker reorients to the most energetically favorable growth direction. The bend persists as basal growth continues.

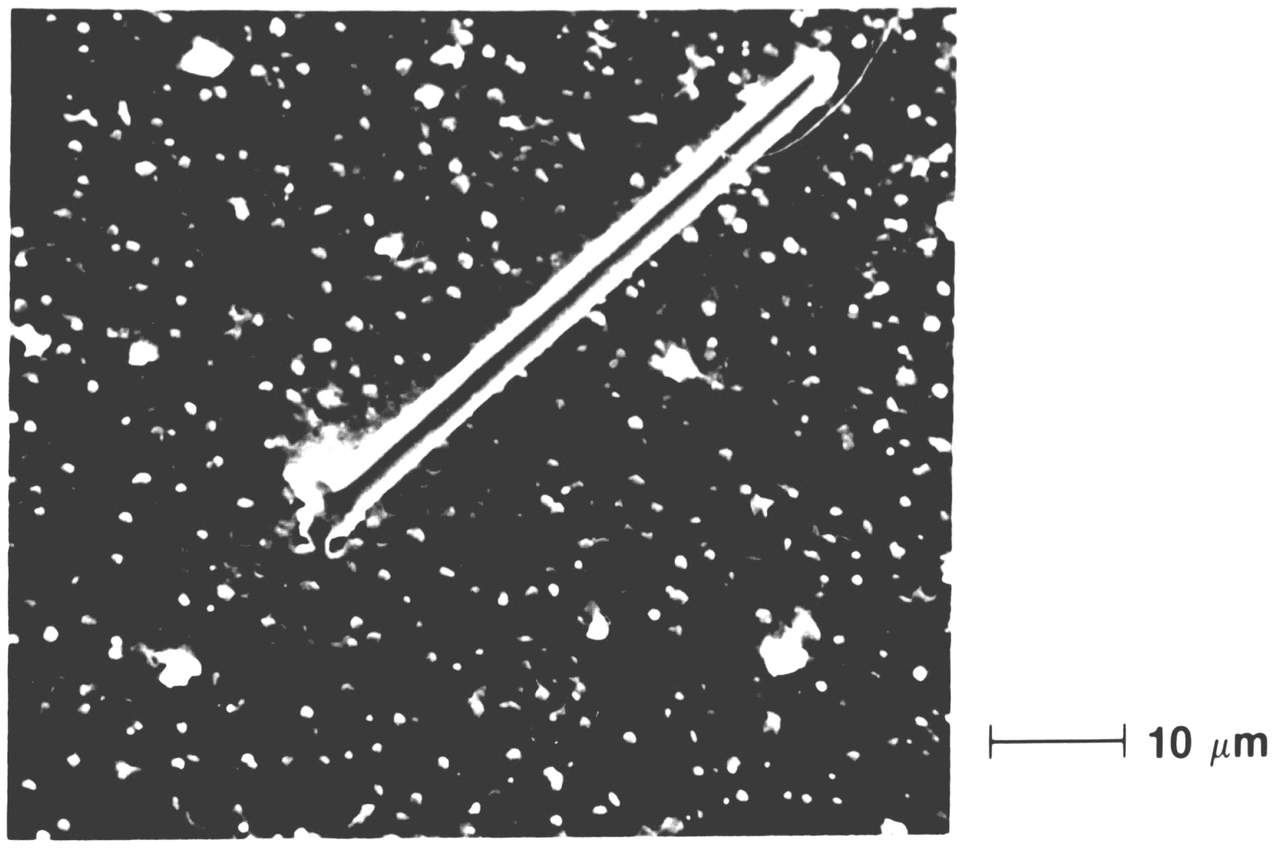

FIGURE 36: SEM MICROGRAPH OF TIN WHISKER ON AGED (75°C, 7000 h.) PLATED SURFACE ON COPPER.

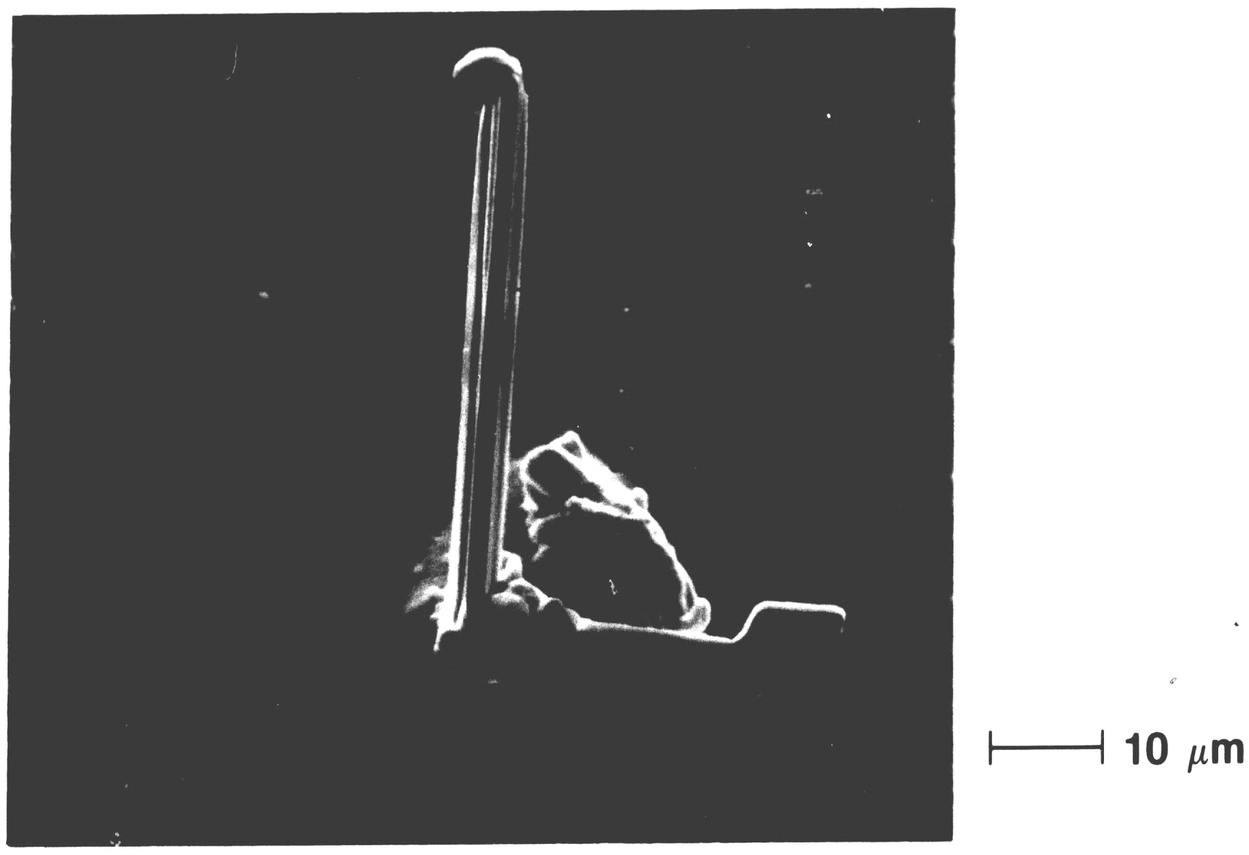

FIGURE 37: SEM MICROGRAPH OF TIN WHISKER ON AGED (75°C, 7000 h.) PLATED SURFACE ON COPPER.

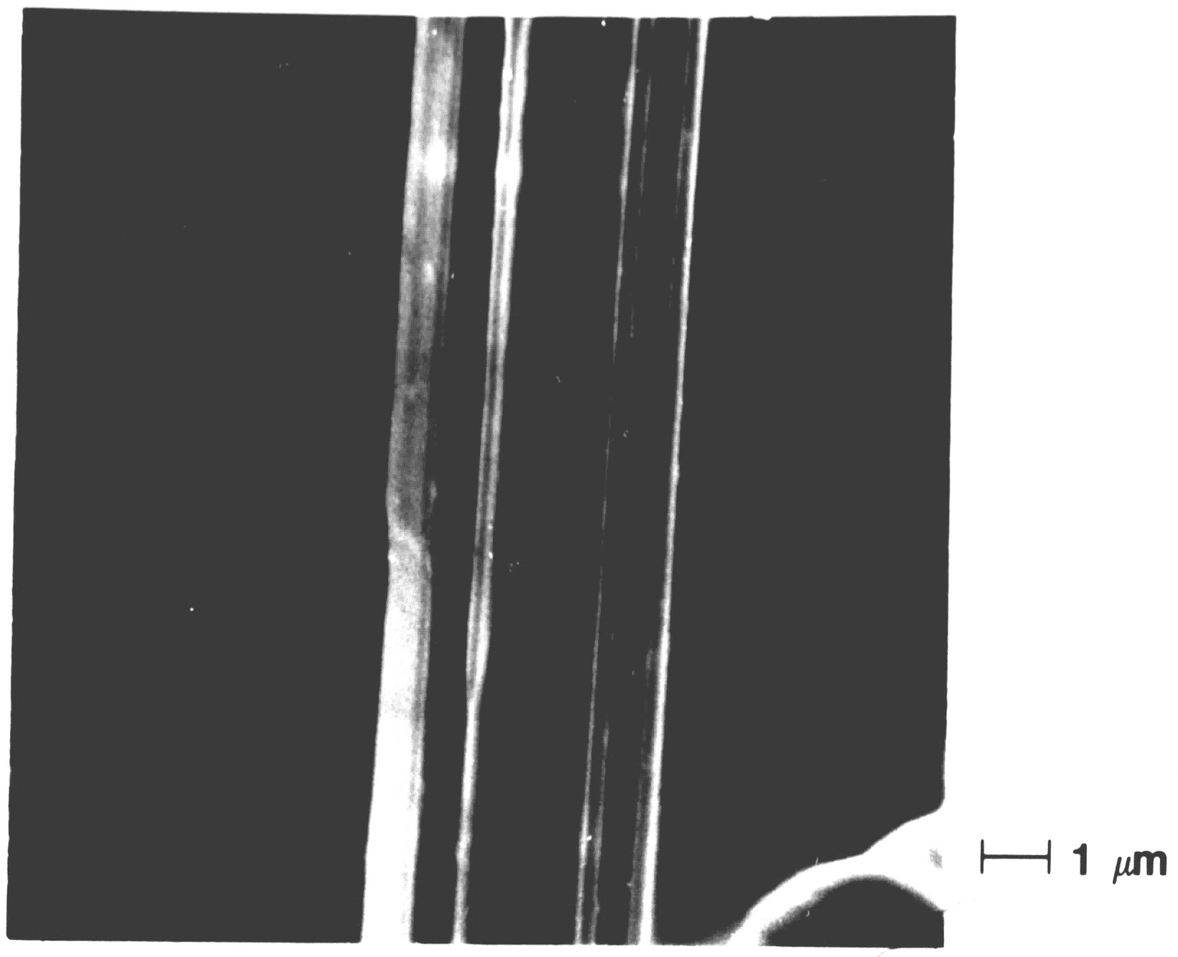

FIGURE 38: SEM MICROGRAPH SHOWING DETAILS OF STRIATIONS OF TIN WHISKER PRESENTED IN FIGURE 37.

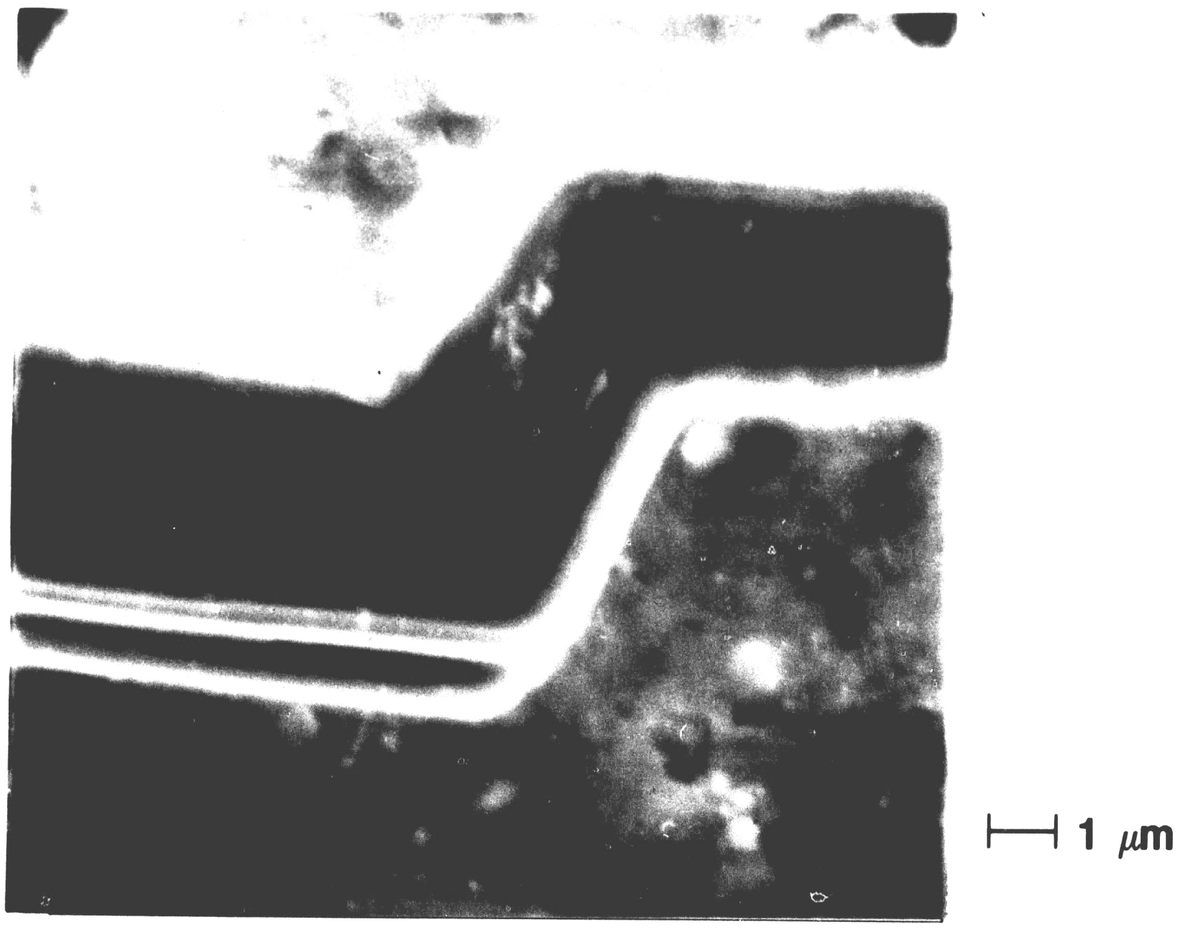

FIGURE 39: SEM MICROGRAPH SHOWING DETAILS OF KINK OF TIN WHISKER PRESENTED IN FIGURE 37.

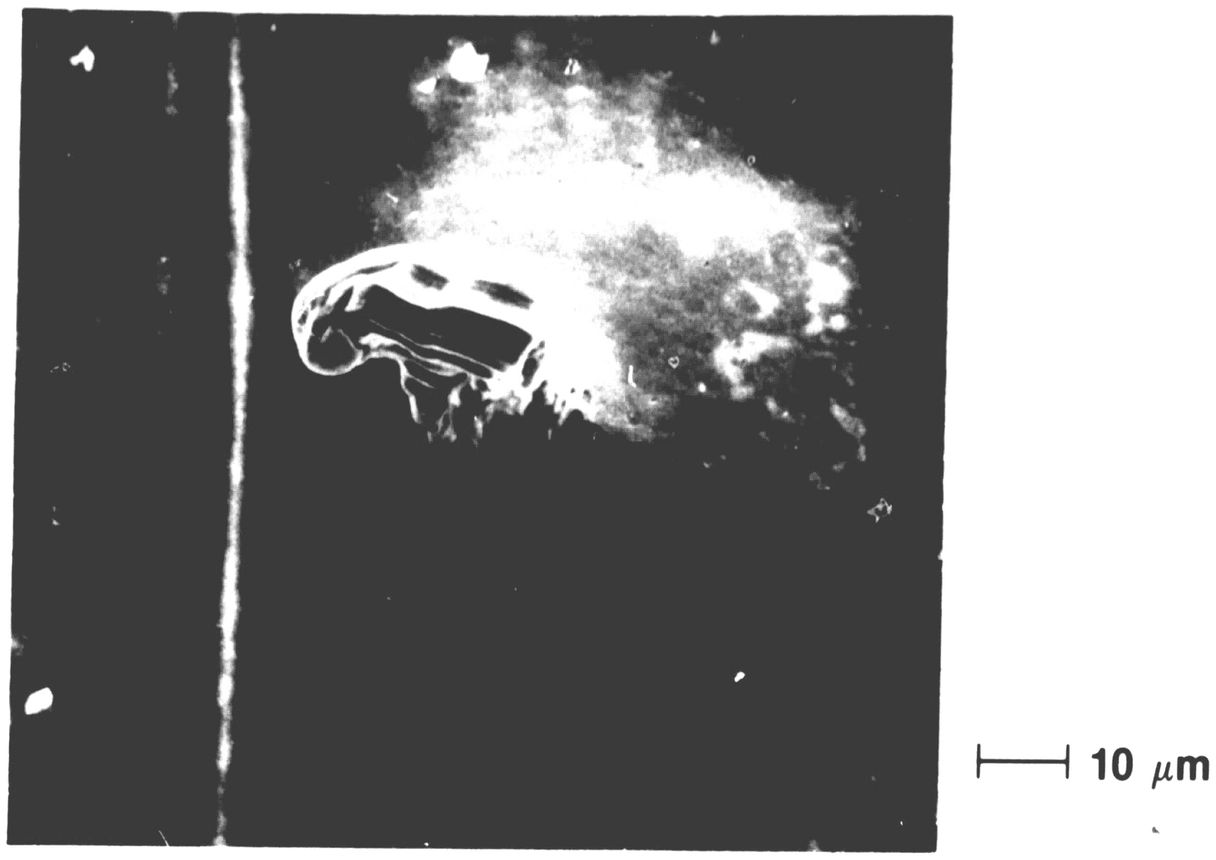

FIGURE 40: SEM MICROGRAPH OF TIN WHISKER ON AGED (100°C, 7000 h.) PLATED SURFACE ON COPPER.

FIGURE 41: SEM MICROGRAPH OF TIN WHISKER ON AGED (100°C, 7000 h.) PLATED SURFACE ON COPPER.

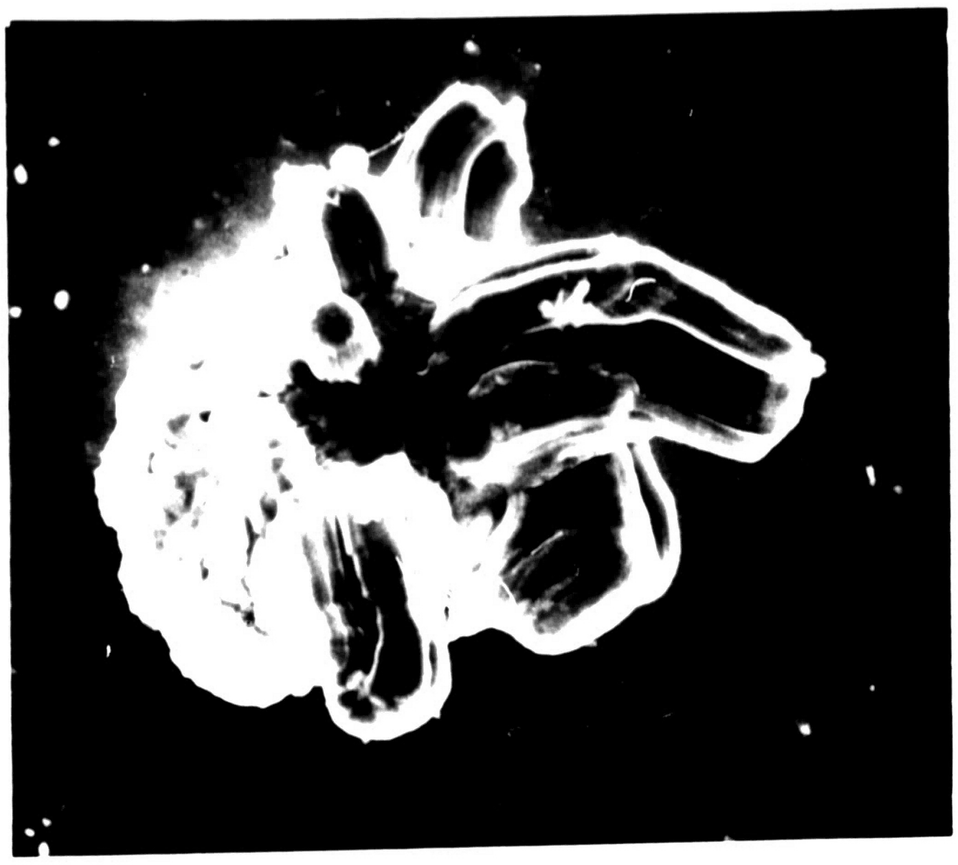

FIGURE 42: SEM MICROGRAPH OF TIN WHISKERS ON AGED (100°C, 7000 h.) PLATED SURFACE ON COPPER.

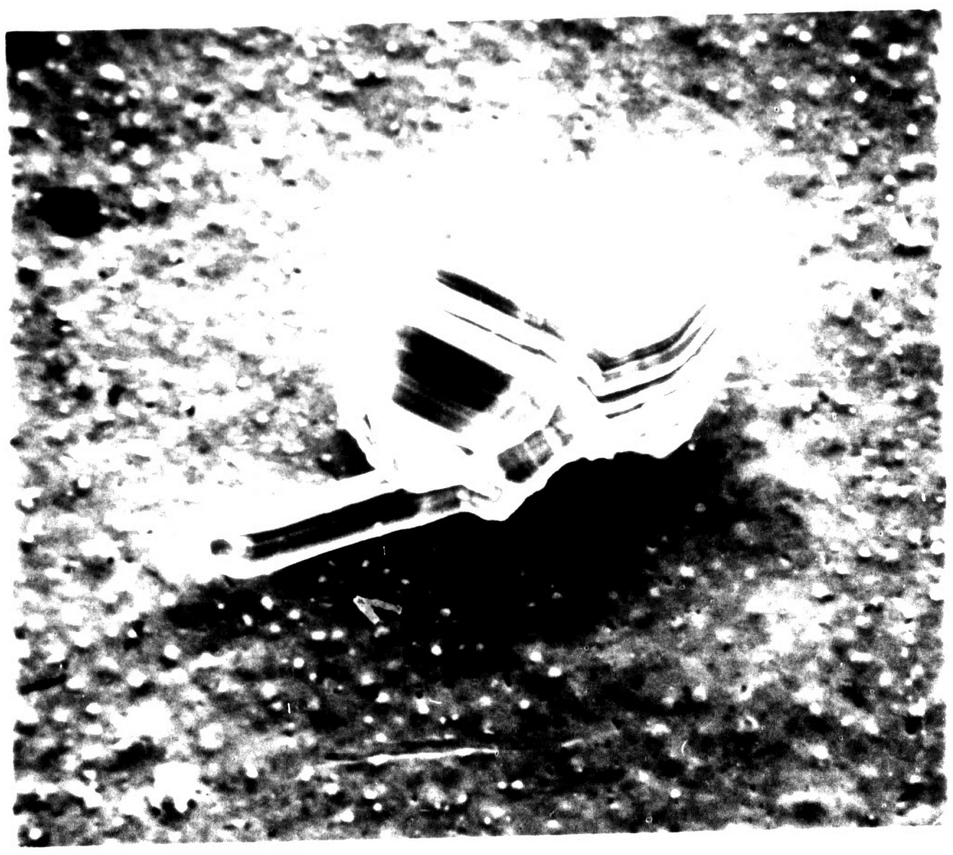

FIGURE 43: SEM MICROGRAPH OF TIN WHISKER ON AGED (75°C, 7000 h.) PLATED SURFACE ON COPPER.

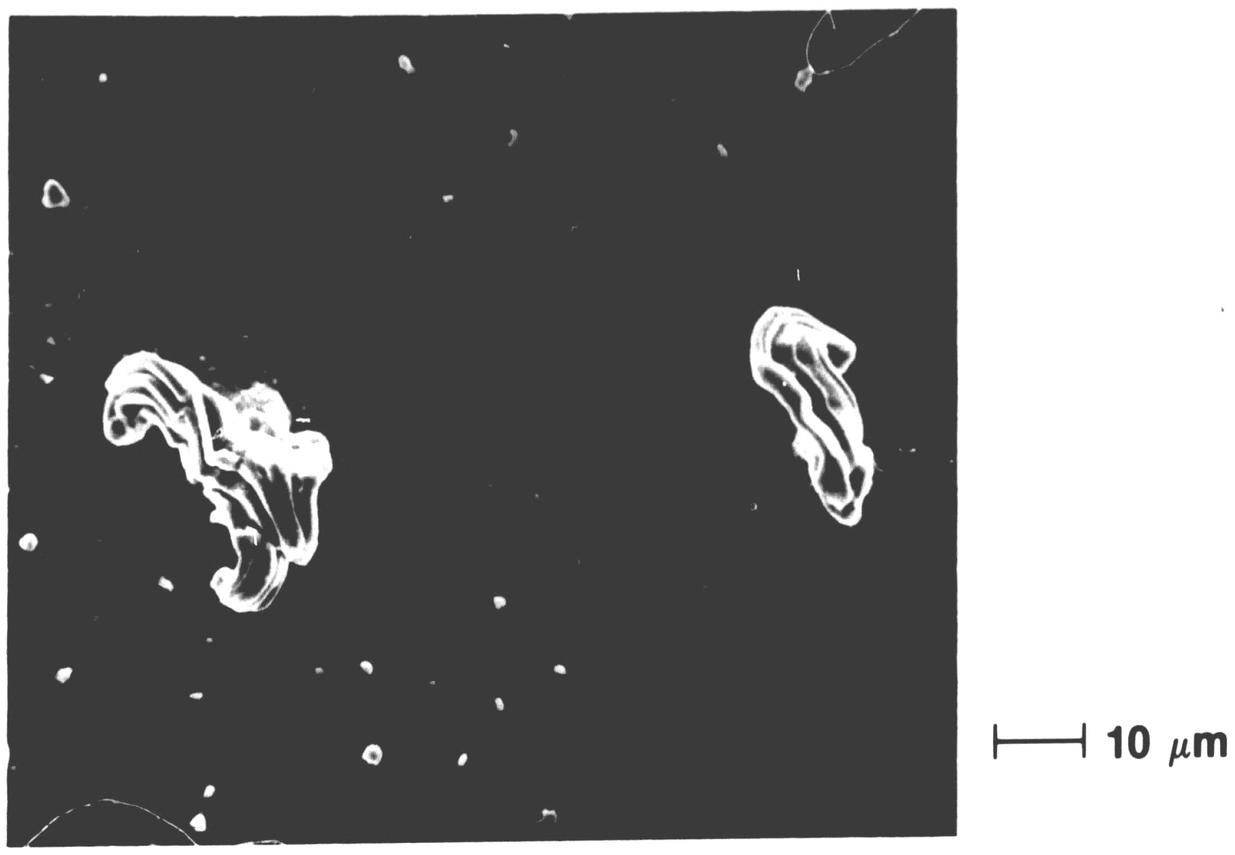

FIGURE 44: SEM MICROGRAPH OF TIN WHISKERS ON AGED (75°C, 7000 h.) PLATED SURFACE ON COPPER.

FIGURE 45: SEM MICROGRAPH OF TIN WHISKER GROWTH ON AGED (75°C, 7000 h.) PLATED SURFACE ON COPPER.

5.2.2 Effects of Temperature and Substrate Differences in the coefficients of thermal expansion between the substrate and tin electroplate appear irrelevant in this investigation. Large differences in thermal expansion cause stresses in the material that may lead to tin whisker growth. Based on the coefficients of thermal expansion for tin, copper and alloy 42 (23 μm/mK [65], 17 μm/mK [65] and 12 μm/mK, [67] respectively), the largest difference exists between tin and alloy 42. Since the plated alloy 42 lead frames did not exhibit whisker growth, the relevance of expansion differences is unresolved.

Tin plated copper lead frames aged at 75 and 100°C for 7000 hours exhibited the highest tin growth densities. In contrast, plated alloy 42 lead frames contained a low density of hillock growths after 7000 hours at 100°C (Table XII). In all cases, a considerable amount of time elapsed before growths were detected. Based on the formation of copper-tin intermetallics at the plating/substrate interface, Tu [68] hypothesized that the formation of $\eta' - Cu_6Sn_5$ at the interface compresses the unreacted tin and produces tin whiskers at the surface. Approaching the growth phenomenon as an energy potential with a threshold, Tu's investigation can provide the basis for a tentative explanation; sufficient intermetallic phase must form before the induced stresses in the tin layer reach the level for whisker growth. Since diffusion and consequently intermetallic formation is time and temperature dependent, the incubation period and temperature effects can be resolved. At higher temperatures, (75 and 100°C) copper-tin intermetallic compound formation occurs rapidly thus allowing the critical stress level for whisker growth to be reached sooner.

The interdiffusion of copper in tin is known to be rapid. At 25°C, the diffusion coefficient of copper along the *c* and *a* axis of tin is approximately $.4\times10^{-8}$ and $2\times10^{-6} cm^2/sec.$, respectively.[69] Tin whisker growth commonly occurs in the copper-tin electroplate system.[30] [45] [66] [68] The tin electroplated iron-nickel alloys rarely exhibits whisker growth. The lack of growth observed on the tin plated alloy 42 lead frames implies

that the interdiffusion of iron and nickel in tin is lower than that of copper. As a result, intermetallic formation proceeds slowly, and attainment of critical stress levels for whisker growth in the tin electroplate requires exceedingly long times.

5.2.3 Effect of Macrostresses In the present investigation, a potential correlation between tin whisker growth and electroplate internal macrostresses was evaluated. Previous investigations [70] [71] developed contrary relationships between whisker growth and internal macrostresses. Tables IX and X contain the internal macrostress results for the present investigation. Since tin whiskers grew only on plated copper lead frames aged at 75 and 100°C for 7000 hours, the first step in the evaluation concentrates on the stress results for these samples (Table X). Comparison of these stress values to the other stress results for the remaining samples that did not grow whiskers reveals insignificant differences. Consequently, it appears that internal macrostresses in the tin electroplate exert no detectable effects on tin whisker growth in the present investigation.

Figures 46 to 51, however, depict an interesting phenomenon that may be related to internal microstresses in the tin electroplate. During the plating operation, current concentrates at projections and edges of the sample.[72] Higher current cathodic densities increase defects and stresses in the metal film,[3] [37] creating regions of high microstresses. Examining Figure 50, the density of tin growths increases at the protuberance of the lead frame. This observation suggests that local microstresses induced by higher cathodic current densities promote tin growths. Furthermore, high percentages of substrate deformation resulting from forming operations in this region can be eliminated since tin growth density did not increase in the area of the stamped codes on the lead frames. Figure 51 shows the same region of another sample that was aged at 100°C for 7000 hours. The tin growth density appears uniform without noticable concentrations around the edge of the protrusion. At the higher temperature, accelerated formation of intermetallic compounds, Cu_5Sn_6, may

overshadow any microstress effects induced during electroplating.

The plated alloy 42 lead frames (Figures 46 and 47) did not exhibit this edge phenomenon observed for the plated copper lead frames (Figures 48 and 49). Tin whisker growth from the electroplated alloy 42 samples must therefore require a higher driving force that is not provided by the local microstresses and the aging temperatures and times used in the present investigation.

FIGURE 46: SEM MICROGRAPH OF TIN PLATED ALLOY 42 LEAD FRAME AGED AT 50°C, 7000 h.

FIGURE 47: SEM MICROGRAPH OF TIN PLATED COPPER LEAD FRAME AGED AT 50°C, 7000 h.

FIGURE 48: SEM MICROGRAPH OF TIN PLATED COPPER LEAD FRAME AGED AT 75°C, 7000 h.

FIGURE 49: SEM MICROGRAPH OF TIN PLATED COPPER LEAD FRAME AGED AT 100°C, 7000 h.

H 10 μm

FIGURE 50: SEM MICROGRAPH OF PORTION OF TIN PLATED COPPER LEAD FRAME AGED AT 75°C, 7000 h.

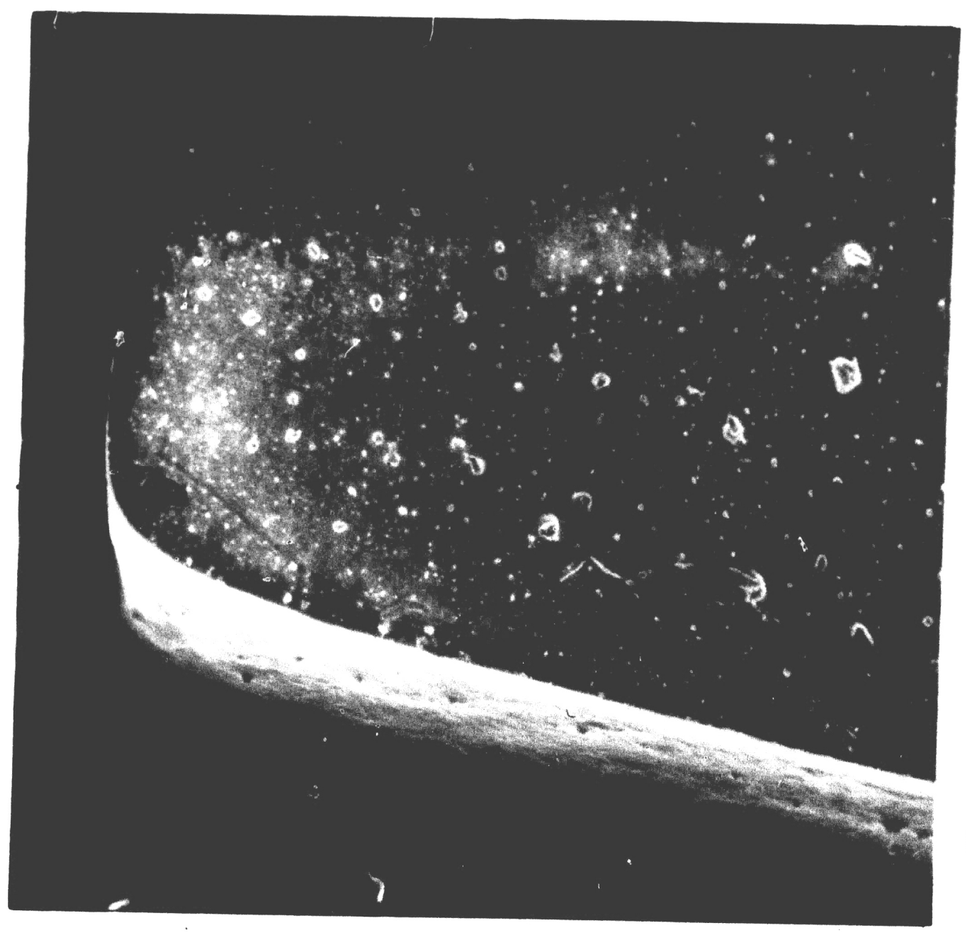

H 10 μm

FIGURE 51: SEM MICROGRAPH OF PORTION OF TIN PLATED COPPER LEAD FRAME AGED AT 100°C, 7000 h.

5.3 Device Reliability Implications

Tables XI and XII summarize all data concerning the whisker length. The total number of leads investigated for commercial devices was 800. The longest whisker observed out of this many leads, some after 5 years of storage, was only 20 μm. Also more significantly, aging at the optimum whisker growth conditions (50°C ≈ 75°C) did not result in appreciable increase in length (less than 6 μm).

The total number of leads investigated for laboratory-plated lead frames was 1000. The longest whisker observed for this group of leads was 60 μm, and the number of whiskers of this length was very small.

The inter-lead separation in a standard commercial DIP is 1270 μm. Therefore, based on the whisker length observed in the present study, the probability of whiskers bridging two leads seems very small. This finding is in agreement with that of M.C. Lin. [11]

6. CONCLUSIONS

1. Variations of characteristic tin whisker morphology were frequently observed but surface striations extending from the whisker base to tip were always present.

2. Commercial devices from all three manufacturers exhibited tin hillock or tin whisker growth in the as-received and all aged conditions.

3. Tin whisker growth on laboratory plated lead frames was found to be temperature dependent.

4. Laboratory plated Cu lead frames were more susceptible to tin whisker growth than plated alloy 42 lead frames.

5. The internal macrostresses in the laboratory-plated bright tin were determined to be compressive.

6. Macrostresses in the tin plating were not observed to be significant in whisker growth from laboratory samples.

7. No evidence for the exact mechanism for tin whisker growth was revealed in this investigation; however, basal growth was observed.

8. The driving forces for tin whisker growth appeared to be supplied by a complex interaction of internal microstresses. The sources for the microstresses may stem from stresses induced by high cathodic current density and the formation of intermetallics.

9. The maximum length of whiskers observed under the optimum whisker formation conditions was only 60 microns. Since the minimum lead separation on a DIP is 1270 microns, the probability of whiskers causing inter-lead shorts is very small. Therefore, tin plating on integrated circuits does not pose a reliability problem.

REFERENCES

1. Arnold, S.M., "The Growth of Metal Whiskers on Electrical Components," Proceedings of Electrical Components Conference, 1959, pp. 75-82.

2. Compton, K.G., Mendizza, A., Arnold, S.M., "Filamentary Growths on Metal Surfaces - 'Whiskers'," Corrosion, *1*, 1951, pp. 327-333.

3. Jafri, A., "Fighting Whisker Growth in the Communication Industry," Telesis, *2*, No. 4, 1972, pp. 15-19.

4. Diehl, R.P., "Eliminate Whisker Growth on Contacts By Using a Tin Alloy Plate," Insulation/Circuits, *22*, No. 4, 1976, pp. 37-39.

5. Dunn, B.D., "Whisker Formation on Electronic Materials," Circuit World, *2*, No. 4, 1976, pp. 32-40.

6. Arnold, S.M., "The Growth and Properties of Metal Whiskers," Proceedings of American Electroplaters' Society, *43*, 1956, pp. 26-31.

7. Key, P.L., Baker, R.G., "Finishes Approved for Replacement of the 562 Tin Finish," Bell Laboratories Memorandum for Record, May 21, 1971, Case 544 23-5 and 39091-102.

8. Britton, S.C., "Spontaneous Growth of Whiskers on Tin Coatings: 20 Years of Observation," Trans. of the Institute of Metal Finishing, *52*, 1974, pp. 95-102.

9. Arnold, S.M., " Repressing the Growth of Tin Whiskers," Plating, *53*, No. 1, 1966, pp. 96-99.

10. Baker, R.G., "Restrictions on the Use of Electrodeposited Tin," Bell Laboratories Memorandum for Record, February 15, 1968, Case 54423-5.

11. Lin, M.C., "Tin Whisker Growth on IC Lead Finish - A Review," Bell Laboratories Technical Memorandum 52221-840709-01, July 9, 1984.

12. Howey, J. H., "The Non-Cubic Growth of Single Crystal Silver by Condensation from Vapor," Phys. Rev., *55*, 1939, pp. 578-581.

13. Andrade, E. N. da C., Martindale, J. G., "Crystallisation of Metals from Sparse Assemblages," Nature, *134*, 1934, pp. 321-322.

14. Hardy, H. K., "Filamentary Growth of Metals," Prog. Metal Phys., *6*, 1956, pp. 45-73.

15. Nabarro, F.R.N., Jackson, P.J., "Growth of Metal Whiskers," *Growth and Perfection of Crystals*, ed. R.H. Doremus, B.W. Roberts and D. Turnbull, John Wiley and Sons, Inc., New York, 1958, pp. 13-102.

16. Herring, C., Galt, J.K., "Elastic and Plastic Properties of Very Small Metal Specimens," Phys. Rev., *85*, 1952, pp. 1060-1061

17. Smith, H.G., Rundle, R.E., "X-Ray Investigation of the Perfection in Tin Whiskers," J. Appl. Phys., *29*, No. 4, 1958, pp. 679-683.

18. Pauling, L., Carpenter, D.C., "The Crystal Structure of Metaldehyde," J. Amer. Chem. Soc., *58*, 1954, pp. 1204-1205.

19. Johnson, E.R. Amick, J.A., "Formation of Single Crystal Silicon Fibers," J. Appl. Phys., *25*, 1954, pp. 1204-1205.

20. Frank, F.C., "Crystal Growth and Dislocations," Adv. Phys., *1*, 1952, pp. 91-109.

21. Brenner, S.S., "The Growth of Whiskers by the Reduction of Metal Salts," Acta Met., *4*, 1956, pp. 62-74.

22. Davis, M.E., Lever, R.I., "Vapor Phase Crystal Growth of Germanium from Thermally Decomposed Germane," J. Appl. Phys., *27*, 1956, pp. 835-836.

23. Cobb, H.L., "Cadmium Whiskers," Monthly Review of American Electroplaters' Society, *33*, 1946, pp. 28ff.

24. Glazunova, V.K., Gorbunova, K.M., "Spontaneous Growth of Whiskers from Electrodeposited Coatings," J. Crystal Growth, *10*, 1971, pp. 85-90.

25. Ellis, W.C., "Morphology of Whisker Crystals of Tin, Zinc, and Cadmium Grown Spontaneously from the Solid," Trans. AIME, *236*, 1966, pp. 872-875.

26. Arnold, S.M., Koonce, S.E., "Filamentary Growths on Metals at Elevated Temperatures," J. Appl. Phys., *27*, p. 964.

27. Hada, Y., Marikawa, O., Togami, H., "Study of Tin Whiskers on Electromagnetic Relay Parts," presented at 26th Annual National Relay Conference, 1978.

28. Britton, S.C., Clarke, M., "Effects of Diffusion from Brass Substrates into Electrodeposited Tin Coatings on Corrosion Resistance and Whisker Growth," Trans. Inst. Metal Finishing, *40*, 1963, pp. 205-211.

29. Marchand W., Trans. Inst. Metal Finishing, *38*, 1961.

30. Ellis, W.C., Gibbons, D.F., Treuting, R.G., "Growth of Metal Whiskers from the Solid," *Growth and Perfection of Crystals*, ed. R.H. Doremus, B.W. Roberts and D. Turnbull, John Wiley and Sons, Inc., New York, 1958, pp. 102-120.

31. Key, P.L., "Surface Morphology of Whisker Crystals of Tin, Zinc and Cadmium," Proc. 20th Electronic Components Conference, 1970, pp. 155-160.

32. Arnold, S.M., Koonce, S.E., "Metal Whiskers," J. Appl. Phys., *25*, 1954, pp. 134-135.

33. Franks, J., "Growth of Whiskers in the Solid Phase," Acta Met., *6*, 1958, pp. 103-109.

34. Koonce, S.E., Arnold, S.M., "Growth of Metal Whiskers," J. Appl. Phys., *24*, 1953, pp. 365-366.

35. Bradley, D.E., Franks, J., Rush, P.E., "Electron Microscopy of Tin Whiskers using Carbon Replicas," Proc. Phys. Soc. of London, *70B*, 1957, pp. 889-892.

36. Thomas, E.E., "Tin Whisker Studies. Observation of Some Hollow Whiskers and Some Sharply Irregular External Forms," Acta Met., *4*, 1956, p. 94.

37. Polyitycki, A., Kehrer, H.P., "Investigation of the Growth of Tin Whiskers," Z. Metallk., *59*, 1968, pp. 309-323.

38. Kehrer, H.P., Kadereit, H.G., "Tracer Experiments on the Growth of Tin Whiskers," Appl. Phys. Letters, *16*, 1970, pp. 411-412.

39. Treuting, R.G., Arnold, S.M., "Orientation Habits of Metal Whiskers," Acta Met., *5*, 1957, p. 598

40. Morris, R.B., Bonfield, W., "The Crystallography of Alpha-Tin Whiskers," Scripta Met., *8*, 1974, pp. 231-236.

41. Baker, G.S., "Angular Bends in Whiskers," Acta Met., *5*, 1957, pp. 353-357.

42. Furuta, N., "Growing Process of Kinked Tin Whiskers," Jap. J. Appl. Phys., *4*, 1955, pp. 155-156.

43. Levy, P.W., Kammerer, "'Spiral Polygon' Tin Whiskers," J. Appl. Phys., *26*, 1955, pp. 1182-1183.

44. Amelinckx, S., Bontinck, W., Dekeyser, W., Seitz, F., "On the Formation and Properties of Helical Dislocations," Phil. Mag. *2*, 1957, pp. 355-378.

45. Frank, F.C., "On Tin Whiskers," Phil. Mag., *44*, 1953, pp. 854-860.

46. Eshelby, J.D., "A Tentative Theory of Metallic Whisker Growth," Phy. Rev., *91*, 1953, pp. 755-756.

47. Franks, J., "Growth of Whiskers in the Solid Phase," Acta Met., *6*, 1958, pp. 103-109.

48. Lindborg, U., "A Model for the Spontaneous Growth of Zinc, Cadmium and Tin Whiskers," Acta Met., *24*, 1976, pp. 181-186.

49. Furuta, N., Hamamura, K., "Growth Mechanism of Proper Tin Whisker," Jap. J. Appl. Phys., *8*, 1969, pp. 1404-1410.

50. Hasiguti, R.R., "A Tentative Explanation for the Accelerated Growth of Tin Whiskers," Acta Met., *3*, 1955, pp. 200-201.

51. Kakeshita, T., Shimizu, K., Kawanaka, R., Hasegawa, T., "Grain Size Effect of Electroplated Tin Coatings on Whisker Growth," J. Mat. Sci., *17*, 1982, pp. 2560-2566.

52. Fisher, R.M., Darken, L.S., Carroll, K.G., "Accelerated Growth of Tin Whiskers," Acta Met., *2*, 1954, pp. 368-373.

53. Peach, M.O., "Mechanism of Growth of Whiskers on Cadmium," J. Appl. Phys., *23*, 1952, pp. 1401-1403.

54. Rozen, M., "Practical Whisker Growth Control Methods," Plating, *55*, 1968, pp. 1155-1160.

55. Asthner, B., "Tin Whisker Growth on Electrodeposited Tin Coatings," Galvanotrommel, *10-13*, 1976.

56. Zakraysek, L., "Whisker Growth from a Bright Acid Tin Electrodeposit," Plating, *64*, 1977, pp. 38-43.

57. Hitachi, Ltd., "Prevention of Dendrite Formation in Plated Tin (patent)," Jpn. Kokai Tokkyo Koho, *80, 138, 067*, 1980.

58. Ascher, D., Hiesboeck, H.G., "Largely Whisker-Free-Tin-Electroplated Material (patent)," Ger. Offen. DE *3, 331, 212*, 1984.

59. Ohsawa, K., Kaizumi, T., "Prevention of Whisker Formation on Electrodeposited Tin (patent)," Japan. Kokai, *77, 45, 539,* 1977.

60. Kawanaka, R., Fujiwara, K., Nago, S., Hasegawa, T., "Influence of Impurities on the Growth of Tin Whiskers," Jap. J. Appl. Phys., *22,* 1983, pp. 917-922.

61. Burggraaf, P.S., "IC Lead Finishing: Issues and Options," Semiconductor International, July 1983, pp. 64-69.

62. Tsujita, Y., Nakamura, K., Kaizuka, T., "Whisker Formation Inhibition of Bright Electroplated Tin Coatings (patent)," Japan. Kokai, *76, 143, 533,* 1976.

63. Cullity, B.D., *Elements of X-Ray Diffraction, 2nd ed.*, Addison-Wesley Publishing Co., Inc., Reading, Mass., 1978.

64. Barrett, C., Massalski, T.B., *Structure of Metals, 3rd ed.* Pergamon Press Ltd., New York, 1980.

65. American Society for Metals, *Metals Handbook, vol. 2, 9th ed.*, Metals Park, Ohio, 1979.

66. Tu, K. N., Thompson, R. D., "Kinetics of Interfacial Reaction in Bimetallic Cu-Sn Thin Films," Acta Met., *30,* 1982, pp. 947-952.

67. Touloikian, Y.S., Kirby, R.K., Taylor, R.E., Desai, P.D., *Thermophysical Properties of Matter; The TPRC Data Series,* vol. 12, IFI, Plenum, New York, 1975, pp. 848-860.

68. Tu, K. N., "Interdiffusion and Reaction in Bimetallic Cu-Sn Thin Films," Acta Met., *21,* 1973, pp. 347-354.

69. Dyson, B.F., Anthony, T.R., Turnbull, D., "Interstitial Diffusion of Copper in Tin," J. Appl. Phys., *38*, 1967, p. 3408.

70. Sugiarto, H., Christie, I.R., Richards, B.P., "Studies of Zinc Whiskers Formation and Growth from Bright Zinc Electrodeposits," Trans. Inst. Met. Finish., Autumn 1984, pp.

92-97.

71. Lindborg, U., "Observations on the Growth of Whisker Crystals from Zinc Electroplate," Met. Trans., Vol. *6A*, 1975, pp. 1581-1586.

72. Graham, A.K., ed., *Electroplating Engineering Handbook, 3rd ed.*, Van Nostrand Reinhold Co., New York, pp. 56-65.

VITA

Barbara Ann Shollock was born January 5, 1962 in Bristol, Pennsylvania and is the daughter of Paul and CeCelia Shollock.

In June 1983, Ms. Shollock graduated with honors from Lehigh University with a degree of Bachelor of Science in Metallurgy and Materials Engineering. She was employed as a member of the technical staff at AT&T Bell Laboratories, Allentown in the Failure Analysis and Reliability Group during the summer of 1984. During the summer of 1985, she was employed by AT&T Bell Laboratories, Reading in the Lightwave Device Packaging Group. Ms. Shollock is a joint member of ASM-AIME.